Loma Linda University Electronic Theses, Dissertations & Projects

9-2014

Role of Astrocyte Network in Edema after Juvenile Traumatic Brain Injury

Andrew Minoru Fukuda

LOMA LINDA UNIVERSITY
School of Medicine
in conjunction with the
Faculty of Graduate Studies

_____

Role of Astrocyte Network in Edema after Juvenile Traumatic
Brain Injury

by

Andrew Minoru Fukuda

_____

A Dissertation submitted in partial satisfaction of
the requirements for the degree
Doctor of Philosophy in Physiology

_____

September 2014

Each person whose signature appears below certifies that this dissertation in his/her opinion is adequate, in scope and quality, as a dissertation for the degree Doctor of Philosophy.

_____, Chairperson
Jerome Badaut, Assistant Professor of Pediatrics and Physiology

_____
Stephen Ashwal, Distinguished Professor of Pediatrics and Neurology

_____
Eduardo Candelario-Jalil, Assistant Professor of Neuroscience, University of Florida

_____
Kerby Oberg, Professor of Pathology and Human Anatomy

_____
John Zhang, Professor of Physiology, Anesthesiology, Neurology, Neurosurgery, Pathology & Human Anatomy

ACKNOWLEDGEMENTS

There are so many people who have played an integral part in my life so far to shape me the way I am so that I can be at this stage in my life, and one page is not enough to thank you all individually, so I would first like to express my gratitude to those unnamed friends here.

The following are key people who have played essential and direct roles in the completion of my PhD.

First, I would like to express my deepest gratitude to Dr. Badaut for teaching me the ways of biomedical research and guiding me as a mentor for the past few years. Although my PhD training is finished, there are still many more things I have yet to learn from you, so regardless of where we end up in the world, you will always be my teacher and friend.

Next, I would like to thank my committee members for their advice and direction. Dr. Zhang, Dr. Ashwal, Dr. Oberg, and Dr. Candelario, thank you all very much for sparing your valuable time to provide me with scientific and academic insights. Additional gratitude goes to Dr. Obenaus and Dr. Hartman for their expertise regarding magnetic resonance imaging and neurobehavioral testing. Your facilities and expert knowledge were essential for the completion of my work.

I would also like to extend a special thanks to my mentor and friend, Dr. John Perumal, from my undergraduate years for instilling within me the passion for research - I would not have pursued the MD/PhD path were it not for you. I would also like to thank Dr. Oberg who, having gone through this MD/PhD program already in the past, gave me invaluable insights and encouragements during crucial moments during my training.

Without your kind professional advice, I most likely would not have decided to complete my PhD.

To my loving parents, thank you very much for always watching over me and supporting me. I would like to especially thank my father, who has always been, and continue to be, my inspiration and role model as I continue with my career: I will always strive to emulate your unconditional kindness to humbly help the sick and injured while never forgetting the joyful pursuit to quench our unending curiosity for knowledge.

To my loving and patient wife, Keila, I would not have been able to do this without your understanding support and unwavering confidence in my ability to succeed. During those countless days and nights when I was unsure of myself, you were the one who always brought me back up.

And above all else, I continually thank God for allowing me to encounter all of these amazing people and giving me this opportunity to pursue science as a means to make a positive difference in this world.

CONTENTS

TABLE

FIGURES

ABBREVIATIONS

jTBI	Juvenile Traumatic Brain Injury
CCI	Controlled Cortical Impact
AQP1	Aquaporin 1
AQP4	Aquaporin 4
AQP9	Aquaporin 9
Cx30	Connexin 30
Cx43	Connexin 43
MRI	Magnetic Resonance Imaging
T2	T2 Weighted Imaging
DWI	Diffusion Weighted Imaging
ADC	Apparent Diffusion Coefficient
IHC	Immunohistochemistry
WB	Western Blot
GFAP	Glial Fibrillary Acidic Protein
siRNA	Small Interference Ribonucleic Acid
IgG	Immunoglobulin G
EBA	Endothelial Barrier Antigen
NeuN	Neuronal Nuclei
BBB	Blood Brain Barrier
ROI	Regions of Interests
MWM	Morris Water Maze

ABSTRACT OF THE DISSERTATION

Role of Astrocyte Network in Edema after Juvenile Traumatic
Brain Injury

by

Andrew Minoru Fukuda

Doctor of Philosophy, Graduate Program in Physiology
Loma Linda University, September 2014
Dr. Jerome Badaut, Chairperson

Juvenile traumatic brain injury (jTBI) is the leading cause of death and disability

in young children and adolescents. Despite its lasting detrimental effects on the

developing brain, no pharmacological treatment exists. One of the pathological hallmarks

of jTBI is edema. Astrocytes play a key role in the edema process, and have been

hypothesized that numerous astrocyte networks allow communication and propagation of

edema and secondary injury spread. Two key astrocyte proteins are hypothesized to have

a central role in the edema process: Aquaporin 4 (AQP4) and Connexin 43 (Cx43). AQP4

is expressed extensively in astrocyte endfeet, which surrounds the blood vessels as part of

the blood brain barrier (BBB). Cx43 is central in astrocyte to astrocyte connection and

communication. We hypothesized that AQP4 acted as one of the potential passageway of

water into the astrocyte, whereas Cx43 acted as the bridge between astrocytes once inside

the brain. By blocking these strategically located pathways, we hypothesized that edema

would decrease post-jTBI. In order to achieve specific inhibitions of APQ4 or Cx43, we

utilized small interference RNA (siRNA), which is also an endogenous mechanism.

We observed that after jTBI both AQP4 and Cx43 was significantly upregulated,

edema was prominent, and reactive astrogliosis occurred. When siAQP4 was

administered after jTBI, there was functional improvement, decreased edema, and decreased reactive astrogliosis. When siCx43 was administered, there was functional improvement and decreased reactive astrogliosis, but the level of edema did not change. From these findings, it can be seen that (1) AQP4 and Cx43 are upregulated acutely after jTBI, (2) both siAQP4 and siCx43 have therapeutic potentials after jTBI leading to functional recovery, (3) although both target astrocyte endfeet proteins, the mechanism of action seem to be different and AQP4 may play a more direct role in the edema process than Cx43.

Future studies could focus on (1) a more clinically relevant delivery of siRNA for jTBI, (2) elucidating the mechanism behind functional improvement of siCx43, and (3) the relationship between AQP4 and Cx43 regarding astrocyte pathology after jTBI.

CHAPTER ONE

INTRODUCTION

**Clinical Relevance of Juvenile Traumatic
Brain Injury**

Traumatic brain injury affects at least 1.7 million people in the U.S. directly; and

this number does not include patients in military, federal, or veterans affair hospitals, or

people who are not medically treated (Faul et al., 2010). TBI contributes to 30.5% of all

injury related deaths in the U.S. and causes a huge financial burden. Of especially great

concern is juvenile traumatic brain injury (jTBI), which is the major cause of death and

disability in children and adolescents, causing about half a million to get emergency care,

and the number is still growing (Faul et al., 2010). jTBI causes long lasting debilities that

can affect the children's physical, mental, and emotional ability well into adulthood.

Despite the damages jTBI cause at the individual, communal, and national level, no

effective pharmacological treatment exists to date.

One can say that TBI causes an onset of two stages of injury: primary and

secondary. Primary injuries are the initial damages resulting from a direct and immediate

mechanical disruption of the brain tissue and leads to secondary injuries, which are

indirect and more delayed mechanisms. The severity of primary injuries have been

decreased in recent years due to increased public and legislative awareness concerning

preventive measures such as wearing helmets when engaging in a potential TBI causing

event such as riding bicycles. Thus, research in the development of efficient post-injury

therapeutic treatments should focus on targeting secondary injuries (Morales et al., 2005).

In order to accomplish this, a better understanding of the pathophysiological molecular changes that occur in the brain at later time points post injury is needed. This knowledge of the long term alterations post-injury is critical in jTBI because the brain is still developing, and secondary injuries may have a more severe and long lasting effect in the child's cognitive, emotional, and motor functions than in adult. One such key secondary pathological hallmark responsible for the deaths and disabilities after jTBI is cerebral edema (Huh and Raghupathi, 2009).

Cerebral Edema

Edema is an abnormal accumulation of water, whether inside the cell or in the extracellular space. Traditionally, cerebral edema has been categorized into two general types: cytotoxic and vasogenic (Klatzo, 1967). Cytotoxic edema refers to the cellular swelling due to water moving from the extracellular space into the intracellular space without disruption of the blood brain barrier (BBB), and vasogenic edema refers to the accumulation of water from the blood to the brain parenchyma, due to the disruption of the BBB (Papadopoulos and Verkman, 2007). However, recent findings have led some to suspect cerebral edema to be a more complicated process with further stages of characterization (Simard et al., 2007; Unterberg et al., 2004). One example of this is a further categorization of cerebral edema into three stages: anoxic edema, ionic edema, and vasogenic edema (Badaut et al., 2011b), taking into consideration the recent knowledge on molecular and cellular mechanisms involved in edema formation. Anoxic edema occurs within minutes after the cessation of oxygen and energy (such as glucose) supplies that result in ionic gradient abnormality, finally causing astrocytic swelling as described for cytotoxic edema. In a continuous gradient, the endothelial cells suffer from

2

the energy depletion, which contributes to ionic pump dysfunction which results in water flow into the brain extracellular space before physical disruption of BBB. This phase is called ionic edema that further exacerbates astrocyte swelling and neuronal cell death. The final stage termed vasogenic edema occurs because of a massive disruption of BBB due to endothelial tight junction destruction, causing leakage of plasma proteins into the brain parenchyma, with water following. Regarding TBI, during anoxic and ionic edema, cellular swelling and the resultant damage most likely spreads from the initial impact site to regions further away, affecting more distant cells due to the characteristic network organization of astrocytes, connected by gap junctions. As such, edema most likely involves several proteins in the astrocyte, especially those expressed in the perivascular astrocyte and astrocyte-astrocyte junctions. Thus, we believe that reducing edema formation by targeting these key components of the edema process is an effective strategy to facilitate recovery or reduce the secondary damages caused after jTBI.

Aquaporin 4, a Key Astrocyte Water Channel Protein is
Responsible for Edema Formation

Aquaporin is a family of water channel protein that is expressed in most organisms, including rodents and humans. To date 13 AQPs have been identified in mammals, and 3 AQPs in the brain have been characterized so far: AQP1, AQP4, and AQP9 (Badaut et al., 2011b). The aquaporin family exhibits a common structure with six membrane spanning alpha helical domains, a consensus motif composed of Asparagine-Proline-Alanine (NPA) constituting part of the pore, and an approximate molecular weight of 30 kDa (Gonen and Walz, 2006). AQP4 is the most abundant AQP found in the primate and rodent brains, mainly in the perivascular astrocyte endfeet (Badaut et al.,

2002). AQP4 is assembled in homo-tetramers where each individual aquaporin represents a water channel (Yu et al., 2006). The assemblage of four molecules of AQP4 forms a central pore, through which water, cations, and gases such as CO2 flow (Musa-Aziz et al., 2009). The main function of AQP4 is widely accepted as facilitating water mobility (Badaut et al., 2011b), and thus have been studied in relationship with the edema process (Fukuda and Badaut, 2012). Recently, this was observed using *in vivo* inhibition of expression of AQP4 with specific siRNA targeting AQP4 (Badaut et al., 2011a), and using diffusion weighted magnetic resonance imaging (DWI), which is widely accepted as a measure of water mobility (Badaut et al., 2011a).

Connexin 43, a Key Protein Forming the Astrocyte Network may be Responsible for Edema Spread

In the brain, not only neurons, but also astrocytes form a network in which individual astrocytes connect with each other, exchange information, and influence each other and the network as a whole. Appropriately, the term astrocyte network (Giaume et al., 2010) is frequently used to describe this characteristic. In the network, astrocytes are interconnected with each other through gap junctions, which are made of connexin proteins: predominantly connexin 43 (Cx43), but also connexin 30 (Cx30), that facilitate intercellular communication, and possibly intracellular communication (Wolff et al., 1998). The connexin subtypes are named according to their molecular weight, thus Cx43 has a molecular weight of 43kDa and Cx30 has that of 30kDa. Six connexin proteins form a connexon, which is a hemichannel, and when a hemichannel from one cell is aligned with another hemichannel of an adjacent cell, that is called a gap junction. Therefore, 12 connexins make up one gap junction. Of these connexins, Cx43, which is

4

predominantly astrocytic (Giaume et al., 2010; Rash et al., 2001), is one of the most studied connexin in the brain and highly expressed because astrocytes far outnumber other cell types in the brain, including neurons (Sofroniew and Vinters, 2010). Connexin 43 form a hemichannel, which form a gap junction, which has an aqueous pore and selectively permits flow of small endogenous molecules such as second messengers, amino acids, nucleotides, small peptides, and also water intercellularly between astrocytes (Giaume et al., 2010; Goodenough and Paul, 2003; Herve and Derangeon, 2012; Wallraff et al., 2006). Although various cell types such as neurons, oligodendrocytes, and endothelial cells swell after injury, astrocytes are the first cell types to swell, and the swelling lasts the longest; in fact, perivascular astrocyte endfeet can swell within minutes after injury (Grange-Messent and Bouchaud, 1994), and this swelling may spread from primary injury site to distant sites because of the astrocyte network mediated by gap junctions. This hypothesized spread of detrimental factors from the primary injury site to more distant sites mediated by gap junctions is often referred to as "bystander effect" (Andrade-Rozental et al., 2000; Cronin et al., 2008; Perez Velazquez et al., 2003). Thus, the inhibition of connexin 43 will decrease this bystander effect and lead to better recovery after jTBI. Accordingly, several studies have shown that administering gap junction inhibitors such as carbenoxolone and octanol after brain pathology resulted in beneficial outcome (Andersson et al., 2011; Frantseva et al., 2002; Perez Velazquez et al., 2006; Rawanduzy et al., 1997) . However, gap junction inhibitors are not specific for individual connexins or particular cell types and have side effects, thus unable to pinpoint the function of each connexins in a definitive manner, and difficult to transition as a clinical therapeutic (Goodenough and Paul, 2003). Furthermore,

recent studies have shown that non gap junction forming hemichannels may have specific functions as well such as extracellular signaling of ATP and glutamate under physiological and pathological conditions (Kar et al., 2012). Therefore, the usage of specific connexin inhibitors will be of paramount importance not only in learning about the physiological functions under normal and pathological conditions, but also as potential therapeutics.

T2 Weighted Imaging and Diffusion Weighted Imaging in the Assessment of Edema

Clinically, Diffusion Weighted Imaging (DWI) alongside the standard T2 weighted imaging (T2WI) is used widely as a diagnostic tool in clinical and research settings; among them to assess edematous damage after various brain pathologies from ischemic stroke to TBI (Chastain et al., 2009; Obenaus and Ashwal, 2008; Tourdias et al., 2009; Tourdias et al., 2011). The computed T2 value is believed to represent the water content within brain tissues; where increased T2 values correspond to water accumulation in pathological conditions (Obenaus and Ashwal, 2008).

DWI makes use of the characteristic property of water motion when excited by magnetic field gradients, and the rate of diffusion of water can be assessed (Bydder et al., 2001). The rate of diffusion of water is most often interpreted in a value termed the apparent diffusion coefficient (ADC). The first published data for DWI usage in the pediatric population was published in 1991 (Rutherford et al., 1991; Sakuma et al., 1991) and is now quite routinely used in pediatric neuropathologies including jTBI (Badaut et al., 2007; Galloway et al., 2008; Hou et al., 2007; Utsunomiya, 2011). In animal studies, DWI has also started to gain popularity (Badaut et al., 2007; Badaut et al., 2011a;

Bertolizio et al., 2011; Obenaus and Ashwal, 2008; Wang et al., 2007), although there are many more studies done in adults than juvenile animals. Because there are differences in brain structure and physiology between the pediatric population and adult population such as higher water content in pediatric brain, adult TBI studies should not be directly translated into the pediatric population without careful research and clinical evidence.

Despite the usage of DWI, the exact molecular mechanisms that contribute to ADC differences are still unknown. But we hypothesize that aquaporin 4 (AQP4), which has been proposed as a key player in the cerebral edema process in several brain disorders including TBI, contributes to ADC values. Because DWI detects changes observed via the excitation of protons, and water molecules are the main source of protons being detected in the brain, the presence of the water channel protein, AQP4, in astrocytes suggests a possible involvement. A decrease in the ADC is classically associated with a decrease in the extracellular space during cellular swelling after brain injury (Obenaus and Ashwal, 2008). More recently, ADC changes have been hypothesized to be linked with the level of expression of AQP4. Several experiments have shown increases in AQP4 expression and increased ADC (Tourdias et al., 2009) and decreased AQP4 expression with decreased ADC (Badaut et al., 2011a; Meng et al., 2004). Of note, Tourdias et al. (Tourdias et al., 2011) have shown in a model of acute brain pathology that AQP4 upregulation was associated with early edema formation via increased ADC and BBB disruption. With our hypothesized role of Cx43 in edema spread, we also propose that Cx43, in conjunction with AQP4 will affect ADC values.

Evidences Linking AQP4 and Cx43

So far, we have covered how AQP4 and Cx43 can play major roles in the edema process after jTBI independently. However, in order to maintain homeostasis, astrocyte proteins have to work in an intricate concerted manner. Is there a possibility that AQP4 and Cx43 have regulatory functions on each other? Interestingly, a decrease in Cx43 protein expression and a concomitant decrease in gap junction function after administration of siRNA against AQP4 in primary astrocyte culture have been reported (Nicchia et al., 2005). Additionally, brain cell cultures taken from AQP4 -/- mice have also shown lower Cx43 protein level compared to wildtype (Kong et al., 2008). And also, transgenic mice lacking Cx43 and Cx30 have decreased AQP4 levels (Ezan et al., 2012).

Small Interference RNA as a Research and Therapeutic Tool to Downregulate AQP4 and Cx43

In order to test our hypothesis that AQP4 and Cx43 played key regulatory roles in the post traumatic edema process, we needed to find a tool to specifically downregulate these astrocyte proteins post-injury. A recently discovered tool that fit this criterion was the small interference RNA molecules.

Small interference RNA (siRNA) is a short double-stranded molecule composed of about 20 nucleotide base pairs organized in corresponding sense and antisense strands. These short double-stranded molecules are produced as a result of an enzyme called Dicer (Bernstein et al., 2001; Ketting et al., 2001), which cleaves a longer double-stranded RNA present in the cell cytoplasm. These double-stranded RNA composed of both the sense and antisense strand is a necessary trigger for the generation of siRNA. This was elegantly demonstrated by Mello and Fire, when phenotypic changes were

8

observed in *C. elegans* following insertion of both the sense and antisense mRNA of a particular protein, but no changes occurred upon delivery of a single strand of either the sense or antisense strand (Fire et al., 1998; Montgomery et al., 1998). Once siRNA is made, it enters a protein complex called the RNA induced silencing complex (RISC) where Argonaut 2 cleaves the sense strand away from the antisense strand. The antisense strand remaining within RISC is now free to target complementary endogenous mRNA for subsequent cleavage by the RISC-Argonaut2-siRNA complex, thereby interfering with the translation process of that specific protein (Ketting et al., 2001). This ultimately leads to significant down-regulation of the protein normally encoded by the targeted mRNA (Figure 1).
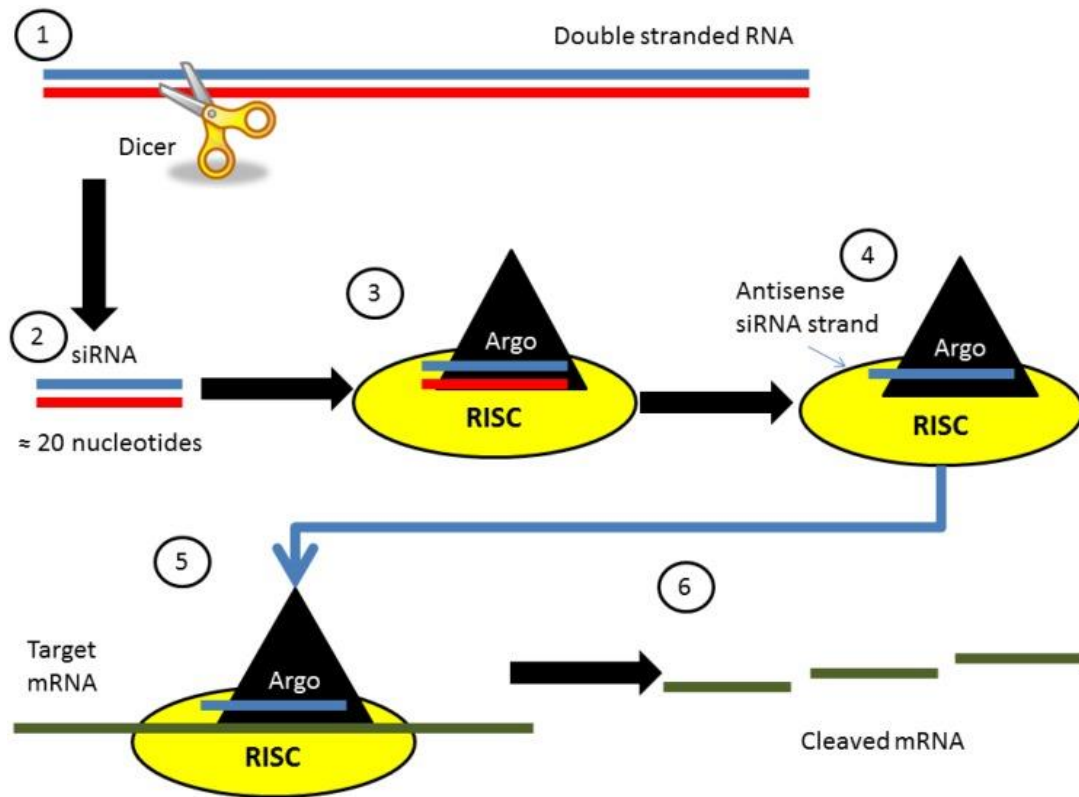
Figure 1. Basic molecular mechanism of siRNA. 1) The enzyme, dicer, cleaves a double stranded RNA in the cell cytoplasm. 2) This cleavage forms a shorter double-stranded RNA composed of both the sense and antisense strand. 3) Once siRNA is made, it enters a protein complex called the RNA induced silencing complex (RISC) where 4) Argonaut 2 cleaves the sense strand away from the antisense strand. 5) The antisense strand remaining within RISC is now free to target complementary endogenous mRNA for subsequent cleavage by the RISC-Argonaut2-siRNA complex, 6) thereby interfering with the translation process of that specific protein.

This elegant yet simple mechanism allowed the advent of numerous basic science discoveries and research advances due to the specificity and potency of the RNA interference mechanism in targeting proteins of interests. Ongoing research interests include translational approaches of this newfound mechanism into clinical practice, and using siRNA as a therapeutic agent against diseases including acute brain injuries (Fukuda and Badaut, 2013).

Small interfering RNA (siRNA) transfection offers a new exciting therapeutic possibility for brain disorders, through specific inhibition of translation of one targeted protein. siAQP4 injection in non-injured rat brains resulted in a significant decrease of water movement evaluated with magnetic resonance imaging (MRI) and the apparent diffusion coefficient (ADC) values (Badaut et al., 2011a). Importantly, *in vivo* siAQP4 injection did not produce adverse side effects or mortalities compared to naïve animals, suggesting the safety of this method for early inhibition of AQP4 expression after brain injury (Badaut et al., 2011a). Small interference RNA targeting AQP4 (siAQP4) and Cx43 (siCx43) are expected to decrease edema formation and improve outcomes after jTBI. Thus, the dissertation research's unique purpose is to determine the contribution of the astrocyte network in jTBI pathophysiology.

Previous experiments have shown that siAQP4 injection in non-injured juvenile rat brains induced a 50% decrease in water mobility as interpreted from MRI ADC values, along with a 30% reduction in AQP4 protein expression (Badaut et al., 2011a). These discrepancies between the two percentage values suggest the possible involvement of additional molecular players such as Cx43 as proposed above.

Summary

In summary, jTBI is a serious health concern with no therapeutic treatment available. Edema, which can be visualized by the usage of DWI, is an effective target to ameliorate secondary damage caused by jTBI, facilitating improved recovery. In order to accomplish this, the inhibition of the gap junction protein, Cx43, and the perivascular astrocyte endfeet water channel protein, AQP4, will be very effective.

Study Objectives

Using AQP4 and Cx43 as siRNA targets provides a unique platform to study the role of the astrocyte network in water diffusion contributing to edema formation after juvenile traumatic brain injury.

We will have three different aims split up into three chapters (Ch. 2-4) to answer our question proposed above. Aim 1 (Ch. 2) will characterize the expression of the aquaporins after our juvenile traumatic brain injury (jTBI) model, correlating these protein levels with edema. Aim 2 (Ch. 3) will explore novel therapeutic administration of siAQP4 *in vivo* after jTBI with measures on edema formation via MRI, behavior outcome, AQP4 expressions and histology of the neurovascular unit. Aim 3 (Ch. 4) is to characterize the expression of the connexins after our juvenile traumatic brain injury (jTBI) model and explore novel therapeutic administration of siCx43 *in vivo* after jTBI with measures on edema formation via MRI, behavior outcome, and Cx and GFAP expressions.

Together, these novel studies will provide new information and knowledge on astrocyte pathophysiology and contribute to the development of new therapeutic approaches for jTBI and other brain injuries associated with the edema process.

Key Novelties of the Studies

Characterization of Aquaporin and
Connexin after jTBI

Our study will be looking at the changes in the expression pattern of water channels and gap junctions after jTBI. Characterization of these proteins has not been performed in models of jTBI. We will be looking at the spatial and temporal changes of these proteins along the process of edema formation and resolution. Of particular importance to our astrocyte network hypothesis, the key astrocyte aquaporin-AQP4 and connexin-Cx43 will be our central focus in our characterization.

Usage of siRNA against AQP4 or Cx43
In Vivo in the Brain after jTBI

Small interference RNA has been gaining considerable attention and is used as both a molecular tool and a potential therapeutic agent. However, very few studies use siRNA *in vivo* in the brain under pathological and non-pathological conditions. This study will be the first to use siAQP4 and siCx43 *in vivo* after jTBI as a therapeutic agent.

Astrocyte Network as a Target to Decrease Edema

We will be the first to target key proteins of the astrocyte network as therapeutic targets after jTBI. Little is known regarding the changes in astrocyte fates after brain injuries and the contribution of the astrocyte network in edema formation and resolution. We hypothesize that the inhibition of AQP4 or Cx43 will result in edema decrease and better behavioral recovery after jTBI.

References

Andersson, H.C., Anderson, M.F., Porritt, M.J., Nodin, C., Blomstrand, F., Nilsson, M., 2011. Trauma-induced reactive gliosis is reduced after treatment with octanol and carbenoxolone. Neurol Res. 33, 614-24.

Andrade-Rozental, A.F., Rozental, R., Hopperstad, M.G., Wu, J.K., Vrionis, F.D., Spray, D.C., 2000. Gap junctions: the "kiss of death" and the "kiss of life". Brain Res Brain Res Rev. 32, 308-15.

Badaut, J., Lasbennes, F., Magistretti, P.J., Regli, L., 2002. Aquaporins in brain: distribution, physiology, and pathophysiology. J Cereb Blood Flow Metab. 22, 367-78.

Badaut, J., Ashwal, S., Tone, B., Regli, L., Tian, H.R., Obenaus, A., 2007. Temporal and regional evolution of aquaporin-4 expression and magnetic resonance imaging in a rat pup model of neonatal stroke. Pediatr Res. 62, 248-54.

Badaut, J., Ashwal, S., Adami, A., Tone, B., Recker, R., Spagnoli, D., Ternon, B., Obenaus, A., 2011a. Brain water mobility decreases after astrocytic aquaporin-4 inhibition using RNA interference. J Cereb Blood Flow Metab. 31, 819-31.

Badaut, J., Ashwal, S., Obenaus, A., 2011b. Aquaporins in cerebrovascular disease: a target for treatment of brain edema? Cerebrovasc Dis. 31, 521-31.

Bernstein, E., Caudy, A.A., Hammond, S.M., Hannon, G.J., 2001. Role for a bidentate ribonuclease in the initiation step of RNA interference. Nature. 409, 363-6.

Bertolizio, G., Bissonnette, B., Mason, L., Ashwal, S., Hartman, R., Marcantonio, S., Obenaus, A., 2011. Effects of hemodilution after traumatic brain injury in juvenile rats. Paediatr Anaesth. 21, 1198-208.

Bydder, G.M., Rutherford, M.A., Hajnal, J.V., 2001. How to perform diffusion-weighted imaging. Childs Nerv Syst. 17, 195-201.

Chastain, C.A., Oyoyo, U.E., Zipperman, M., Joo, E., Ashwal, S., Shutter, L.A., Tong, K.A., 2009. Predicting outcomes of traumatic brain injury by imaging modality and injury distribution. J Neurotrauma. 26, 1183-96.

Cronin, M., Anderson, P.N., Cook, J.E., Green, C.R., Becker, D.L., 2008. Blocking connexin43 expression reduces inflammation and improves functional recovery after spinal cord injury. Mol Cell Neurosci. 39, 152-60.

Ezan, P., Andre, P., Cisternino, S., Saubamea, B., Boulay, A.C., Doutremer, S., Thomas, M.A., Quenech'du, N., Giaume, C., Cohen-Salmon, M., 2012. Deletion of astroglial connexins weakens the blood-brain barrier. J Cereb Blood Flow Metab.

Faul, M., Xu, L., Wald, M.M., Coronado, V., 2010. Traumatic brain injury in the United States: emergency department visits, hospitalizations, and deaths, 2002–2006. . National Center for Injury Prevention and Control. Atlanta, GA: CDC.

Fire, A., Xu, S., Montgomery, M.K., Kostas, S.A., Driver, S.E., Mello, C.C., 1998. Potent and specific genetic interference by double-stranded RNA in Caenorhabditis elegans. Nature. 391, 806-11.

Frantseva, M.V., Kokarovtseva, L., Naus, C.G., Carlen, P.L., MacFabe, D., Perez Velazquez, J.L., 2002. Specific gap junctions enhance the neuronal vulnerability to brain traumatic injury. J Neurosci. 22, 644-53.

Fukuda, A.M., Badaut, J., 2012. Aquaporin 4: a player in cerebral edema and neuroinflammation. J Neuroinflammation. 9, 279.

Fukuda, A.M., Badaut, J., 2013. siRNA Treatment: "A Sword-in-the-Stone" for Acute Brain Injuries. Genes (Basel). 4, 435-56.

Galloway, N.R., Tong, K.A., Ashwal, S., Oyoyo, U., Obenaus, A., 2008. Diffusion-weighted imaging improves outcome prediction in pediatric traumatic brain injury. J Neurotrauma. 25, 1153-62.

Giaume, C., Koulakoff, A., Roux, L., Holcman, D., Rouach, N., 2010. Astroglial networks: a step further in neuroglial and gliovascular interactions. Nat Rev Neurosci. 11, 87-99.

Gonen, T., Walz, T., 2006. The structure of aquaporins. Q Rev Biophys. 39, 361-96.

Goodenough, D.A., Paul, D.L., 2003. Beyond the gap: functions of unpaired connexon channels. Nat Rev Mol Cell Biol. 4, 285-94.

Grange-Messent, V., Bouchaud, C., 1994. Effects of soman on cerebral astrocyte plasma membranes: a freeze-fracture study. Neurosci Lett. 178, 77-80.

Herve, J.C., Derangeon, M., 2012. Gap-junction-mediated cell-to-cell communication. Cell Tissue Res.

Hou, D.J., Tong, K.A., Ashwal, S., Oyoyo, U., Joo, E., Shutter, L., Obenaus, A., 2007. Diffusion-weighted magnetic resonance imaging improves outcome prediction in adult traumatic brain injury. J Neurotrauma. 24, 1558-69.

Huh, J.W., Raghupathi, R., 2009. New concepts in treatment of pediatric traumatic brain injury. Anesthesiol Clin. 27, 213-40.

Kar, R., Batra, N., Riquelme, M.A., Jiang, J.X., 2012. Biological role of connexin intercellular channels and hemichannels. Arch Biochem Biophys. 524, 2-15.

Ketting, R.F., Fischer, S.E., Bernstein, E., Sijen, T., Hannon, G.J., Plasterk, R.H., 2001. Dicer functions in RNA interference and in synthesis of small RNA involved in developmental timing in C. elegans. Genes Dev. 15, 2654-9.

Klatzo, I., 1967. Presidental address. Neuropathological aspects of brain edema. J Neuropathol Exp Neurol. 26, 1-14.

Kong, H., Fan, Y., Xie, J., Ding, J., Sha, L., Shi, X., Sun, X., Hu, G., 2008. AQP4 knockout impairs proliferation, migration and neuronal differentiation of adult neural stem cells. J Cell Sci. 121, 4029-36.

Meng, S., Qiao, M., Lin, L., Del Bigio, M.R., Tomanek, B., Tuor, U.I., 2004. Correspondence of AQP4 expression and hypoxic-ischaemic brain oedema monitored by magnetic resonance imaging in the immature and juvenile rat. Eur J Neurosci. 19, 2261-9.

Montgomery, M.K., Xu, S., Fire, A., 1998. RNA as a target of double-stranded RNA-mediated genetic interference in Caenorhabditis elegans. Proc Natl Acad Sci U S A. 95, 15502-7.

Morales, D.M., Marklund, N., Lebold, D., Thompson, H.J., Pitkanen, A., Maxwell, W.L., Longhi, L., Laurer, H., Maegele, M., Neugebauer, E., Graham, D.I., Stocchetti, N., McIntosh, T.K., 2005. Experimental models of traumatic brain injury: do we really need to build a better mousetrap? Neuroscience. 136, 971-89.

Musa-Aziz, R., Chen, L.M., Pelletier, M.F., Boron, W.F., 2009. Relative CO_2/NH_3 selectivities of AQP1, AQP4, AQP5, AmtB, and RhAG. Proc Natl Acad Sci U S A. 106, 5406-11.

Nicchia, G.P., Srinivas, M., Li, W., Brosnan, C.F., Frigeri, A., Spray, D.C., 2005. New possible roles for aquaporin-4 in astrocytes: cell cytoskeleton and functional relationship with connexin43. FASEB J. 19, 1674-6.

Obenaus, A., Ashwal, S., 2008. Magnetic resonance imaging in cerebral ischemia: focus on neonates. Neuropharmacology. 55, 271-80.

Papadopoulos, M.C., Verkman, A.S., 2007. Aquaporin-4 and brain edema. Pediatr Nephrol. 22, 778-84.

Perez Velazquez, J.L., Frantseva, M.V., Naus, C.C., 2003. Gap junctions and neuronal injury: protectants or executioners? Neuroscientist. 9, 5-9.

Perez Velazquez, J.L., Kokarovtseva, L., Sarbaziha, R., Jeyapalan, Z., Leshchenko, Y., 2006. Role of gap junctional coupling in astrocytic networks in the determination of global ischaemia-induced oxidative stress and hippocampal damage. Eur J Neurosci. 23, 1-10.

Rash, J.E., Yasumura, T., Davidson, K.G., Furman, C.S., Dudek, F.E., Nagy, J.I., 2001. Identification of cells expressing Cx43, Cx30, Cx26, Cx32 and Cx36 in gap junctions of rat brain and spinal cord. Cell Commun Adhes. 8, 315-20.

Rawanduzy, A., Hansen, A., Hansen, T.W., Nedergaard, M., 1997. Effective reduction of infarct volume by gap junction blockade in a rodent model of stroke. J Neurosurg. 87, 916-20.

Rutherford, M.A., Cowan, F.M., Manzur, A.Y., Dubowitz, L.M., Pennock, J.M., Hajnal, J.V., Young, I.R., Bydder, G.M., 1991. MR imaging of anisotropically restricted diffusion in the brain of neonates and infants. J Comput Assist Tomogr. 15, 188-98.

Sakuma, H., Nomura, Y., Takeda, K., Tagami, T., Nakagawa, T., Tamagawa, Y., Ishii, Y., Tsukamoto, T., 1991. Adult and neonatal human brain: diffusional anisotropy and myelination with diffusion-weighted MR imaging. Radiology. 180, 229-33.

Simard, J.M., Kent, T.A., Chen, M., Tarasov, K.V., Gerzanich, V., 2007. Brain oedema in focal ischaemia: molecular pathophysiology and theoretical implications. Lancet Neurol. 6, 258-68.

Sofroniew, M.V., Vinters, H.V., 2010. Astrocytes: biology and pathology. Acta Neuropathol. 119, 7-35.

Tourdias, T., Dragonu, I., Fushimi, Y., Deloire, M.S., Boiziau, C., Brochet, B., Moonen, C., Petry, K.G., Dousset, V., 2009. Aquaporin 4 correlates with apparent diffusion coefficient and hydrocephalus severity in the rat brain: a combined MRI-histological study. Neuroimage. 47, 659-66.

Tourdias, T., Mori, N., Dragonu, I., Cassagno, N., Boiziau, C., Aussudre, J., Brochet, B., Moonen, C., Petry, K.G., Dousset, V., 2011. Differential aquaporin 4 expression during edema build-up and resolution phases of brain inflammation. J Neuroinflammation. 8, 143.

Unterberg, A.W., Stover, J., Kress, B., Kiening, K.L., 2004. Edema and brain trauma. Neuroscience. 129, 1021-9.

Utsunomiya, H., 2011. Diffusion MRI abnormalities in pediatric neurological disorders. Brain Dev. 33, 235-42.

Wallraff, A., Kohling, R., Heinemann, U., Theis, M., Willecke, K., Steinhauser, C., 2006. The impact of astrocytic gap junctional coupling on potassium buffering in the hippocampus. J Neurosci. 26, 5438-47.

Wang, R., Ashwal, S., Tone, B., Tian, H.R., Badaut, J., Rasmussen, A., Obenaus, A., 2007. Albumin reduces blood-brain barrier permeability but does not alter infarct size in a rat model of neonatal stroke. Pediatr Res. 62, 261-6.

Wolff, J.R., Stuke, K., Missler, M., Tytko, H., Schwarz, P., Rohlmann, A., Chao, T.I., 1998. Autocellular coupling by gap junctions in cultured astrocytes: a new view on cellular autoregulation during process formation. Glia. 24, 121-40.

Yu, J., Yool, A.J., Schulten, K., Tajkhorshid, E., 2006. Mechanism of gating and ion conductivity of a possible tetrameric pore in aquaporin-1. Structure. 14, 1411-23.

CHAPTER TWO

DELAYED INCREASE OF ASTROCYTIC AQUAPORIN 4 AFTER JUVENILE

TRAUMATIC BRAIN INJURY: POSSIBLE ROLE IN EDEMA RESOLUTION?

By

Andrew M Fukuda, Viorela Pop, David Spagnoli, Stephen Ashwal,

André Obenaus, Jérôme Badaut

Title: Delayed increase of astrocytic aquaporin 4 after juvenile traumatic brain injury: possible role in edema resolution?

Author: Andrew M Fukuda[1], Viorela Pop[2], David Spagnoli[3,4], Stephen Ashwal[2], André Obenaus[2,3,4,5], Jérôme Badaut[1,2,]

Affiliations: Departments of Physiology[1], Pediatrics[2], Radiation Medicine[3], Biophysics and Engineering[4], Loma Linda University, Loma Linda, CA.

Department of Neuroscience[5], University of California, Riverside, CA 92521

Running Title: Astrocyte-AQP contribution after juvenile TBI

* **Corresponding Author**:

Jerome Badaut, PhD
Departments of Pediatrics, Pharmacology and Physiology
Loma Linda University School of Medicine
Coleman Pavilion, Room A1120
11175 Campus Street
Loma Linda, CA 92354 USA

Key words: Edema, Astrocyte, Aquaporin, juvenile traumatic brain injury

Highlights:

-1) Diffuse edema formation in a rodent model of juvenile traumatic brain injury

-2) Astrocytic AQP4 expression parallels the edema resolution after jTBI

-3) Neuronal AQP1 expression is increased after jTBI

-4) Long-term changes of AQP4 and AQP1 after jTBI

Conflict of Interest: none

Abstract

Traumatic brain injury (TBI) is one of the leading causes of death and disability in children and adolescents. The neuropathological sequelae that result from TBI are a complex cascade of events including edema formation, which occurs more frequently in the pediatric than the adult population. This developmental difference in the response to injury may be related to higher water content in the young brain and also to molecular mechanisms regulating water homeostasis. Aquaporins (AQPs) provide a unique opportunity to examine the mechanisms underlying water mobility, which remain poorly understood in the juvenile post-traumatic edema process. We examined the spatiotemporal expression pattern of principal brain AQPs (AQP1, 4, and 9) after juvenile TBI (jTBI) related to edema formation and resolution observed using magnetic resonance imaging (MRI).

Using a controlled cortical impact in post-natal 17 day-old rats as a model of jTBI, neuroimaging analysis showed a global decrease in water mobility (apparent diffusion coefficient, ADC) and an increase in edema (T2-values) at 1 day post-injury, which normalized by 3 days. Immunohistochemical analysis of AQP4 in perivascular astrocyte endfeet was increased in the lesion at 3 and 7 days post-injury as edema resolved. In contrast, AQP1 levels distant from the injury site were increased at 7, 30, and 60 days within septal neurons but did not correlate with changes in edema formation. Group differences were not observed for AQP9. Overall, our observations confirm that astrocytic AQP4 plays a more central role than AQP1 or AQP9 during the edema process in the young brain.

Introduction

Traumatic brain injury (TBI) has been termed a 'silent epidemic' in the United States in recent years because of its increased medical and financial burden. TBI affects about 1.7 million people annually and contributes to 30.5% of all injury-related deaths in the U.S. An important subgroup of this population are children and adolescents ranging in age from 0-14 years, of which half a million visit emergency departments for TBI (Faul M, 2010). Juvenile TBI (jTBI) is the primary cause of death and disability in children and adolescents (Schneier et al., 2006) with long-term impairments in motor and cognitive abilities, including deficits in intellectual functioning, attention, memory, language, sensorimotor, visual-spatial, and executive skills (Adelson and Kochanek, 1998, Adelson et al., 1998). Despite increases in prevalence and resulting catastrophic effects of jTBI, there are no effective pharmacological treatments.

TBI in infants and children is more frequently associated with severe brain swelling than in adults (Lang et al., 1994, Bauer and Fritz, 2004) that may affect the edema process. Two mechanisms may account for these age-related differences: (i) increased post-injury cerebral blood flow in the young, and (ii) developmental and mechanical properties of the brain and skull (Kochanek, 2006). Experimental studies suggest that post-traumatic edema in the immature brain may also be related to enhanced diffusion of excitotoxic neurotransmitters, an intensified inflammatory response (Kochanek, 2006), and higher brain water content in the young rat compared to the adult rat (Dobbing and Sands, 1981).

Developmental differences in water homeostasis between children and adults may also account for the observed greater risk of post-traumatic edema in the younger population. Aquaporins (AQPs), a family of water channel proteins, are recognized to

22

have an important role in brain water regulation (Badaut et al., 2011b). In rodents and humans, AQP4 and AQP1 show increased expression during brain development (Wen et al., 1999, Gomori et al., 2006, Hsu et al., 2011). To date, three different AQPs (AQP1, AQP4, and AQP9) have been identified *in vivo* in the brain and each are hypothesized to play different roles during normal physiological and neuropathological states (Badaut et al., 2007). For example, AQP1 in epithelial cells of the choroid plexus appears to contribute primarily to cerebrospinal fluid formation whereas the neuronal AQP1 may play a role in pain processing (Oshio et al., 2006). AQP9 in astrocytes and catecholaminergic neurons may contribute to the regulation of brain energy metabolism (Badaut, 2010). In contrast, AQP4 appears to have multiple roles including: (i) water homeostasis and edema formation (Papadopoulos et al., 2004, Badaut et al., 2011a, Badaut et al., 2011b, Lee et al., 2011); (ii) regulation of synaptic plasticity with regulation of p75NTR (Skucas et al., 2011); and (iii) modulation of neurogenesis (Zheng et al., 2010).

The intricate role of brain AQPs after injury may depend on underlying pathology and type of edema (Badaut et al., 2011b), and AQP findings in several TBI studies using adult rodents have provided conflicting results. In some reports, AQP4 expression is increased (Sun et al., 2003, Guo et al., 2006, Ding et al., 2009, Higashida et al., 2011, Tomura et al., 2011) whereas other investigators have reported decreased expression (Ke et al., 2001, Kiening et al., 2002, Zhao et al., 2005). Interestingly, more recent studies have shown both AQP1 (Tran et al., 2010, Oliva et al., 2011) and AQP9 (Ding et al., 2009, Oliva et al., 2011) increasing after injury. Notably, these previous studies were undertaken in adult rats and the majority only examined AQP4 expression for up to 48

hours, without correlations of AQP levels with edema formation and resolution via neuroimaging. In other injury models, AQP expression is observed acutely and in the long-term, such as in spinal cord injury where AQP1 (Nesic et al., 2008) and AQP4 (Nesic et al., 2010) are increased 5 and 11 months after injury.

Developmental differences in water homeostasis and AQP expression between children and adults raises the question whether AQPs play a critical role in regulating brain water content in the developing brain after TBI. To address this question, we examined edema formation and resolution using magnetic resonance imaging (MRI) in conjunction with protein levels of AQP1, 4, and 9 by immunohistochemistry and western blot in a model of jTBI.

Material and Methods

Animals

All protocols and procedures were in compliance with the U.S. Department of Health and Human Services Guide and were approved by the Institutional Animal Care and Use Committee of Loma Linda University. Briefly, juvenile male Sprague-Dawley rats (P10, Harlan, Indianapolis, IN) were housed with their dams on a 12-hour light-dark cycle schedule, at constant temperature and humidity, for seven days prior to surgery at P17. Upon weaning at seven days after surgery, the rats were housed two per cage. Animals were fed with standard lab chow and water *ad libitum*.

Juvenile Traumatic Brain Injury Model

Controlled cortical impact (CCI) was induced in 17 day old rat pups as previously described (Ajao et al., in press). Briefly, P17 juvenile rats were anesthetized with

isoflurane (Webster Veterinary Supply, Inc., Sterling, MA) and placed into a stereotaxic frame (David Kopf Instruments, USA). Following a midline skin incision over the skull, a 5mm craniotomy was performed over the right frontal-parietal cortex (Bregma: -1mm anterior-posterior and 2mm medial-lateral). CCI was induced in the jTBI group using a 3mm rounded-tip metal impactor fixed to an electromechanical actuator and centered over the exposed dura at a 20° angle to the cortical surface (Leica Microsystems Company, Richmond, IL). The CCI was delivered at a 1.5 mm depth with impact duration of 200 ms at a velocity of 6 m/s. The surgical site was sutured after recording any bleeding or herniation of cortical tissues (Ajao et al., in press). After the craniotomy, the dura was intact in all of the animals in both groups (sham and jTBI). After induction of jTBI none of the animals had bleeding and all of the animals had a similar minimal damage on the dura. Body temperature was maintained at 37°C during surgery. Following surgery, animals received one subcutaneous injection of buprenorphine (0.01mg/kg; dilution: 0.01mg/ml) for pain relief before the animals were returned to their cages.

Magnetic Resonance Imaging and Analysis

Magnetic Resonance Imaging (MRI) was performed at 1, 3, 7, and 30 days post-injury (d). Rats were lightly anesthetized using isoflurane (1.0%) and then imaged on a Bruker Avance 11.7 T MRI (Bruker Biospin, Billerica MA, 8.9 cm bore) for the 1, 3, and 7d timepoints, or on a larger bore (40 cm) 4.7T MRI (Bruker Biospin, Billerca, MA) for the 30d scan, based on the size of the animals (Badaut et al., 2011a; Ajao et al., in press). Two imaging data sets were acquired: 1) a 10 echo T2 weighted imaging (T2WI), and 2)

a diffusion weighted imaging (DWI) sequence where each sequence collected twenty coronal slices (1 mm thickness and interleaved by 1 mm). The T2 sequence had the following parameters: TR/TE = 4600 ms/10.2 ms, matrix = 128 X 128, field of view (FOV) = 3 cm, NEX = 2 and acquisition time = 20 min. The spin echo diffusion sequence parameters were TR/TE = 3000 ms/25 ms, b-values = 0.72, 1855.64 s/mm^2, matrix = 128 X 128, FOV = 3 cm, NEX = 2 and acquisition time = 25 min.

Spin-spin relaxation time (T2) and apparent diffusion coefficient (ADC) values were quantified using standardized protocols (Badaut et al., 2007). T2 relaxation rates were determined for each pixel and T2 maps generated. ADC maps were calculated using a linear two point fit. Four primary regions of interest (ROIs) within ipsi- and contralateral hemispheres (cortex and striatum) were delineated on T2WI. These ROIs were overlaid onto corresponding T2 and ADC maps and the mean, standard deviation, number of pixels, and area for each ROI were extracted. MRI analysis was performed blinded without knowledge of experimental group. Data were represented as percentage of sham values to facilitate comparison to AQP changes.

Tissue Processing

Rats were transcardially perfused with 4% paraformaldehyde (PFA) prepared in phosphate buffered saline (PBS) at 1, 3, 7, 30, and 60 d. Brains were immersed in 30% sucrose at 4°C for 48 hours and then frozen on dry ice and stored at -20°C (Badaut et al., 2004). Free-floating coronal sections were cut on a cryostat (Leica CM1850, Leica Microsystems GmbH, Wetzlar, Germany) at 15µm thickness for 1, 3, 7, and 30 d tissue, and at 50µm thickness for 60d tissue.

Immunohistochemistry

All antibody incubations were carried out in PBS (Fisher Scientific, Pittsburgh, PA) containing 0.25% Triton X-100 and 0.25% bovine serum albumin (BSA) (both from Sigma-Aldrich Co., St. Louis, MO). Briefly, after washes in PBS, sections were pre-incubated for 90 minutes in PBS with 1% BSA, and then incubated overnight at 4°C with the various primary antibodies and their respective dilutions as described in Table 1. After rinsing, sections were incubated for 90 minutes at room temperature with the secondary antibodies (Table 1). After subsequent washes in PBS for 3x10min, sections on glass slides were cover-slipped with anti-fading medium VectaShield containing DAPI (Vector, Vector laboratories, Burlingame, CA). Negative control staining where the primary antibody was omitted showed no detectable labelling, and depletion of the AQP4 antibody by an excess of the specific peptide (Chemicon International, Temecula, CA) was also carried out and gave negative results as previously observed (Ribeiro Mde et al., 2006).

Table 1. Antibodies and dilutions used in this study.

Antibody name	Company	Dilution
Anti-AQP1 (rabbit)	Millipore	1:300
Anti-AQP4 (rabbit)	Millipore	1:300
Anti-AQP4 (rabbit)	Alpha diagnostics	1:300
Anti-AQP9 (rabbit)	Alpha diagnostics	1:100
Anti-GFAP (chicken)	Millipore	1:1000
Alexa 594 goat anti-rabbit	Invitrogen	1:1000
Alexa 488 goat anti-rabbit	Invitrogen	1:1000
Alexa 568 goat anti-chicken	Invitrogen	1:1000
Alexa 488 goat anti-chicken	Invitrogen	1:1000
Alexa 488 goat anti-mouse	Invitrogen	1:1000

Immunohistochemistry Analysis

Intensity of the AQP4 immunoreactivity was quantified using the LI-COR-Odyssey analysis software as previously described (Badaut et al., 2011a). Briefly, the level of fluorescence was quantified in ROIs similar to that of MRI analysis: ipsilateral hemisphere (lesion and perilesion) and contralateral hemisphere (cortex and striatum). Values obtained for the jTBI were also normalized to the sham values of the corresponding ROIs.

Non-infrared stained tissues were observed under an epifluorescent light microscope (Olympus, BX41, Center Valley, PA USA) and pictures were obtained using Fluo-Up (Explora-Nova, La Rochelle, France) and confocal microscope (Zeiss). AQP1 and 4 immunostaining were scored using a relative scale including a combination of the intensity and pattern of staining. AQP1 was scored in the following brain structures: choroid plexus, ependymal cells of the lateral and third ventricle, and lateral septal nucleus (n=5-8 animals/region/timepoint). Scoring was given a value from 0-4 with (0) no staining seen; (1) faint staining in a few positive cells, (2) bright staining in a small area, or low intensity staining in a larger area (more positive cells), (3) bright staining in a larger area, or (4) very intense staining over a large area. AQP4 staining was scored on the tissue collected at 60d with a scale representing the distribution patterns of the protein on astrocyte endfeet along brain vessels in the ipsilateral and contralateral sides of the lesion at multiple coronal bregma levels, from 4.2mm to -5.2mm throughout the longitudinal brain axis (demonstrated in Figure 5). The regions scored for AQP4 were: dorsal frontal-parietal cortex and lateral parietal temporal cortex in the sham and jTBI (n=5-8 animals/region). The AQP4 scale was from 0-4 with (0) no perivascular staining,

(1) few scattered areas of perivascular staining at moderate brightness, (2) many areas of perivascular staining at moderate brightness, (3) several high density areas of perivascular staining at moderate brightness (4) entire region has extensive and very bright staining of AQP4 on perivascular astrocyte endfeet. No analysed regions received a score of 0, and category 4 was most often observed in anterior sections far from the injury site.
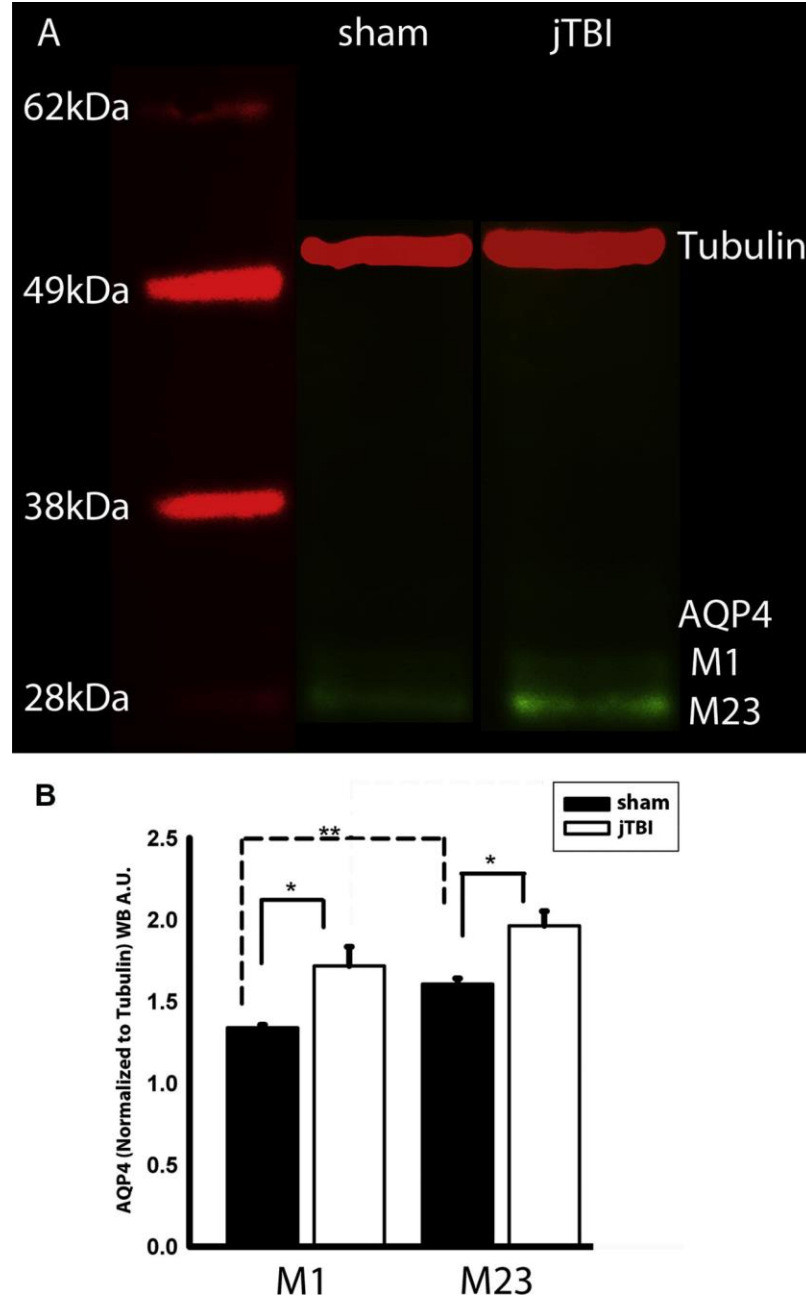
Figure 5. Aquaporin 4 Western Blot Analysis Sham vs jTBI. (A) Western blot of AQP4 at 7d shows two distinct bands of AQP4 at around 30kDa, corresponding to the M1 and M23 isoforms of AQP4. (B) jTBI shows a significantly higher expression of both M1 and M23 compared to sham. AQP4-M23 was significantly higher than the M1 in sham. (AQP4, aquaporin 4; kDa, kilo Dalton; jTBI, juvenile traumatic brain injury; *p<0.05, **p<0.01).

AQP4 Western Blot Analysis

After magnetic resonance imaging at 7d, brains from 3 animals per group were freshly dissected with collection of cortex adjacent to the site of the impact. Tissues were prepared in RIPA buffer with protease inhibitor cocktail (PIC, Roche, Basel, Switzerland) and sonicated for 30 seconds. One μg of protein was then subjected to SDS polyacrylamide gel electrophoresis on a 4-12% gel (Nupage, Invitrogen, Carlsbad, CA). Proteins were then transferred to a polyvinylidene fluoride membrane (PerkinElmer, Germany). The blot was incubated with a polyclonal antibody against AQP4 (Millipore, California, 1:2000) and a monoclonal antibody against tubulin (Sigma, Switzerland, 1:25,000) in Odyssey blocking buffer (LI-COR, Bioscience, Germany) for 2 hrs at room temperature. After washing in PBS, the filter was incubated with two fluorescence-coupled secondary antibodies (1:10,000, anti-rabbit Alexa-Fluor-680nm, Molecular Probes, Oregon and anti-mouse infra-red-Dye-800-nm, Roche, Germany) for 2 hours at room temperature. After washing in PBS, the degree of fluorescence was measured using an infra-red scanner (Odyssey, LI-COR, Germany).

Statistical Analysis

For MRI, infrared ROI, and western blot analysis, a student's t-test was performed between groups. Categorical data were assessed using a non-parametric Mann-Whitney U (M-W) test to assess group differences.

Results

Apparent Diffusion Coefficient (ADC)
and T2 Values

To address the time course of edema following TBI in our juvenile rat model, ADC and T2 values were analysed in the ipsilateral cortex including the lesion and the perilesion regions. Analysis was also performed distant from the injury site, for the contralateral cortex, ipsilateral striatum and contralateral striatum (Fig. 1). ADC and T2 values were reported relative to sham values. At 1d, ADC was significantly decreased within the lesion ($39.5 \pm 2.4\%$) and perilesion ($45.0 \pm 2.7\%$) regions compared to shams. A significant decrease in ADC values was also observed in the contralateral cortex ($41.1 \pm 9.4\%$) and striatum ($41.3 \pm 9.4\%$) (Fig 1A, B, C). ADC values normalized at 3 and 7d in all regions (Figure 1A, B, C). However, ADC became significantly elevated in the jTBI animals at 30 d within the lesion.

Parallel to the ADC changes, T2 values were significantly higher in the jTBI animals compared to shams at 1d ($44.4 \pm 3.3\%$ increase in the lesion, $47.5 \pm 6.9\%$ in the perilesion, $46.1 \pm 1.6\%$ in contralateral cortex and $46.3 \pm 3.5\%$ in the striatum). Edema remained elevated at 3d for all the regions assessed but returned to sham values at 7 and 30d (Figure 1 D, E, F).
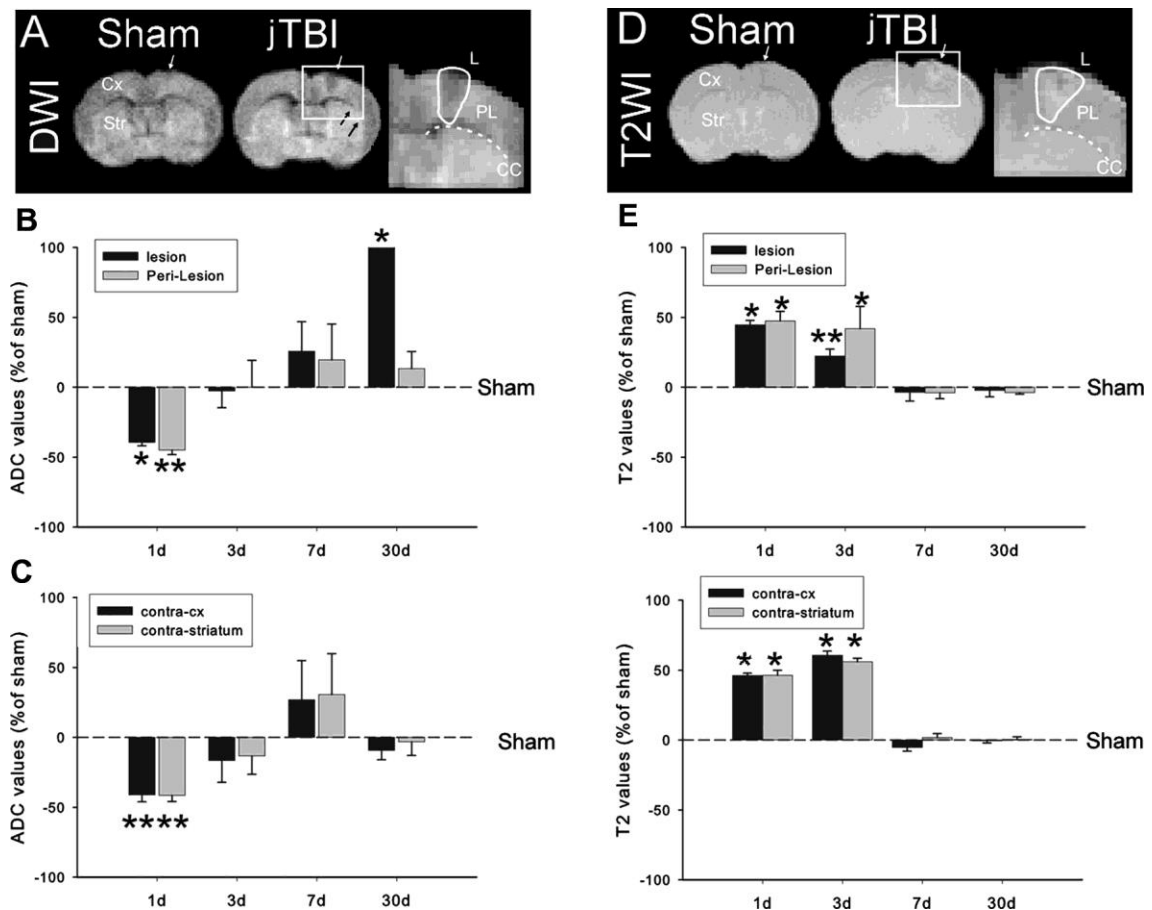
Figure 1. Changes in T2 and ADC in Sham vs jTBI. (A) DWI at 24hours after jTBI shows an increase in the size of the lesion and the perilesion compared to the sham group (B, C) Relative changes of the ADC values in the lesion and perilesion regions (B) and contralateral cortex (contra-cx) and contra-striatum show a decrease in the ADC values in all ROIs at 1d then increase at 30d in the lesion (*p<0.01). (D) T2 weighted images (T2) at 24h after jTBI show the increase of T2 signal in different brain regions compared to the sham. (E, F) Relative changes of the T2 values in the lesion and perilesion (B) and contralateral cortex (contra-cx) and contra-striatum show an increase of the T2 values in all ROIs at 1and 3d before to be normalized in all ROIs. (DWI, diffusion weighted images; jTBI, juvenile traumatic brain injury; ADC, apparent diffusion coefficient; ROI, region of interest; d, days post injury; *p<0.01).

Increase of AQP1 Expression in
Neurons after jTBI

To address the contribution of AQPs following jTBI, we first evaluated AQP1 levels by immunohistochemistry. AQP1 staining was predominantly observed in the apical membrane of the choroid plexus at similar levels between jTBI and sham groups (Figure 2 A and B). The absence of differences between groups may be due to the relatively large distance between the choroid plexus and the site of the impact, which is approximately 2mm.

A few AQP1 positive neurons were observed in the ipsilateral and contralateral parietal cortex in sham and jTBI rat pups at each time point as reported previously (Ribeiro Mde et al., 2006). No overt differences of the AQP1 staining were observed in the cortical and striatal regions where ADC and T2 values were changed. However, a striking increase in AQP1 staining was observed in jTBI rat pups after 7d, specifically in the neuronal dendrites in the dorso-lateral septal nucleus, just below the medial corpus callosum (Figure 2C-E). While quantification based on the intensity and pattern of the AQP1 staining at 1 and 3 d showed no significant differences, jTBI animals exhibited a significant increase at 7, 30, and 60 d ($p<0.001$) with greater staining intensity on several neuronal processes compared to sham (Figure 2). The changes in AQP1 expression starting at 7d strongly suggested that the changes in neuronal AQP1 expression may not be directly related to edema formation and resolution as observed in MRI.
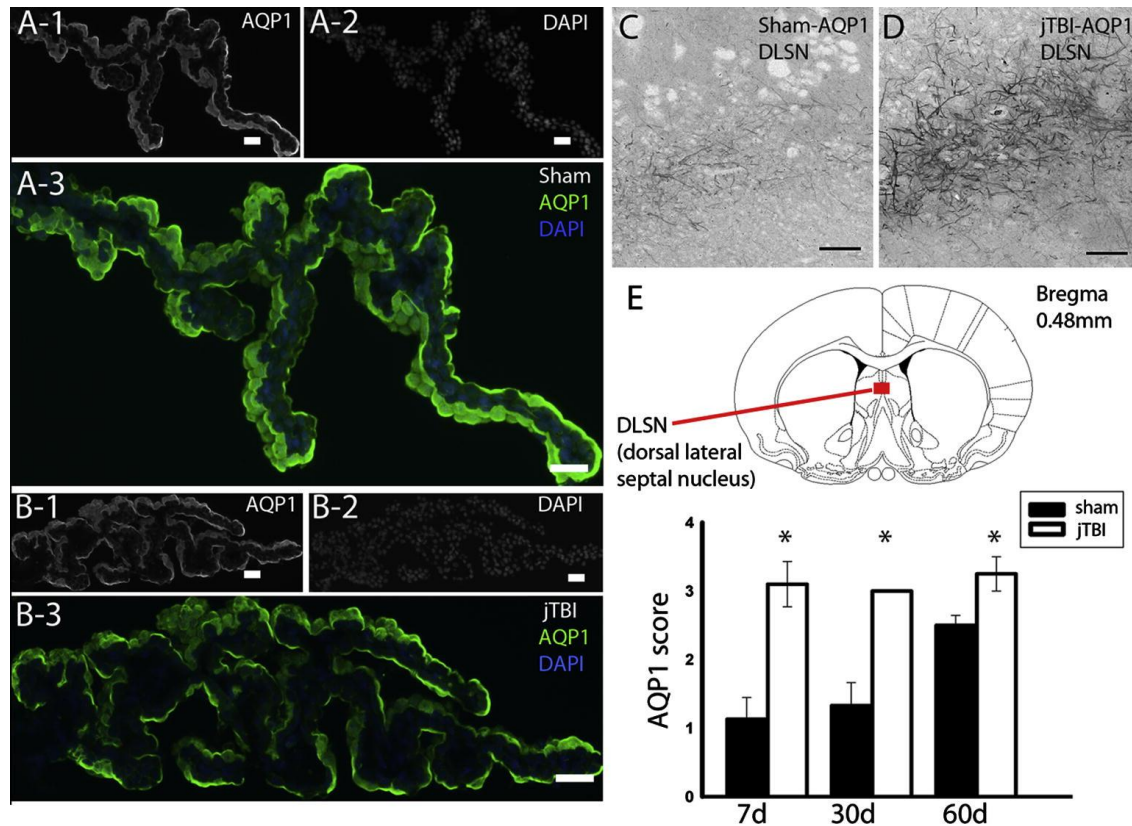
Figure 2. Aquaporin 1 Changes Sham vs jTBI. (A) AQP1 staining in the choroid plexus of sham and (B) jTBI shows no difference in intensity or pattern of staining. (C) AQP1 staining in the dorso-lateral septal nucleus of sham compared to that of (D) jTBI shows a (E) significant increase in staining in the jTBI animals at 7d, 28d, and 60d.
(AQP1, aquaporin1; jTBI, juvenile traumatic brain injury; DLSN, dorsal lateral sepal nucleus; d, days post injury; scale bar = 100 μm, *p<0.01).

AQP4 Expression in Astrocytes

We determined the evolution of AQP4 immunoreactivity (IR) using infra-red labelling over several post-injury timepoints and compared our results with MRI detection. Our data indicate several changes over time in the areas ipsilateral to the lesion (Figure 3) and on the contralateral side (Figure 4). Quantification of AQP4-IR using infra-red labeling (Figure 3C, 4C) was confirmed at higher magnification with classical immunostaining (Figure 3B, 4B). The intensity of the AQP4-IR using infra-red labelling was not significantly changed within the ipsilateral lesion and perilesional cortex between jTBI and sham animals at 1d (Figure 3). However, AQP4-IR was significantly decreased in the contralateral striatum in jTBI compared to sham animals, but not in the contralateral cortex at 1d (Figure 4). When ADC values and T2 values normalized (Figure 1), AQP4-IR significantly increased within the lesion at 3 and 7d (Figure 3). No differences were observed in AQP4 staining at 3 and 7 d in the contralateral cortex or striatum (Figure 4). AQP4-IR normalized at 30 d in all regions (Figure 3C, 4C).
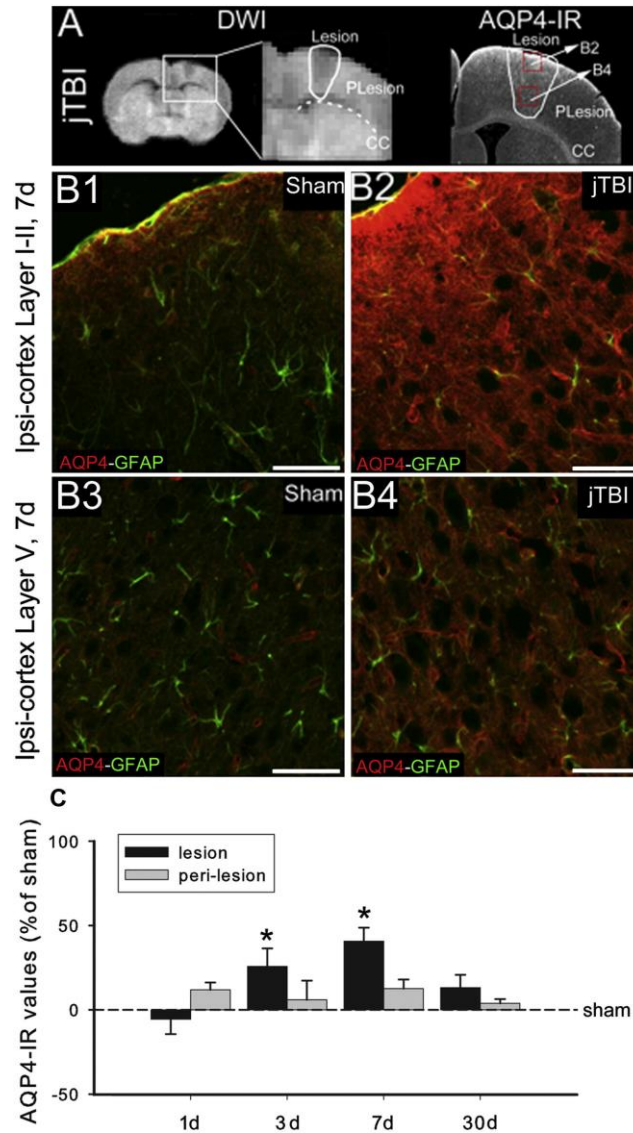
Figure 3. Aquaporin 4 Changes Ipsilateral Sham vs jTBI. (A) DWI, (A left) and AQP4 immunoreactivity (A, right) at 7d after jTBI show the location of the lesion and perilesion ROIs used for the analysis and the location of the pictures, B2 and B4 in the red boxes. (B1, B2, B3, B4) AQP4 (red) and GFAP (green) staining in the lesion area of the ipsilateral cortex near the surface in cortical layers I-II (B1, B2) and at the layer V (B3, B4) shows an increase of the AQP4 staining intensity at the glia limitans of jTBI (B2) compared to the shams (B1) and in the intracortical astrocytes in jTBI (B4) compared to sham (B3). (Scale bar = 100 μm.). (C) AQP4 staining quantification was performed in the ROIs (lesion, perilesion, contralaral cortex and striatum, see figure 4). AQP4 immunoreactivity shows a significant increase of the in the lesion and perilesion at 3 and 7d (*p<0.05). (DWI, diffusion weighted imaging; AQP4, aquaporin 4; d, days post injury; jTBI, juvenile traumatic brain injury; ROIs, regions of interest; GFAP, glial fibrillary acidic protein).
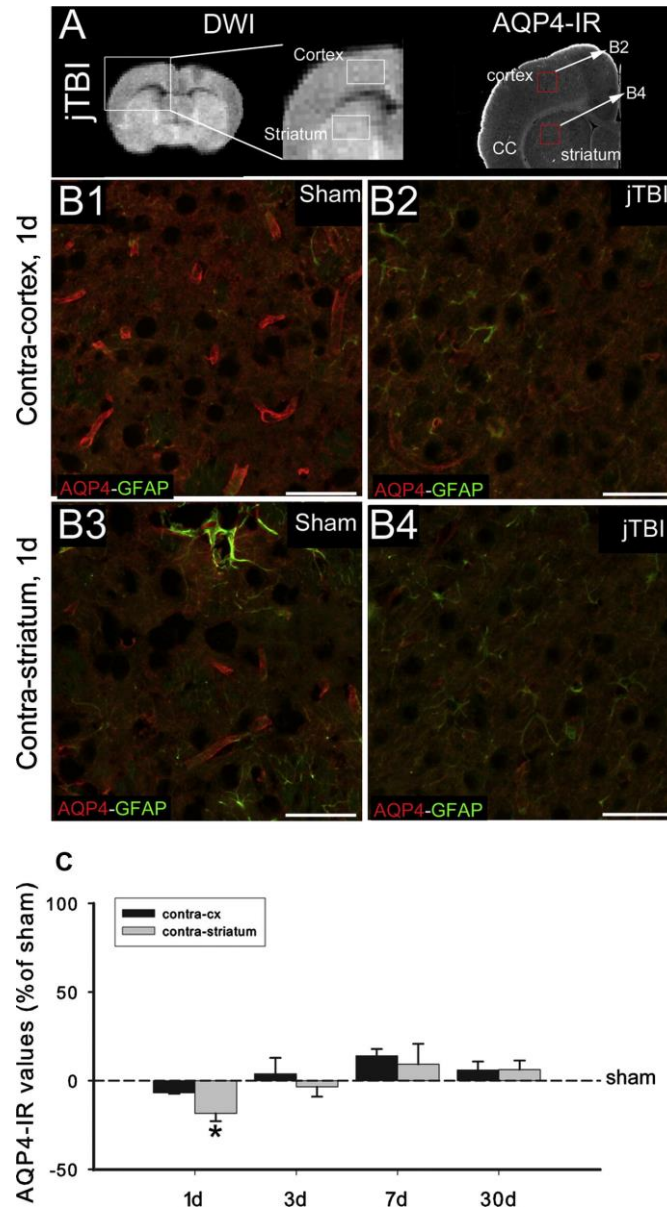
Figure 4. Aquaporin 4 Changes Contralateral Sham vs jTBI. (A) DWI (left) and AQP4 immunoreactivity (right) at 1d after jTBI show the location of the contralateral cortex and striatum ROIs used for the analysis as well as the location of the pictures B2 and B4 in the red boxes. (B1, B2, B3, B4) AQP4 (red) and GFAP (green) staining in the contra-cortex (B1, B2) and contra-striatum (B3, B4) show a decrease of the perivascular AQP4 staining in contra-cortex and contra-striatum of jTBI rats (B2, B4) compared to sham (B1, B3). Scale bar = 100 μm. (C) AQP4 staining quantification shows a significant decrease of the AQP4 staining in the contra-striatum at 1d (*p<0.05). (DWI, diffusion weighted imaging; AQP4, aquaporin 4; d, days post injury; jTBI, juvenile traumatic brain injury; ROIs, regions of interest; GFAP, glial fibrillary acidic protein).

More specifically, the higher magnification images show decreased AQP4 labeling on the astrocyte endfeet in contact with blood vessels in the contralateral striatum of jTBI compared to the sham rats at 1d (Figure 4B). At 3 and 7d, the increased AQP4 IR was not only on astrocyte endfeet but also on astrocyte processes and in the glia limitans (Figure 3B). The increase in immunoreactivity of AQP4-IR at 7 d was confirmed by western blot (Figure 5). We observed a significant increase in both isoforms of AQP4 (M23, M1) in jTBI compared to sham animals (Figure 5A). While the ratio of M23 to M1 did not differ between groups, the level of M23 expression was significantly higher than M1 expression in both sham and jTBI animals (Figure 5B).

At 60d, infra-red analysis showed no overall differences between groups; however, at higher magnification, AQP4 immunoreactivity revealed differences in the pattern of the staining (Figure 6). The density and distribution of AQP4 staining was categorized as Types 0-4 (see Methods and Figure 6C-F). Specifically, jTBI animals exhibited a scattered pattern of AQP4 immunostaining on the perivascular astrocyte endfeet in the dorsal parietal cortex region surrounding the lesion cavity at bregma -0.4, -1.4, -2.6 ($p < 0.05$) (Figure 6G) at 60d. No changes were observed between sham and jTBI groups in the dorsal frontal cortex region at more anterior bregma levels (data not shown). Notably, the areas of reduced AQP4-staining correspond to the coronal slices with a visible lesion cavity at 60d. As expected, high AQP4-IR was observed in the glial scar immediately surrounding the lesional cavity in jTBI animals at 60d (Figure 6B).
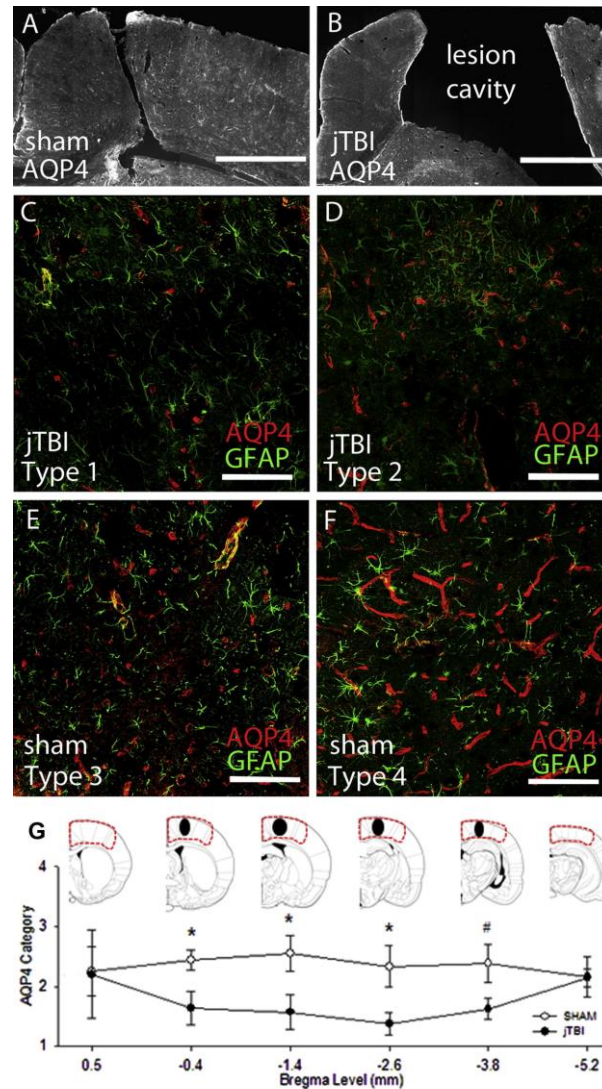
Figure 6. Aquaporin 4 60 days Sham vs jTBI. (A) A mosaic 10X image of representative Sham with AQP4 in perilesional cortex near Bregma level -2.6mm. (B) A mosaic 10X image of representative Sham with AQP4 in perilesional cortex near Bregma level -2.6mm. (bars in A, B= 500 μm) (C-F) Representative images from the parietal cortex showing four immunostaining patterns on astrocyte endfeet resting on micro- and macro-vessels. AQP4 was scored according to positive perivascular staining patterns as either Type 1, Type 2, Type 3, or Type 4. (bars in C-F = 100 μm) (G) Approximated drawing of the lesion size and location in jTBI animals at 60d (black ovals) located in the somatosensory cortex and spans a few coronal levels. Categorical AQP4 scores were assigned to the outlined area at each of the 6 coronal levels depicted. Different staining pattern of AQP4 protein expression was found in the ipsilateral dorsal cortex of jTBI nearest to the lesion cavity at Bregma -0.4mm, -1.4mm, -2.6mm, and a trend of smaller decrease more posteriorly at -3.8mm. (AQP4, aquaporin 4; jTBI, juvenile traumatic brain injury; d, days post injury; * $p < 0.05$, # $p < 0.06$).

41

Taken together, these data suggest that the delayed increase in AQP4 expression at 7 d is possibly related to the edema resolution (Figure 8) during the first week post-injury. However, by 60d when post-traumatic edema is no longer present, changes in AQP4 distribution may reflect other pathophysiological changes occurring near the lesion site and at distance from the impact (Ajao et al., in press).
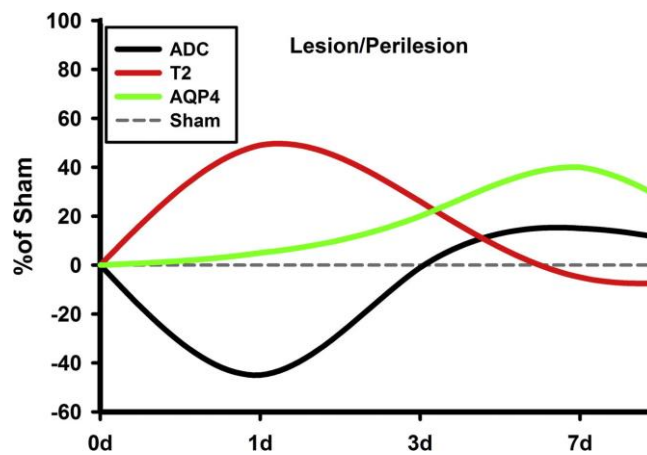
Figure 8. Summary Schematic of the Relative Changes in ADC, T2, and AQP4 after jTBI. Summary Schematic of the Relative Changes in ADC, T2, and AQP4 at the region encompassing the site of impact: The values are normalized to the sham values, which is set at 0%. Notice the initial decrease of ADC and increase of T2, accompanied by a gradual increase in AQP4 values. As AQP4 increases, T2 and ADC start to normalize, signifying a possible resolution of edema. (AQP4, aquaporin 4; d, days post injury; ADC, apparent diffusion coefficient).

Absence of Astrocytic AQP9 Changes after jTBI

Due to the involvement of several AQPs post-injury (Ribeiro Mde et al. 2006), we also evaluated the pattern of AQP9 in our model. AQP9 staining was observed in astrocytes of the corpus callosum (CC) and other white matter tracts such as the lateral olfactory tract (LOT) (Figure 7), in the astrocytes of the subfornical organs, tanycytes and ependymal cells as previously reported (Badaut et al., 2004). No significant differences in AQP9 staining were observed between the sham and jTBI animals at any time points.
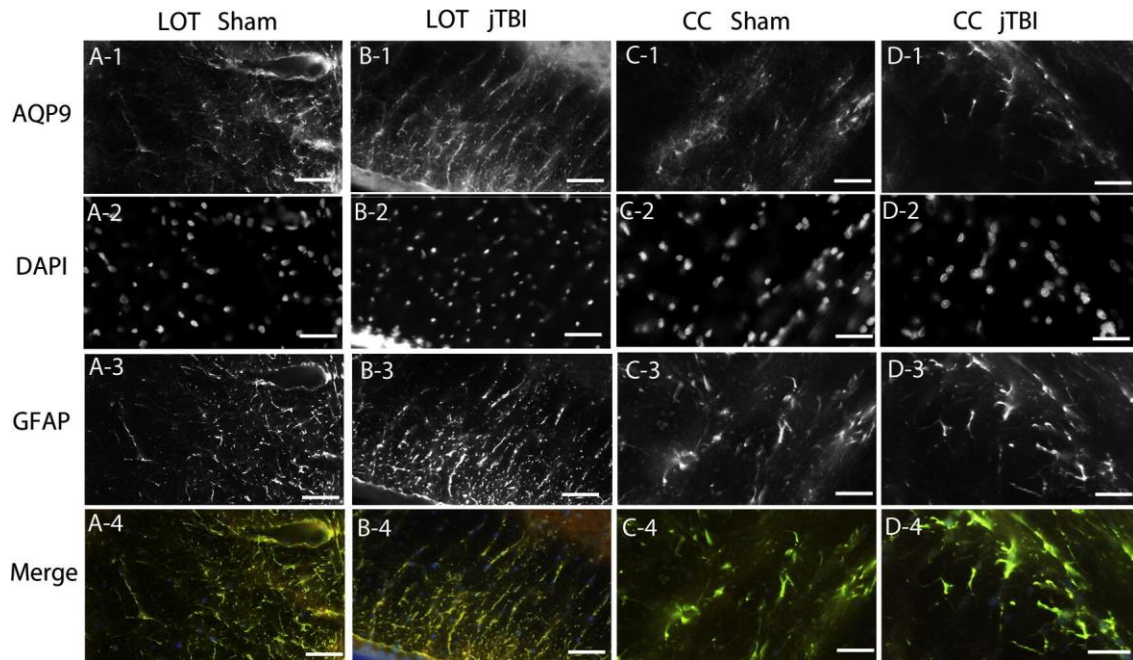
Figure 7. Aquaporin 9 Sham vs jTBI. AQP9 showed no significant differences in intensity of staining or pattern of staining between sham and jTBI at any of the studied time points. (A1-A4) AQP9 staining of sham colocalized with DAPI and GFAP in the lateral olfactory tract. (B1-B4) AQP9 staining of jTBI colocalized with DAPI and GFAP in the lateral olfactory tract. (C1-C4) AQP9 staining of sham colocalized with DAPI and GFAP in the corpus callosum. (D1-D4) AQP9 staining of jTBI colocalized with DAPi and GFAP in the corpus callosum. (AQP9, aquaporin 9; GFAP, glial acidic fibrillary protein; jTBI, juvenile traumatic brain injury; LOT, lateral olfactory tract; CC, corpus callosum; scale bar = 100 μm).

Discussion

Our data suggest that AQP4 plays a significant and more important role than AQP1 and AQP9 in regulating edema in the immature brain during the first week after jTBI. Similar to clinical observations, we observed a diffuse increase of brain water content and decrease of water mobility from regions close to, and far from, the lesion site in both hemispheres at 1 and 3d post-injury. By 7d, MRI values normalized in parallel with increases in AQP4 immunoreactivity, a pattern similar to stroke models (Ribeiro Mde et al., 2006, Badaut et al., 2007). At a distance from the lesion and primary sites of edema, we observed consistently higher AQP1 staining at 7, 30, and 60 d in neuronal filaments in the dorsolateral septum, thus highlighting the functional consequences of neuronal AQP1.

Clinically, diffusion weighted imaging (DWI) and T2 weighted imaging (T2WI) are useful modalities in the assessment of injury severity and outcome, particularly for edema formation and resolution (Obenaus and Ashwal, 2008, Chastain et al., 2009, Badaut et al., 2011b). At 1d, we observed bilateral increases in water content (higher T2) and decreases in water mobility, as shown by lower ADC values (Figure. 1). It is known that widespread edema at sites distant from the original impact are more common in juvenile than adult patients. These changes may be associated with differential susceptibility to blood-brain barrier (BBB) breakdown and cellular swelling following TBI (Pop and Badaut, 2011). Later, our ADC values returned to sham values by 3d but then increased by 30d, while T2 values normalized by 7d and remained stable. However, the pattern of acute ADC changes described in our study was not observed in a previously published paper using a rat jTBI model (Bertolizio et al., 2011). This discrepancy could be due to a difference in the magnet used for the MRI (11.7 T in our

study vs 4.7T) and also to the definition of the ROI used for analysis (Bertolizio et al., 2011). In fact, few publications address both ADC and T2 changes in rodent jTBI. Comparable ADC and T2 changes to our animals were described in focal (Badaut et al., 2007) and global (Meng et al., 2004) rat pup models of hypoxia-ischemia. Overall, the patterns in our ADC and T2 data suggest that edema formation in the immature brain may have cytotoxic and vasogenic components at different post-injury timepoints.

AQPs have been proposed to account for MRI changes reflecting edema formation/resolution in several rodent models of brain injury (Meng et al., 2004, Tourdias et al., 2009, Badaut et al., 2011a, Badaut et al., 2011b, Tourdias et al., 2011). Here, we provided an extensive evaluation of several AQPs at multiple timepoints after jTBI, to address distinctive profiles during the post-traumatic period in the immature brain. At 1d, we observed stable levels of AQP4 near the lesion and decreased AQP4 in the contralateral striatum, in spite of MRI changes occurring bilaterally throughout the brain hemispheres. One explanation may be that stable AQP4 levels adjacent to the site of impact may contribute to water entry leading to cellular swelling (lower ADC) and increased edema (increased T2). At a distance, ADC changes may reflect cellular swelling secondary to reduced AQP4 (Figure 4), associated with transient water accumulation. Other models of normal or pathological brain show concomitant decreases in AQP4 expression and ADC (Meng et al., 2004, Badaut et al., 2011a), or increased AQP4 and ADC in hydrocephalus and inflammation models (Tourdias et al., 2009). Notably, a 30% decrease in AQP4 expression using small interference RNA led to a 50% decrease in ADC values in normal rats (Badaut et al., 2011a). However, in neonatal stroke models (Badaut et al., 2007) and neuroinflammation in adult rats (Tourdias et al.,

2011), decreased ADCs did not correlate with AQP4 at 1d, similar to the discrepancies in our model. These global changes and heterogeneity of AQP4 expression underlie the complexity of molecular changes behind the fluctuations in water content and mobility during the edema process after jTBI.

Evidently, AQP4 may not be solely responsible for changes in water mobility associated with edema development after jTBI, suggesting the participation of other channel proteins. Two likely candidates are the gap junction protein Connexin-43 (Cx43) and inwardly rectifying potassium channel 4.1 (Kir4.1). Cx43 is down-regulated after silencing RNA against AQP4 in primary astrocyte cultures (Nicchia et al., 2005), while Kir4.1 co-localizes with AQP4 in astrocytic endfeet (Nagelhus et al., 2004). In addition, cellular potassium reuptake is impaired in an AQP4 knock-out epilepsy model (Binder et al., 2006) and potassium has been linked with water flux during astrocytic swelling (Dibaj et al., 2007). It is possible that AQP4, Cx43, and Kir 4.1 may be working in concert to address brain edema following jTBI.

Edema is a complex molecular process as shown in previous studies examining post-TBI AQP expression in adult TBI models. Reports of increased AQP4 (Sun et al., 2003, Guo et al., 2006, Ding et al., 2009, Higashida et al., 2011, Tomura et al., 2011) versus decreased AQP4 (Ke et al., 2001, Kiening et al., 2002, Zhao et al., 2005) are likely due to differences in injury type, rodent strains, and age at impact. We expect our juvenile cortical impact in P17 rats to differ from observations in adult animals, especially as early brain trauma may interfere with developmental phases and the evolution and mechanisms of injury. We observed increases in AQP4 at 3 and 7d near the lesion site in perivascular astrocyte endfeet, astrocyte processes, and the glia limitans.

48

These changes may indicate that excess AQP4 could facilitate edematous fluid

elimination through the subarachnoid space (Papadopoulos and Verkman, 2007, Tait et

al., 2010, Tourdias et al., 2011). For example, increased AQP4 in the glia limitans may

compensate for water accumulation at 1 and 3d (higher T2), with a gradual increase of

AQP4 at 3d and normalization of both AQP and T2 values by 7d. This increase of AQP4

at 3 and 7d also parallels the restoration of the BBB with decreased IgG extravasation at

3d and no disruption by 7d (Pop and Badaut, 2011). Although AQP4 improves water

removal, it can also regulate the initial formation of edema (based on increased T2 values

at 1d) as previously proposed (Papadopoulos and Verkman, 2007, Tait et al., 2010).

Thus, inhibiting AQP4 immediately after juvenile injury could be beneficial for edema

reduction as shown in several other injury models (Manley et al., 2000, Papadopoulos

and Verkman, 2005, Saadoun et al., 2008, Badaut et al., 2011b, Higashida et al., 2011,

Igarashi et al., 2011).

Disproportionate levels of AQP4 isoforms and their ratios may interfere with the

protein's function, due to incorrect formation of the orthogonal array of particles, as

described in stroke models (Badaut et al., 2011b). Moreover, although there is no general

consensus and it remains controversial *in vivo*, some data show that the M1 isoform may

have a higher water permeability than the M23 isoform (Fenton et al., 2010). This

difference in water permeability may account for significant increases in the M1 isoform

alone during stroke-related edema (Hirt et al., 2009). In our model, we detected higher

protein levels of both isoforms on the impacted side compared to sham animals (Figure

5), higher levels of M23 than M1 in both groups, and no changes in isoform ratios.

Together, these data suggest that the individual orthogonal array of particle arrangement

may be similar between sham and jTBI by 7d, when the majority of edema and BBB disruption processes are nearly resolved.

We provide an evaluation at delayed post-injury timepoints, in contrast to reports in the adult literature focusing on the acute phase. Although AQP4-IR intensity was similar at 60d between groups, the pattern of AQP4 staining was different in jTBI animals. Notably, fewer scattered areas of perivascular AQP4 staining were observed in the parietal cortex near the lesion site in jTBI compared to sham by 60d. Long-term changes of AQP4 have been observed in other models such as spinal cord injury (Nesic et al., 2010), mouse models of Alzheimer disease (Wilcock et al., 2009, Yang et al., 2011), and Alzheimer disease patients (Wilcock et al., 2009, Moftakhar et al., 2010). These findings strengthen the concept that AQP4 may have additional roles that are not edema-related after certain injuries, such as cell migration (Saadoun et al., 2005, Auguste et al., 2007). In human and rat models of spinal cord injury, the ratio of GFAP to AQP4 in astrocytes around the lesion depend on both the time after injury as well as the severity of injury (Nesic et al., 2010). Thus, it is possible that the gliovascular unit as a whole is chronically affected. Further long-term studies of the gliovascular unit after jTBI should evaluate phenotypic changes in astrocytic networks in microvascular trees and functional correlations of those changes.

A few TBI studies describe increases in neuronal AQP1 (Tran et al., 2010, Oliva et al., 2011) and AQP9 (Ding et al., 2009, Oliva et al., 2011) after injury in adults. In our jTBI model, AQP1 expression in the choroid plexus did not differ between sham and jTBI at any time points. However, we found more intense AQP1 staining in neuronal filaments in the dorsolateral septum in jTBI animals at 7, 30, and 60 d. Neuronal septal

tracts are involved in a number of cognitive pathways including learning, memory, sexual behavior, positive reinforcement, and pain (Gallagher et al., 1995, Singewald et al., 2011). Although consensus has not been established concerning the role of AQP1 in pain processing (Borsani, 2010), AQP1 knock-out mice had reduced pain responses versus wild-types (Oshio, 2006). TBI patients also report varying degrees of acute and chronic pain post-injury (Borsook, 2011; Nampiaparampil, 2008). Thus, septal increases in AQP1 and their influence on pain processing may be further elucidated in this jTBI model, by using appropriate nociceptive testing paradigms.

AQPs likely contribute to the evolution of several nervous system disorders, and can serve as potential therapeutic targets to improve clinical outcomes post-injury. Long-term changes in AQP4 and AQP1 after jTBI highlight differences in the edema process occurring during a developmental period. Notably, edema can have different timelines for resolution in the young versus adult brain. Our data also confirm the importance of optimal timing for the administration of therapeutic agents targeting AQPs. While AQP therapies have been previously suggested for different pathologies such as stroke (Badaut et al., 2011b), optimal results can only be achieved when accounting for injury-specific parameters. It is important to consider age at injury (e.g. adult versus juvenile), type of injury model (e.g. cortical impact, fluid percussion, weight drop, craniotomy versus closed-head), and post-injury evaluation timepoints. Finally, no single model (e.g. TBI or stroke) can define the whole spectrum of a given pathology (e.g. edema) over time. Therefore, observational studies at multiple timepoints are valuable and necessary to adequately characterize post-injury sequelae, towards a comprehensive understanding of differential expression patterns of proteins involved in pathophysiological events. To

determine the exact contribution of AQP4 on edema formation and resolution in parallel with our observations, it will be necessary to pursue a more functional study directed towards blocking or increasing AQP4 expression.

LIST OF ABBREVIATIONS: jTBI (juvenile traumatic brain injury), TBI (traumatic brain injury), AQP (aquaporin), d (days post injury), CCI (controlled cortical impact), DWI (Diffusion Weighted Imaging), T2 weighted imaging (T2WI), ADC (Apparent Diffusion Coefficient), MRI (Magnetic Resonance Imaging), ROI (Region of Interest), GFAP (Glial Fibrillary Acidic Protein), LOT (lateral olfactory tract), CC (corpus callosum)

Author's Contributions

AF, AO, DS, JB and VP: generated the data, the analysis, and writing;

experimental design and writing, AO, JB, SA

References

Adelson PD, Kochanek PM (1998) Head injury in children. J Child Neurol 13:2-15.

Adelson PD, Nemoto E, Colak A, Painter M (1998) The use of near infrared spectroscopy (NIRS) in children after traumatic brain injury: a preliminary report. Acta Neurochir Suppl 71:250-254.

Auguste KI, Jin S, Uchida K, Yan D, Manley GT, Papadopoulos MC, Verkman AS (2007) Greatly impaired migration of implanted aquaporin-4-deficient astroglial cells in mouse brain toward a site of injury. FASEB J 21:108-116.

Badaut J (2010) Aquaglyceroporin 9 in brain pathologies. Neuroscience 168:1047-1057.

Badaut J, Ashwal S, Adami A, Tone B, Recker R, Spagnoli D, Ternon B, Obenaus A (2011a) Brain water mobility decreases after astrocytic aquaporin-4 inhibition using RNA interference. J Cereb Blood Flow Metab 31:819-831.

Badaut J, Ashwal S, Obenaus A (2011b) Aquaporins in cerebrovascular disease: a target for treatment of brain edema? Cerebrovasc Dis 31:521-531.

Badaut J, Ashwal S, Tone B, Regli L, Tian HR, Obenaus A (2007) Temporal and regional evolution of aquaporin-4 expression and magnetic resonance imaging in a rat pup model of neonatal stroke. Pediatr Res 62:248-254.

Badaut J, Petit JM, Brunet JF, Magistretti PJ, Charriaut-Marlangue C, Regli L (2004) Distribution of Aquaporin 9 in the adult rat brain: preferential expression in catecholaminergic neurons and in glial cells. Neuroscience 128:27-38.

Bauer R, Fritz H (2004) Pathophysiology of traumatic injury in the developing brain: an introduction and short update. Exp Toxicol Pathol 56:65-73.

Bertolizio G, Bissonnette B, Mason L, Ashwal S, Hartman R, Marcantonio S, Obenaus A (2011) Effects of hemodilution after traumatic brain injury in juvenile rats. Paediatr Anaesth 21:1198-1208.

Binder DK, Yao X, Zador Z, Sick TJ, Verkman AS, Manley GT (2006) Increased seizure duration and slowed potassium kinetics in mice lacking aquaporin-4 water channels. Glia 53:631-636.

Chastain CA, Oyoyo UE, Zipperman M, Joo E, Ashwal S, Shutter LA, Tong KA (2009) Predicting outcomes of traumatic brain injury by imaging modality and injury distribution. J Neurotrauma 26:1183-1196.

Dibaj P, Kaiser M, Hirrlinger J, Kirchhoff F, Neusch C (2007) Kir4.1 channels regulate swelling of astroglial processes in experimental spinal cord edema. J Neurochem 103:2620-2628.

Ding JY, Kreipke CW, Speirs SL, Schafer P, Schafer S, Rafols JA (2009) Hypoxia-inducible factor-1alpha signaling in aquaporin upregulation after traumatic brain injury. Neurosci Lett 453:68-72.

Dobbing J, Sands J (1981) Vulnerability of developing brain not explained by cell number/cell size hypothesis. Early Hum Dev 5:227-231.

Faul M XL, Wald MM, Coronado VG (2010) Traumatic brain injury in the United States: emergency department visits, hospitalizations and deaths 2002-2006.: Atlanta (GA): Centers for Disease Control and Prevention, National center for Injury Prevention and Control.

Fenton RA, Moeller HB, Zelenina M, Snaebjornsson MT, Holen T, MacAulay N (2010) Differential water permeability and regulation of three aquaporin 4 isoforms. Cell Mol Life Sci 67:829-840.

Gallagher JP, Zheng F, Hasuo H, Shinnick-Gallagher P (1995) Activities of neurons within the rat dorsolateral septal nucleus (DLSN). Prog Neurobiol 45:373-395.

Gomori E, Pal J, Abraham H, Vajda Z, Sulyok E, Seress L, Doczi T (2006) Fetal development of membrane water channel proteins aquaporin-1 and aquaporin-4 in the human brain. Int J Dev Neurosci 24:295-305.

Guo Q, Sayeed I, Baronne LM, Hoffman SW, Guennoun R, Stein DG (2006) Progesterone administration modulates AQP4 expression and edema after traumatic brain injury in male rats. Exp Neurol 198:469-478.

Higashida T, Kreipke CW, Rafols JA, Peng C, Schafer S, Schafer P, Ding JY, Dornbos D, 3rd, Li X, Guthikonda M, Rossi NF, Ding Y (2011) The role of hypoxia-inducible factor-1alpha, aquaporin-4, and matrix metalloproteinase-9 in blood-brain barrier disruption and brain edema after traumatic brain injury. J Neurosurg 114:92-101.

Hirt L, Ternon B, Price M, Mastour N, Brunet JF, Badaut J (2009) Protective role of early aquaporin 4 induction against postischemic edema formation. J Cereb Blood Flow Metab 29:423-433.

Hsu MS, Seldin M, Lee DJ, Seifert G, Steinhauser C, Binder DK (2011) Laminar-specific and developmental expression of aquaporin-4 in the mouse hippocampus. Neuroscience 178:21-32.

Igarashi H, Huber VJ, Tsujita M, Nakada T (2011) Pretreatment with a novel aquaporin 4 inhibitor, TGN-020, significantly reduces ischemic cerebral edema. Neurol Sci 32:113-116.

Ke C, Poon WS, Ng HK, Pang JC, Chan Y (2001) Heterogeneous responses of aquaporin-4 in oedema formation in a replicated severe traumatic brain injury model in rats. Neurosci Lett 301:21-24.

Kiening KL, van Landeghem FK, Schreiber S, Thomale UW, von Deimling A, Unterberg AW, Stover JF (2002) Decreased hemispheric Aquaporin-4 is linked to evolving brain edema following controlled cortical impact injury in rats. Neurosci Lett 324:105-108.

Kochanek PM (2006) Pediatric traumatic brain injury: quo vadis? Dev Neurosci 28:244-255.

Lang DA, Teasdale GM, Macpherson P, Lawrence A (1994) Diffuse brain swelling after head injury: more often malignant in adults than children? J Neurosurg 80:675-680.

Lee DJ, Amini M, Hamamura MJ, Hsu MS, Seldin MM, Nalcioglu O, Binder DK (2011) Aquaporin-4-dependent edema clearance following status epilepticus. Epilepsy Res.

Manley GT, Fujimura M, Ma T, Noshita N, Filiz F, Bollen AW, Chan P, Verkman AS (2000) Aquaporin-4 deletion in mice reduces brain edema after acute water intoxication and ischemic stroke. Nat Med 6:159-163.

Meng S, Qiao M, Lin L, Del Bigio MR, Tomanek B, Tuor UI (2004) Correspondence of AQP4 expression and hypoxic-ischaemic brain oedema monitored by magnetic resonance imaging in the immature and juvenile rat. Eur J Neurosci 19:2261-2269.

Moftakhar P, Lynch MD, Pomakian JL, Vinters HV (2010) Aquaporin expression in the brains of patients with or without cerebral amyloid angiopathy. J Neuropathol Exp Neurol 69:1201-1209.

Nagelhus EA, Mathiisen TM, Ottersen OP (2004) Aquaporin-4 in the central nervous system: cellular and subcellular distribution and coexpression with KIR4.1. Neuroscience 129:905-913.

Nesic O, Guest JD, Zivadinovic D, Narayana PA, Herrera JJ, Grill RJ, Mokkapati VU, Gelman BB, Lee J (2010) Aquaporins in spinal cord injury: the janus face of aquaporin 4. Neuroscience 168:1019-1035.

Nesic O, Lee J, Unabia GC, Johnson K, Ye Z, Vergara L, Hulsebosch CE, Perez-Polo JR (2008) Aquaporin 1 - a novel player in spinal cord injury. J Neurochem 105:628-640.

Nicchia GP, Srinivas M, Li W, Brosnan CF, Frigeri A, Spray DC (2005) New possible roles for aquaporin-4 in astrocytes: cell cytoskeleton and functional relationship with connexin43. Faseb J 19:1674-1676.

Obenaus A, Ashwal S (2008) Magnetic resonance imaging in cerebral ischemia: focus on neonates. Neuropharmacology 55:271-280.

Oliva AA, Jr., Kang Y, Truettner JS, Sanchez-Molano J, Furones C, Yool AJ, Atkins CM (2011) Fluid-percussion brain injury induces changes in aquaporin channel expression. Neuroscience 180:272-279.

Oshio K, Watanabe H, Yan D, Verkman AS, Manley GT (2006) Impaired pain sensation in mice lacking Aquaporin-1 water channels. Biochem Biophys Res Commun 341:1022-1028.

Papadopoulos MC, Saadoun S, Binder DK, Manley GT, Krishna S, Verkman AS (2004) Molecular mechanisms of brain tumor edema. Neuroscience 129:1011-1020.

Papadopoulos MC, Verkman AS (2005) Aquaporin-4 gene disruption in mice reduces brain swelling and mortality in pneumococcal meningitis. J Biol Chem 280:13906-13912.

Papadopoulos MC, Verkman AS (2007) Aquaporin-4 and brain edema. Pediatr Nephrol 22:778-784.

Pop V, Badaut J (2011) A Neurovascular Perspective for Long-Term Changes After Brain Trauma. Transl Stroke Res 2:533-545.

Ribeiro Mde C, Hirt L, Bogousslavsky J, Regli L, Badaut J (2006) Time course of aquaporin expression after transient focal cerebral ischemia in mice. J Neurosci Res 83:1231-1240.

Saadoun S, Bell BA, Verkman AS, Papadopoulos MC (2008) Greatly improved neurological outcome after spinal cord compression injury in AQP4-deficient mice. Brain 131:1087-1098.

Saadoun S, Papadopoulos MC, Watanabe H, Yan D, Manley GT, Verkman AS (2005) Involvement of aquaporin-4 in astroglial cell migration and glial scar formation. J Cell Sci 118:5691-5698.

Schneier AJ, Shields BJ, Hostetler SG, Xiang H, Smith GA (2006) Incidence of pediatric traumatic brain injury and associated hospital resource utilization in the United States. Pediatrics 118:483-492.

Singewald GM, Rjabokon A, Singewald N, Ebner K (2011) The modulatory role of the lateral septum on neuroendocrine and behavioral stress responses. Neuropsychopharmacology 36:793-804.

Skucas VA, Mathews IB, Yang J, Cheng Q, Treister A, Duffy AM, Verkman AS, Hempstead BL, Wood MA, Binder DK, Scharfman HE (2011) Impairment of select forms of spatial memory and neurotrophin-dependent synaptic plasticity by deletion of glial aquaporin-4. J Neurosci 31:6392-6397.

Sun MC, Honey CR, Berk C, Wong NL, Tsui JK (2003) Regulation of aquaporin-4 in a traumatic brain injury model in rats. J Neurosurg 98:565-569.

Tait MJ, Saadoun S, Bell BA, Verkman AS, Papadopoulos MC (2010) Increased brain edema in aqp4-null mice in an experimental model of subarachnoid hemorrhage. Neuroscience 167:60-67.

Tomura S, Nawashiro H, Otani N, Uozumi Y, Toyooka T, Ohsumi A, Shima K (2011) Effect of decompressive craniectomy on aquaporin-4 expression after lateral fluid percussion injury in rats. J Neurotrauma 28:237-243.

Tourdias T, Dragonu I, Fushimi Y, Deloire MS, Boiziau C, Brochet B, Moonen C, Petry KG, Dousset V (2009) Aquaporin 4 correlates with apparent diffusion coefficient and hydrocephalus severity in the rat brain: a combined MRI-histological study. Neuroimage 47:659-666.

Tourdias T, Mori N, Dragonu I, Cassagno N, Boiziau C, Aussudre J, Brochet B, Moonen C, Petry KG, Dousset V (2011) Differential aquaporin 4 expression during edema build-up and resolution phases of brain inflammation. J Neuroinflammation 8:143.

Tran ND, Kim S, Vincent HK, Rodriguez A, Hinton DR, Bullock MR, Young HF (2010) Aquaporin-1-mediated cerebral edema following traumatic brain injury: effects of acidosis and corticosteroid administration. J Neurosurg 112:1095-1104.

Wen H, Nagelhus EA, Amiry-Moghaddam M, Agre P, Ottersen OP, Nielsen S (1999) Ontogeny of water transport in rat brain: postnatal expression of the aquaporin-4 water channel. Eur J Neurosci 11:935-945.

Wilcock DM, Vitek MP, Colton CA (2009) Vascular amyloid alters astrocytic water and potassium channels in mouse models and humans with Alzheimer's disease. Neuroscience 159:1055-1069.

Yang J, Lunde LK, Nuntagij P, Oguchi T, Camassa LM, Nilsson LN, Lannfelt L, Xu Y, Amiry-Moghaddam M, Ottersen OP, Torp R (2011) Loss of Astrocyte Polarization in the Tg-ArcSwe Mouse Model of Alzheimer's Disease. J Alzheimers Dis.

Zhao J, Moore AN, Clifton GL, Dash PK (2005) Sulforaphane enhances aquaporin-4 expression and decreases cerebral edema following traumatic brain injury. J Neurosci Res 82:499-506.

Zheng GQ, Li Y, Gu Y, Chen XM, Zhou Y, Zhao SZ, Shen J (2010) Beyond water channel: aquaporin-4 in adult neurogenesis. Neurochem Int 56:651-654.

CHAPTER THREE

POST-TRAUMATIC REDUCTION OF EDEMA WITH AQUAPORIN-4 RNA

INTERFERENCE IMPROVES ACUTE AND CHRONIC FUNCTIONAL

RECOVERY

By

Andrew M Fukuda, Arash Adami, Viorela Pop, John A. Bellone, Jacqueline S. Coats,
Richard E. Hartman, Stephen Ashwal, Andre Obenaus, Jerome Badaut

Title: Post-traumatic reduction of edema with aquaporin-4 RNA interference

improves acute and chronic functional recovery

Authors: Andrew M Fukuda, BS,[1,2*] Arash Adami, BS,[3*] Viorela Pop, PhD,[2] John A. Bellone, MA,[4] Jacqueline S. Coats, BS,[2] Richard E. Hartman, PhD,[4] Stephen Ashwal, MD,[3] Andre Obenaus, PhD[2,3], Jerome Badaut, PhD[1,2]

Affiliations: [1] Department of Physiology, Loma Linda University, Loma Linda, CA 92354

[2] Department of Pediatrics, Loma Linda University Medical Center, Loma Linda, CA 92354

[3] Department of Neuroscience, University of California, Riverside, CA 92521

[4] Department of Psychology, Loma Linda University Loma Linda, CA 92354

Corresponding Author
Jerome Badaut, PhD
Departments of Pediatrics and Physiology
Loma Linda University School of Medicine
Coleman Pavilion, Room A1120
11175 Campus Street
Loma Linda, CA 92354 USA
jbadaut@llu.edu
Phone: +1 (909) 558-8242
Fax: +1 (909) 558-4479

Acknowledgements

Abstract

Traumatic brain injury (TBI) is common in young children and adolescents and is associated with long-term disability and mortality. The neuropathological sequelae that result from juvenile TBI are a complex cascade of events that include edema formation and brain swelling. Brain aquaporin 4 plays a key role in edema formation. Thus, development of novel treatments targeting aquaporin 4 to reduce edema could lessen the neuropathological sequelae. We hypothesized that inhibiting aquaporin 4 expression by injection of small interference RNA targeting aquaporin 4 (siAQP4) after juvenile traumatic brain injury would decrease edema formation, neuroinflammation, neuronal cell death, and improve neurological outcomes.

siAQP4 or a non-targeted-siRNA (siGLO) was injected lateral to the trauma site after controlled cortical impact in postnatal day 17 rats. Magnetic resonance imaging, neurological testing, and immunohistochemistry were performed to assess outcomes.

Pups treated with siAQP4 showed acute (3d post-injury) improvements in motor function and spatial memory at long-term (60d post-injury) compared to siGLO-treated animals. These improvements were associated with decreased edema formation, increased microglial activation, decreased blood-brain barrier disruption, and reduced astrogliosis and reduced neuronal cell death. The effectiveness of our treatment paradigm was associated with a 30% decrease in aquaporin 4 expression at the injection site.

Introduction

Traumatic brain injury (TBI) affects about 1.7 million people annually and contributes to 30% of all injury-related deaths in the United States. An important sub-group are injured children (ages 0-14) of which a half million require treatment in local emergency departments.(1) Despite this increasing incidence of juvenile traumatic brain injury (jTBI), there are currently no effective pharmacological treatments.

TBI is divided into two main types of injuries: primary injuries due to a direct and immediate mechanical disruption of brain tissue; and secondary injuries, a matrix of delayed events affecting neuronal, glial, and vascular structures.(2) The severity of primary injuries has decreased in recent years due to increased public and legislative awareness concerning preventative measures such as regulation of motor vehicle speed limits and wearing protective helmets during competitive sport activities. Thus, development of effective post-injury treatments should focus on targeting secondary injury cascades. This is especially important in jTBI because the brain is still undergoing development and secondary injuries are more severe in the pediatric than in adult population with long lasting cognitive, emotional, and motor effects.(3) Secondary injuries including blood-brain barrier (BBB) disruption and edema formation are pathological hallmarks after jTBI and contribute to the myriad of long lasting consequences of jTBI(4), and make excellent clinical targets for improving outcome. We recently characterized the behavioral changes, brain tissue properties, as well as neurovascular unit transformation up to 60 days after a controlled cortical impact in juvenile rats (post-natal 17 days old) (5-7).

Aquaporin 4 (AQP4) is mainly expressed in perivascular astrocytic endfeet and is the most abundant brain aquaporin and has been shown to play a central role in edema formation in several cerebrovascular diseases.(8) However, the beneficial or deleterious role of AQP4 in edema formation remains unclear and depends on the pathological model(9). We recently showed an increase in edema formation at 1 and 3 days post-injury with concomitant decreased apparent diffusion coefficient (ADC) and increased T2 values in a model of jTBI (6). These MRI changes were associated with increase of the AQP4 expression at 3d, suggesting a central role of AQP4 in edema formation in jTBI (6). Nonetheless, several studies using AQP4 knockout mice have shown significant decreases in edema formation in several injury models, including adult TBI.(10) Despite several recent reports proposing the use of ionic channel inhibitors to block AQP4 channels(11) and pretreatment with certain drugs(12), there are no specific AQP inhibitors available for clinical use.(8) Recently, small interfering RNA (siRNA) to transiently knockdown proteins of interest has garnered considerable translational attention with improvements noted in clinical trials using siRNA against VEGF receptors for the treatment of cancer (13). In our group, we have recently shown that siRNA against AQP4 (siAQP4) can effectively reduce brain AQP4 expression *in vitro* and *in vivo*(14). In the present study, we hypothesized that using siAQP4 injection as a treatment to decrease AQP4 expression after controlled cortical impact (CCI) in juvenile rats would decrease edema formation, BBB disruption and neuroinflammation (astrogliosis and microglia activation) as well as improve neurological outcomes.

Materials and Methods

Animals

Manuscript was written in accordance with the ARRIVE guidelines. Experiments and care of animals were conducted according to the principles and procedures of the Guidelines for Care and Use of Experimental Animals and were approved by the Loma Linda University Institutional Review Board. Sprague Dawley rat pups at postnatal day 17 (P17) were housed in a temperature controlled ($22\text{-}25^{\circ}C$) animal facility on a 12-hour light/dark cycle 7 days before the surgery.

siRNA Preparation

An *in vivo* AQP4 silencing protocol was adapted as described in our previous studies.(14) Briefly, SMART-pool® containing 4 siRNA-duplexes against AQP4 (400ng, siAQP4, Dharmacon Research) and non-targeted siRNA (siGLO RISC-free-control-siRNA, Dharmacon Research) were mixed with interferin® (Polypus-transfection, Illkirch, France) diluted in a saline solution (0.9%) containing 5% glucose for a final volume of 5 µL and incubated on ice for 20 min before injection.

Controlled Cortical Impact (CCI) Injury
and siRNA Injection

Controlled cortical impact (CCI) was carried out in P17 rat pups as previously described.(5) Rats were anesthetized with isoflurane (2%) and placed in a stereotaxic apparatus (David Kopf Instrument, Tujunga, USA) where a 5 mm diameter craniotomy was performed over the right hemisphere at 3 mm posterior from the bregma and 4 mm lateral to the midline. Animals were subjected to a CCI with a 2.7 mm round tip angled

20 degrees at a velocity of 6 m/s to a depth of 1.5 mm below the cortical surface using an electromagnetic impactor (Leica, Richmond, IL). After craniotomy, the dura was intact in both groups and after induction of TBI none of the animals in siGLO and siAQP4 groups had major bleeding or herniation of cortical tissues.

Injection of siRNA was performed 10 min after the injury lateral to the site of the impact using a 30-gauge needle on a Hamilton syringe (3 mm posterior to bregma, 6 mm lateral to midline, and 1.0 mm below cortical surface). The syringe was attached to a nanoinjector (Leica, Richmond, IL) and a volume of 4 μL of siRNA was infused at a rate of 0.4 μL/min. After suturing, all pups received an intraperitoneal injection of buprenorphine (0.01 mg/kg, Tyco Healthcare Group LP, Mansfield, MA) for pain relief and then placed on a warm heating pad for recovery before being returned to their dams. A second siRNA injection was repeated 2 days later in all pups using the same injection protocol. Total number of animals used for the study was 27 rats divided in n=15 rats for siGLO and n=12 for siAQP4 group.

Magnetic Resonance Imaging (MRI)

MRI was performed at 1 and 3d. Pups were lightly anesthetized using isoflurane (1.0%) and imaged on a Bruker Avance 11.7 T (Bruker Biospin, Billerica, MA).(15) Two imaging data sets were acquired: 1) a 10 echo T2- and 2) a diffusion weighted imaging (DWI) sequence in which each sequence collected 20 coronal slices (1 mm thickness and interleaved by 1 mm). The 11.7T T2 sequence had the following parameters: TR/TE = 2357.9 / 10.2 ms, matrix = 128 x 128, field of view (FOV) = 2 cm, and 2 averages. The

DWI sequence had the following parameters: TR/TE = 1096.5 / 50 ms, two b-values (116.960, 1044.422 s/mm^2), matrix = 128 x 128, FOV = 2 cm, and 2 averages.

Region of Interest (ROI) and Volumetric Analysis

T2 and apparent diffusion coefficient (ADC) values were quantified using previously published standard protocols (14). Regions of interest (ROIs) were placed on the imaging section with the maximally detected injury using Cheshire (Parexel International Corp. Waltham, MA). Lesion and ipsilateral hippocampus were delineated on T2 images and overlaid onto corresponding T2 and ADC maps. The mean, standard deviation, and area for each ROI were extracted.

Behavioral Testing

The behavioral evaluation was performed on 2 independent sets of animals. Foot-fault and rotarod testing was performed at 1, 3, 7 and 60 days, where the foot-fault test evaluated sensorimotor and proprioception while the rotarod test evaluated sensorimotor coordination as previously reported in our earlier studies.(5) All tests at each time-point were carried out on siGLO and siAQP4 treated jTBI rats within a 3-hours morning time-block (8 – 11 am). siGLO and siAQP4 treated jTBI rats were interleaved in testing sequence. To further control potential confounds, the same tests were administered in the same order at all of the time points, by the same investigators (AA, VP, JC) blinded to the experimental groups. For the behavioral tests the videos and the extraction of the data were carried out by JB and RH, who were also blinded to the experimental groups.

Foot-fault testing was carried out on an elevated platform (50 cm X 155 cm, ClosetMaid, Ocala, FL) with parallel wire bars 1.5 cm apart and raised 100 cm above the floor at 1d, 3d, 7d, and 60d. Rats were placed in the middle of the platform and movements were video-recorded for a period of 60 sec. in two separate trials, 30 min. apart. When a rodent's paw (fore- or hindlimb) slipped completely through the wire mesh, it was considered as an individual fault. The average foot-fault score was calculated from the total number of faults from two 60 sec trials.

Rotarod evaluation was performed on all the animals at 1d, 3d, 7d, and 60d (SD Instruments, San Diego, CA). A rotating 7 cm-wide spindle with a continuous speed (20 RPM) was used to evaluate performance during two trials (15 min apart). Latency to fall was recorded as a measure of motor coordination and balance. The maximum time spent on the test was 60s, if the rat did not fall. The two fall latencies were summed and express in total time (s) for 2 trials.

At 60 days post injury a battery of tests were performed over 4 days to evaluate the overall cognitive performance of the animals including open field, zero maze, and Morris Water Maze (MWM) (5). 1) Open field was used to assess the overall locomotor activity in a plastic box (50 x 36 x 45 cm), and each rat was monitored for 30 min with an overhead video camera using Noldus Ethovision software (Tacoma, WA). The total distance traveled by each rat was recorded (5). 2) On day 2, the elevated zero maze tests used an elevated circular track 10 cm wide with a 100 cm outer diameter and 2 sets of 30 cm high walls enclosing two opposing quadrants of the track, leaving the other two opposing quadrants open and brightly lit. This test was used to evaluate anxiety-like behavior by a 5 min observation, and the outcome measure was the percentage of the

time spent in the enclosed (dark) half of the maze. 3) Finally, the MWM test was carried out to assess spatial learning and memory in the rats. The test consists of a tank of 100 cm in diameter, filled with opaque water and an 11 cm diameter escape platform was placed. Recording the animal with an overhead camera and the Noldus Ethovision system allowed for assessment of variables such as swim distance, swim speed, and relative angular velocity (left / right turn bias). The first day of testing consisted of the cued learning paradigm, designed to test for non-associative factors that could affect the scoring on the MWM, such as motivation, swimming ability, and vision. The platform was visible by protruding 2 cm above the waterline with a 40 cm wooden rod attached. Animals were placed in the tank and required to simply swim to the visible platform to end the task. Each animal completed 10 trials consisting of 5 blocks of 2 trials each, with their starting location and that of the platform being shifted throughout the task. If the rat had not found the platform after 60 sec, it was guided to the platform, where it remained for 5 seconds. The swim path was recorded and each animal's total swim distance determined for each trial. The following days 2 and 3 of the MWM consisted of the spatial paradigm, designed to measure an animal's ability to learn and remember a hidden platform's location in the tank. During this paradigm, the platforms submerged approximately 2 cm below the water's surface, and release points varied throughout each day although the platform remained stationary. As in the cued paradigm, animals were required to swim to the platform to end the task. Unlike the cued paradigm, hiding the platform's surface under the water's surface required animals to learn and navigate to the location using spatial cues. Each animal completed 10 trials consisting of 5 blocks of 2 trials each. If the animal had not found the platform after 60 sec, it was guided to and

placed on the platform, where it remained for 5 seconds. The dependent variable for the spatial task was cumulative distance to the platform, a variable sensitive to both distance and time defined as a cumulative total of an animal's distance from the platform as measured 5 times every second. After each day of spatial testing, a probe trial was administered to measure an animal's ability to remember the platform's location. This trial was administered 1 hour after the final spatial trial of the day. The platform was removed and animals were allowed to search the tank for 60 sec. Dependent variables for this task included the number of times an animal entered the platform's previous location and percent time spent in the target quadrant.

Immunohistochemistry and Image Analysis

At 3d the animals were transcardially perfused with 4% paraformaldehyde, the brains extracted and put in 30% sucrose for 48 hours and then stored in -22°C. Coronal sections were cut at 20 μm thickness at -22°C on a cryostat (Leica, Richmond, IL) and mounted on slides for immunohistochemical analysis (14-16).

For immunoglobulin (IgG) extravasation immunohistochemistry, sections were washed with PBS, blocked with 1% BSA in PBS, then incubated for 2 hours at room temperature with IRDye 800 conjugated affinity purified goat-anti-rat IgG (1:500, Rockland, Gilbertsville, PA) in PBS containing 0.1% Triton X-100 and 1% bovine serum albumin. After washing, sections were scanned on an infra-red (IR) scanner (Odyssey) to quantify fluorescence for the different ROIs as previously described.(14) Additional immunostaining was done for rabbit polyclonal antibodies for AQP4 (1:300, Alpha Diagnostic, Owings Mill, MD), chicken polyclonal antibodies for glial fibrillary acidic

protein (GFAP, 1:500, Millipore, Billerica, MA), mouse monoclonal antibodies for

endothelial brain antigen (EBA, 1:1000, Covance, Princeton, NJ), mouse monoclonal

antibodies for Neuronal Nuclei (NeuN, 1:200, Abcam, Cambridge, MA), rabbit

polyclonal antibodies for ionized calcium-binding adapter molecule (Iba-1, 1:300, Wako,

Richmond, VA), and mouse monoclonal antibodies for Claudin-5 (1:200, Invitrogen,

Carlsbad, CA) were used. Sections were washed with PBS, blocked with 1% BSA in

PBS, incubated with the respective primary antibodies overnight, then incubated with

affinity purified secondaries conjugated to the desired wavelength to either be scanned on

an IR scanner or to be observed under a confocal microscope (Olympus). All image

acquisition parameters for the same proteins were kept constant for all of the animals for

analysis and visualization purposes. All analysis was carried out in a non-biased, blinded

manner. AQP4, GFAP, Claudin 5, and Iba-1 were quantified in a similar manner to IgG

extravasation staining as published previously (14). In detail, slides were incubated with

secondaries conjugated to the infrared wavelength of either 680 or 800 nm. These slides

were then scanned on an infrared scanner (Odyssey, Lincoln, NE), where images were

saved with resolution of 21 μm per pixel. Three identical circular regions of interests

(ROIs) were drawn in the perilesional cortex (Fig. 3A) at three different bregma levels (-

1.40mm, -2.56mm, and -3.80mm): the bregma level where lesion area was largest, one

slice anterior and one posterior, for a total of 9 regions of interests per animal. The

average fluorescence of these regions of interests was calculated. EBA and NeuN

staining was quantified using the Mercator software (Explora-Nova, La Rochelle,

France). The area of EBA staining was measured by drawing an ROI on the acquired

image with the largest legion as determined and confirmed by MRI, and the total area of

EBA-positive staining was determined and that value was divided by the area of the ROI. Thus, the % of staining per given area was determined for each animal. NeuN positive cells were counted on images acquired using constant parameters: i.e. the same values of the contrast, gain, and brightness were used. Similar to EBA analysis, the tissue section with the largest legion was selected and the NeuN positive cells were counted in an automated fashion via the Mercator software and the density was determined. Microglial activation was quantified by calculating the average form factor (FF= $4\pi*$area/perimeter^2 of each cell) from the Iba-1 positive cells using the image software, MorphoPro (Explora-Nova) on images acquired using constant parameters: i.e. the same values of the contrast, gain, and brightness were used. Negative control staining where the primary antibody or secondary antibody was omitted showed no detectable labelling.
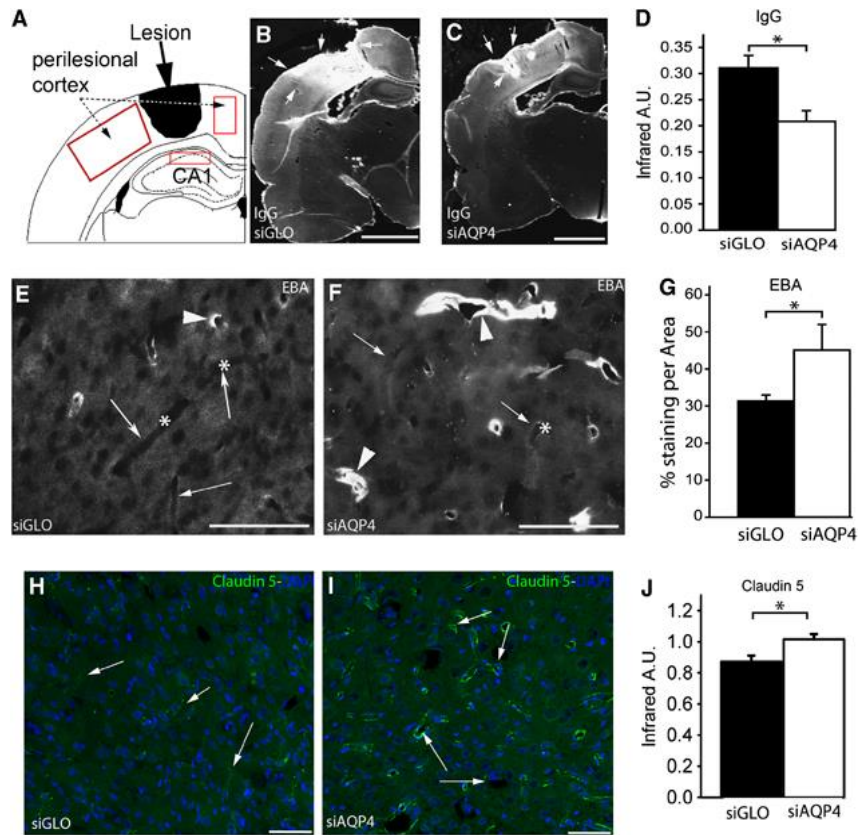
Figure 3. siAQP4 treatment decreases Blood-Brain Barrier disruption after jTBI. Drawing of the region of interests (ROIs) used in the study to quantify protein and histological changes in correlation with the MRI measurements (A). Representative photomicrographs of IgG-extravasation immunofluorescence (arrows) in siGLO (B) and siAQP4 (C) treated rat pups. siAQP4 treated rat pups showed significantly decreased IgG-extravasation staining adjacent to the lesion site compared to siGLO-treated animals (*, p<0.05), suggesting that the siAQP4 treatment mitigates BBB disruption (D). Endothelial Barrier Antigen (EBA) is a marker of intact endothelial cells in rats and disappears when the endothelial layer is disrupted. The arrows in (E) show blood vessels (asterisks) devoid of EBA staining in siGLO treated animals. In contrast siAQP4 rat pups had more EBA-positive staining (arrowheads) in the cortical perilesion tissue (F). Quantification of the EBA staining showed that the siAQP4 treated rat pups had more EBA-positive staining (arrowheads), suggesting decreased damaged blood vessels in the perilesion tissues (*, p<0.05) (G). This result is in accordance with the IgG extravasation data showing improvement of the BBB after siAQP4 treatment (A-C). Similarly, claudin-5 staining, a tight junction protein (in green H, I) showed increased staining in siAPQ4 (I, arrows) compared to siGLO treated rats (H, arrows) and confirmed in the quantification of claudin 5 immunoreactivity (*, p<0.05) (G). Increased levels of claudin-5 suggest less BBB disruption consistent with decreased IgG extravasation and increased EBA staining after siAQP4 treatment. Taken together, siAQP4 treatment results in less BBB disruption at day 3 after injury as seen by more tight junction proteins, more intact blood vessels, and less leakage of IgG from the peripheral blood vessels to brain tissue.
Scale bars in A, B=3mm; D, E=100μm.

Brain Tissue Processing for Western Blotting

A Protein FFPE extraction kit (Qiagen, Hilden, Germany) was used to process perfused brain slices for Western blotting as previously published (7). Parietal cortical tissue around the lesion was excised from three coronal sections at bregma levels -1.40, -2.56 and -3.80mm, that were adjacent to slices of interest used for immunohistochemistry quantification. Briefly, tissue was homogenized and processed according to kit instructions, and then samples were assayed for total protein concentration by bicinchoninic acid assay (BCA, Pierce Biotechnology Inc., Rockford, IL). For gel electrophoresis, all samples were prepared with loading sample buffer and reducing agent (Invitrogen, Carlsbad, CA) for a total of 2 µg of rat protein loaded on a 4-12% SDS polyacrylamide gel (Nupage, Invitrogen, Carlsbad, CA). Proteins were transferred to a polyvinylidene fluoride membrane (PVDF, PerkinElmer, Germany), blocked for 1 hr in Odyssey blocking buffer (Li-Cor Bio-Science, Lincoln, NE), and incubated with a rabbit polyclonal anti-AQP4 (1:3000; Alpha Diagnostic, Owings Mill, MD) and mouse anti-tubulin (1:10,000; Sigma-Aldrich Co., St. Louis, MO), and these blots were co-incubated with goat anti-mouse secondary antibody coupled with Alexa-Fluor-800 (1:10,000; Rockland Immunochemicals, Gilbertsville, PA) and goat anti-rabbit secondary antibody coupled with Alexa-Fluor-680 (1:10,000; Life Technologies: Molecular Probes, Grand Island, NY) for 2 hrs at room temperature. After PBS washes, the PVDF membrane was visualized using the Li-Cor infra-red scanner and fluorescence activity was directly quantified Odyssey software (Li-Cor, Bioscience).

<center>Statistics</center>

MRI and behavioral data were analyzed by two-way repeated measures analysis of variance with a post hoc Bonferroni test. One-way ANOVA was used for immunohistochemistry and western blot analysis. All data are expressed as the mean ± SEM.

<center>**Results**</center>

<center>siAQP4 Treatment Reduces AQP4 Expression Acutely</center>

Injection of siAQP4 induced a 31% decrease ($p<0.05$) in the level of AQP4 expression at 3d (Fig. 1A, B). In support of the Western blot results, siAQP4 treated rats showed a 27% decrease in AQP4 staining within the perilesional tissues around the cavity on the ipsilateral cortex as well as a 33% decrease in the ipsilateral hippocampus compared to siGLO-treated animals ($p<0.05$) (Fig 1C-G). This decrease in AQP4 staining after jTBI was of similar magnitude to that which we previously reported in normal (i.e. no jTBI) juvenile brain tissues after siAQP4 injection(14). In contrast, Western blot and immunohistochemistry analysis showed no differences in AQP4 expression between siGLO and siAQP4 treated animals at 60 days (Fig 6A, B, C). No significant changes found in the contralateral cortex or hippocampus at 3 and 60 days (data not shown).
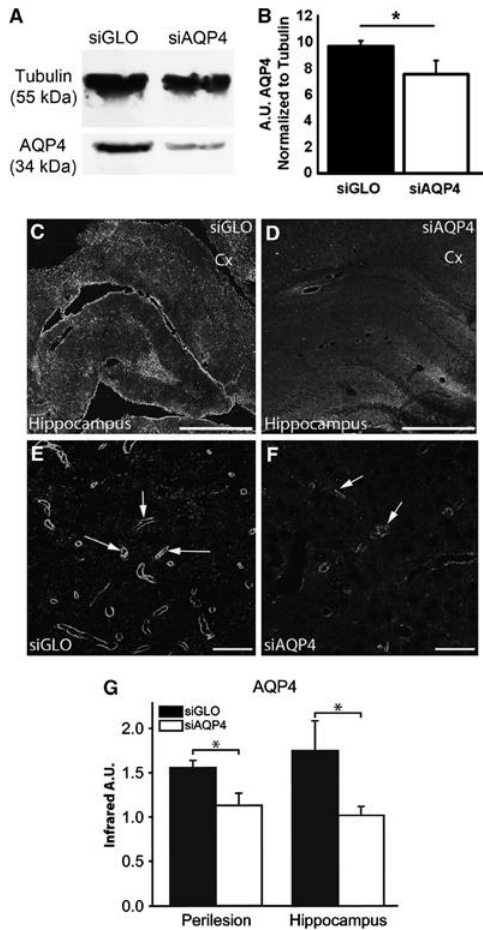
Figure 1. Reduced Expression of AQP4 after siAQP4 injection. AQP4 Western blot from adjacent PFA fixed sections in siGLO and siAQP4 groups showed a band around 34 kDa, with a decrease of the intensity in siAQP4 treated group. Tubulin was used to normalize the loading. The quantification of the intensity of the band showed a significant decrease of AQP4 ($p < 0.05$). Representative images of AQP4-immunoreactivity in the cortical perilesion and hippocampus adjacent to the jTBI cavity (*) in siGLO (C) and siAQP4 treated animals (D) at low magnification. AQP4 staining bordering the cavity is decreased in the siAQP4 (D) compared to the siGLO treated animals (C) at d3 post-injury. Similarly, the AQP4-immunoreactivity is increased in the ipsilateral hippocampus of siGLO group (C) compared to siAQP4 treated animals (D). At higher magnification in perilesional cortex (Cx), AQP4 staining is predominant on astrocyte endfeet in contact with blood vessels (arrows, as previously described, (16)) in siGLO (E) and siAQP4 (F) animals, with decreased staining of AQP4 in the siAQP4 group. This suggests that the siAQP4 treatment after jTBI prevents the increase of AQP4 expression on astrocyte endfeet. (**G**) AQP4 immunoreactivity was quantified and confirmed a significant decrease in AQP4-immunoreactivity in the siAQP4 compared to siGLO treated rats in both the perilesional cortex and ipsilateral hippocampus (*, $p < 0.05$). Taken together, after jTBI, siAQP4 injection induced a decrease of AQP4-immunoreactivity acutely. Abbreviation: Cx, cortex; scale bars C, D = 1mm; E, F=100µm.

siAQP4 Treatment Reduces Acute Edema Formation

As determined by 1d and 3d MRI, we found decreased T2 (edema) and ADC (water mobility) values in siAQP4 compared to siGLO-treated pups (Fig 2), strongly suggesting that siAQP4 reduced edema formation. Whereas T2 values increased in the lesion/perilesion area of siGLO treated rats they were decreased in siAQP4 pups from 1d to 3d (22% in the lesion/perilesion and 15% in the ipsilateral hippocampus). ADC values were also decreased by 21% in the lesion/perilesion at 1d (p <0.005) and by 24% in the ipsilateral hippocampus at 3d (p < 0.001) in the siAQP4 compared to siGLO-treated rats (Fig 2). Overall, the data suggest an association between the regions showing reduced AQP4 staining and reduced edema formation (T2) and improved tissue characteristics (ADC) (Fig 1 and 2).
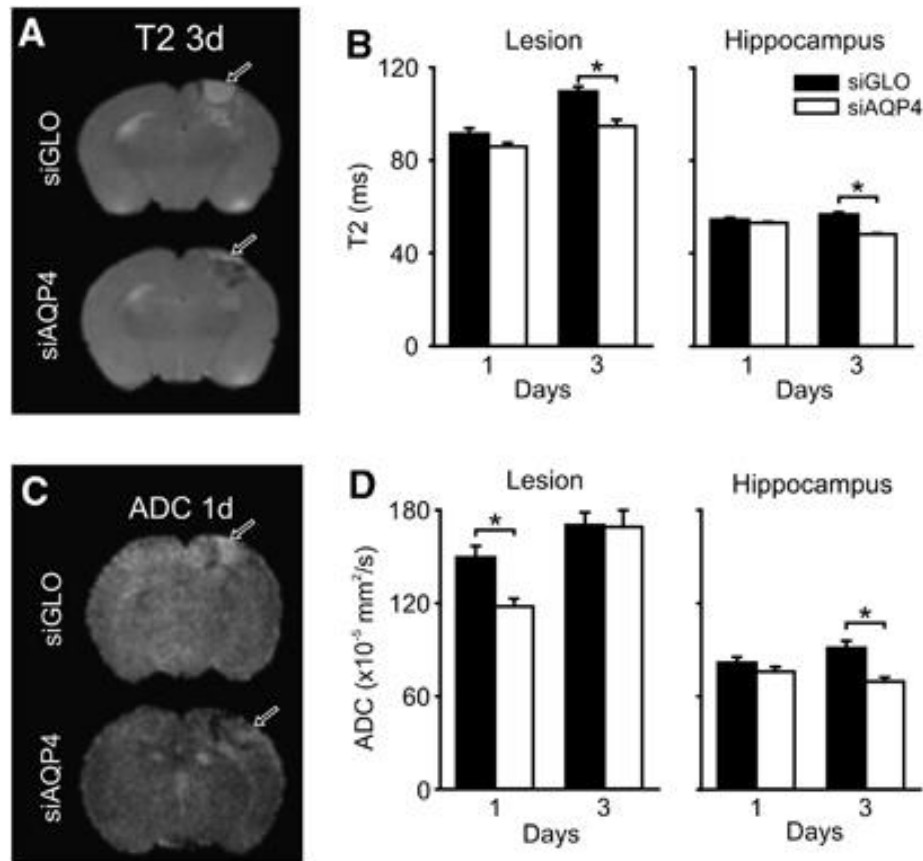
Figure 2. Quantitative neuroimaging of jTBI after siAQP4 treatment reveals decrements in edema. Representative T2 images at day 3 in siGLO and siAQP4-treated pups show decreased edema at the lesion site following siAQP4 treatment (arrows) (A). siAQP4 pups had significantly decreased edema (*, $p < 0.001$) compared to siGLO pups within the lesion at day 3 (B). There was also a significant decrease in edema after siAQP4 treatment at day 3 within the hippocampus, ventral to the injury (*, $p<0.001$) (b). Water mobility (apparent diffusion coefficients, ADC) was reduced in the siAQP4 treated pups (day 1 after injury, arrows) (C). Quantitative ADC revealed significantly decreased water mobility in siAQP4 pups in the lesion at 1 day after injury compared to siGLO (*, $p < 0.001$) (D). siAQP4 pups had significantly decreased ADC in the hippocampus at day 3, but not at 1 day (*, $p < 0.001$) (D). After jTBI, siAQP4 injection mitigated the edema formation associated with a decrease of the AQP4 (Fig 1).

Reduced BBB Disruption in siAQP4
Treated Rat Pups

Edema formation (i.e. increased T2 values) also appeared to be associated with BBB disruption, which improved after siAQP4 treatment. BBB integrity was assessed with claudin-5 (tight junction protein), endothelial barrier antigen (EBA) and IgG extravasation staining in the perilesional cortex and ipsi-hippocampus (Fig 3). Less BBB disruption was also shown through decreased IgG extravasation staining intensity by 30% around the site of the injury in the siAQP4 group ($p < 0.05$) (Fig 3B, C, D). Associated with decreased IgG staining, a 31% increase in the area of EBA staining in siAQP4 rats was observed (Fig 3E, F, G). Similarly, Claudin-5 immunoreactivity was higher in the siAQP4-treated animals around the cavity (Fig 3H, I, J).

Reduced Astrogliosis, Increased Microglial Activation,
and Increased Neuronal Survival in siAQP4 Treated Rat Pups

The effects of siAQP4 on neuroinflammation were evaluated by measurement of astrogliosis with GFAP-immunoreactivity (Fig 4) and microglia activation with Iba-1 staining (Fig 4). GFAP staining intensity was decreased by 39% around the cavity and by 26% in the ipsilateral hippocampus of siAQP4-rat pups compared to the siGLO group ($p < 0.05$, Fig 4). In contrast, we observed an increase in the number of activated microglial cells, showing amoeboid shapes with less ramifications in the lesion site characterized by higher calculated form factor (FF) in siAQP4 compared to siGLO treated rats (Fig 4). This observation was also supported by a higher intensity of Iba-1 staining, a specific marker of microglia, using infrared analysis (Fig 4). No significant differences were observed in the ipsilateral hippocampus.
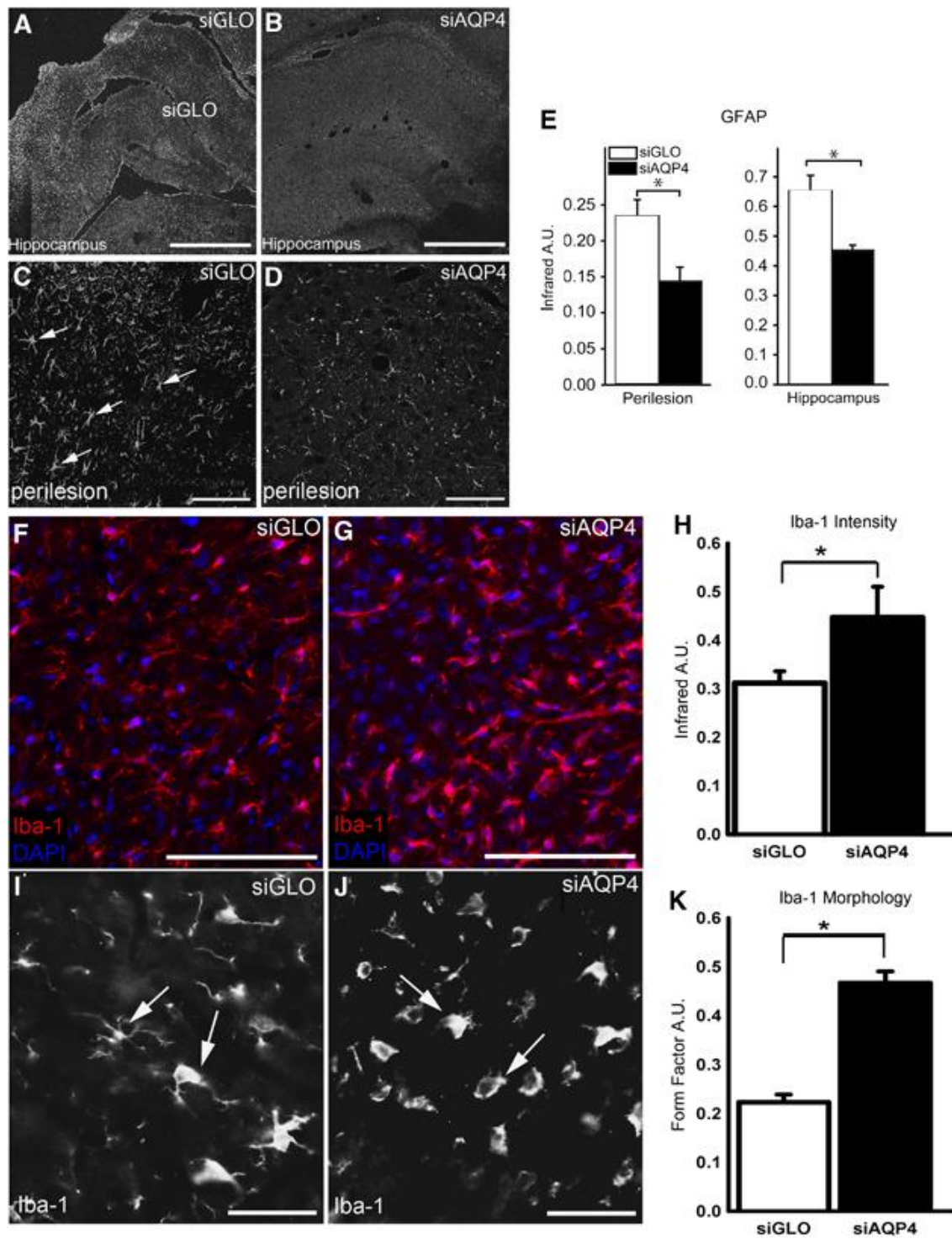
Figure 4. siAQP4 treatment reduces astrogliosis and results in microglial activation acutely after jTBI. Increased GFAP staining after injury is a marker of reactive astrocytes and astrogliosis associated with neuroinflammation. Representative images of regional GFAP-immunoreactivity in the cortical perilesion in the siGLO (A) and siAQP4 treated animals (B). GFAP staining in the region bordering the cavity (*) is decreased in the siAPQ4 treated rats compared to the siGLO-treated animals at day 3 post-injury. Similarly in the hippocampus, the presence of GFAP staining in the reactive astrocytes in the siGLO treated rats (A) is increased compared to siAQP4 treated animals (B). At higher magnification, increased GFAP positive cells with swollen cell bodies and processes in the siGLO group (arrows, C) compared to siAQP4 (D) treated rats were observed in the perilesional cortex. The infrared intensity of the GFAP immunoreactivity was quantified and showed a significant decrease of GFAP staining in the siAQP4 compared to siGLO treated rats in both the perilesional cortex and ipsilateral hippocampus (E) (*, $p<0.05$). The significant decrease of GFAP in the siAQP4 treated rats suggests that siAQP4 treatment mitigates astrogliosis and the swelling of the astrocytes after jTBI. Immunoreactivity of Iba1 (red), a specific marker of microglia, showed a higher intensity of staining in the siAQP4 group (F) compared to siGLO-treated rats (G). At higher magnification, Iba1 staining presents different morphological patterns between the two groups, suggesting that the microglia cells do not have the same level of activation. In the siGLO group (I) Iba1 positive cells appear more ramified (arrows) and have less amoeboid-like shapes than microglial cells in siAQP4 treated rats (J, arrows). The amoeboid-like shapes observed for Iba1 positive cells in the siAQP4-treated group (J, arrows) are associated with a more activated microglia phenotype. To quantify the morphological differences, form factor (FF) analysis was performed where a higher FF correspond to a less ramified and more round cells, suggesting a more activated state for microglia. FF analysis revealed that siAQP4-treated rats had a significantly higher average FF compared to siGLO group (K) (*, $p<0.01$) consistent with a more activated microglia in siAQP4 animals. Infrared analysis showed higher intensity fluorescence in the siAQP4 animals compared to siGLO at the lesion site (H) (*, $p<0.05$).
Scale bars in A, B =1mm; C, D =100μm, F, G, I, J = 20 μm.

The effects of siAQP4 on neuronal survival was also measured by counting the number of NeuN positive cells (5, 17). At 3d, NeuN positive cells were higher in the perilesional cortex adjacent to the cavity (62%) as well as in the ipsilateral hippocampus (56%) in the siAQP4 compared to siGLO-treated pups at 3d (Fig 5).
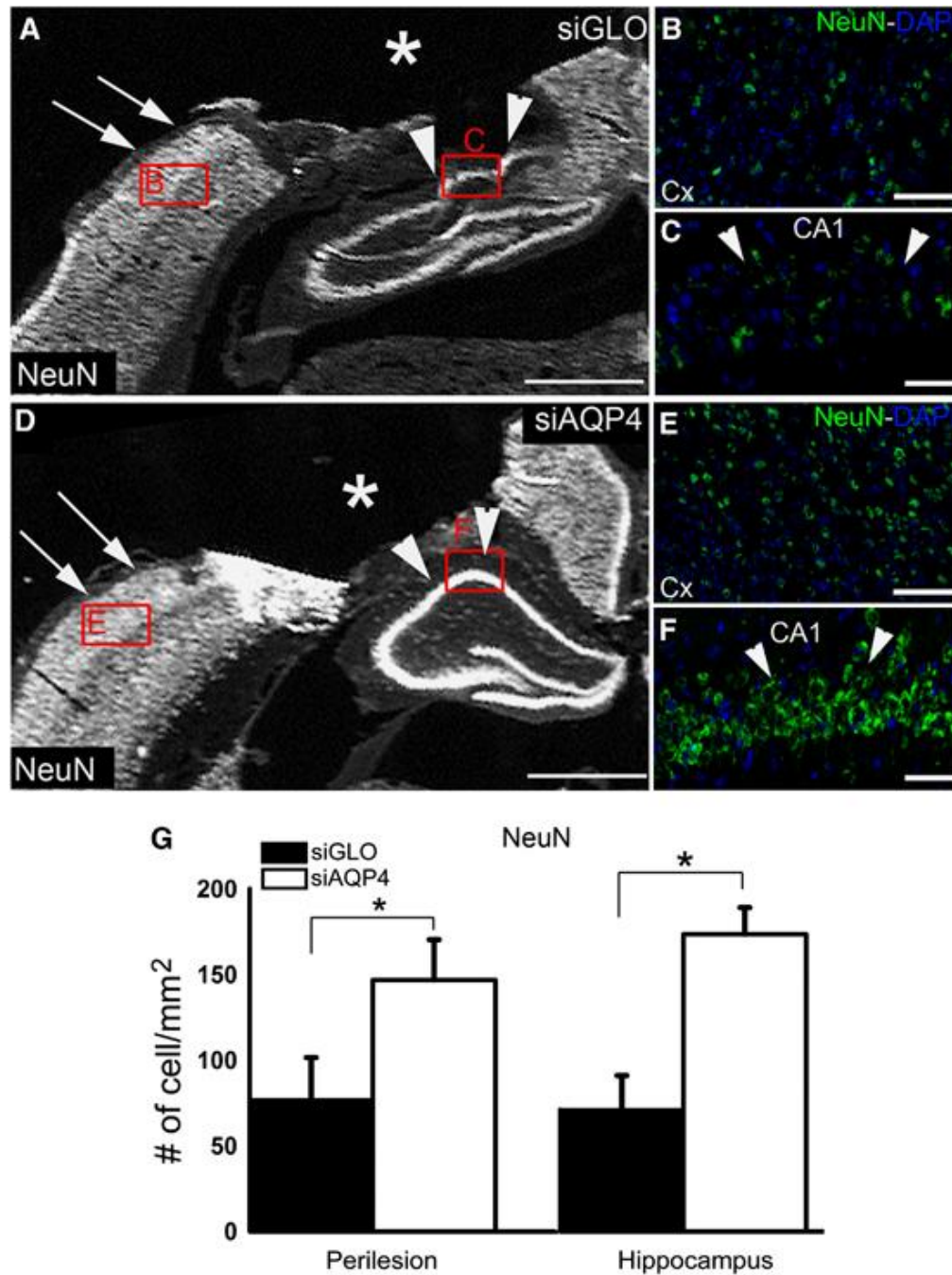
Figure 5. siAQP4 treatment increases neuronal survival at 3d post-injury. NeuN (Neuronal Nuclei) stained sections show a higher staining in the siAQP4 animals (D, E, F) than the siGLO (A, B, C) in the cortex (A, B, D, E) and the hippocampus (A, C, D, F) adjacent to the cavity (*). Neuronal cell counts revealed a significant increase in the number of NeuN positive cells (# of cell/mm^2) in both the perilesion (arrows A, D) and hippocampus (arrowheads, A, C, D, F) of siAQP4 animals (G) (*, $p<0.05$), suggesting improved neuronal survival after injury in siAQP4 treated rat pups compared to siGLO group. Scale bar A, D = 1.25mm; B, E = 50 μm; C, F = 20 μm.

At 60d, there were no differences in AQP4 and GFAP staining (Fig 6A, B, and C). No changes in microglial activation were observed at 60d (Fig 6D). In contrast there was a significantly higher number of NeuN positive cells in the CA1 region of the ipsilateral hippocampus in siAQP4 animals compared to siGLO, however no changes were observed in the ipsilateral cortex (Fig 6F, G, I).
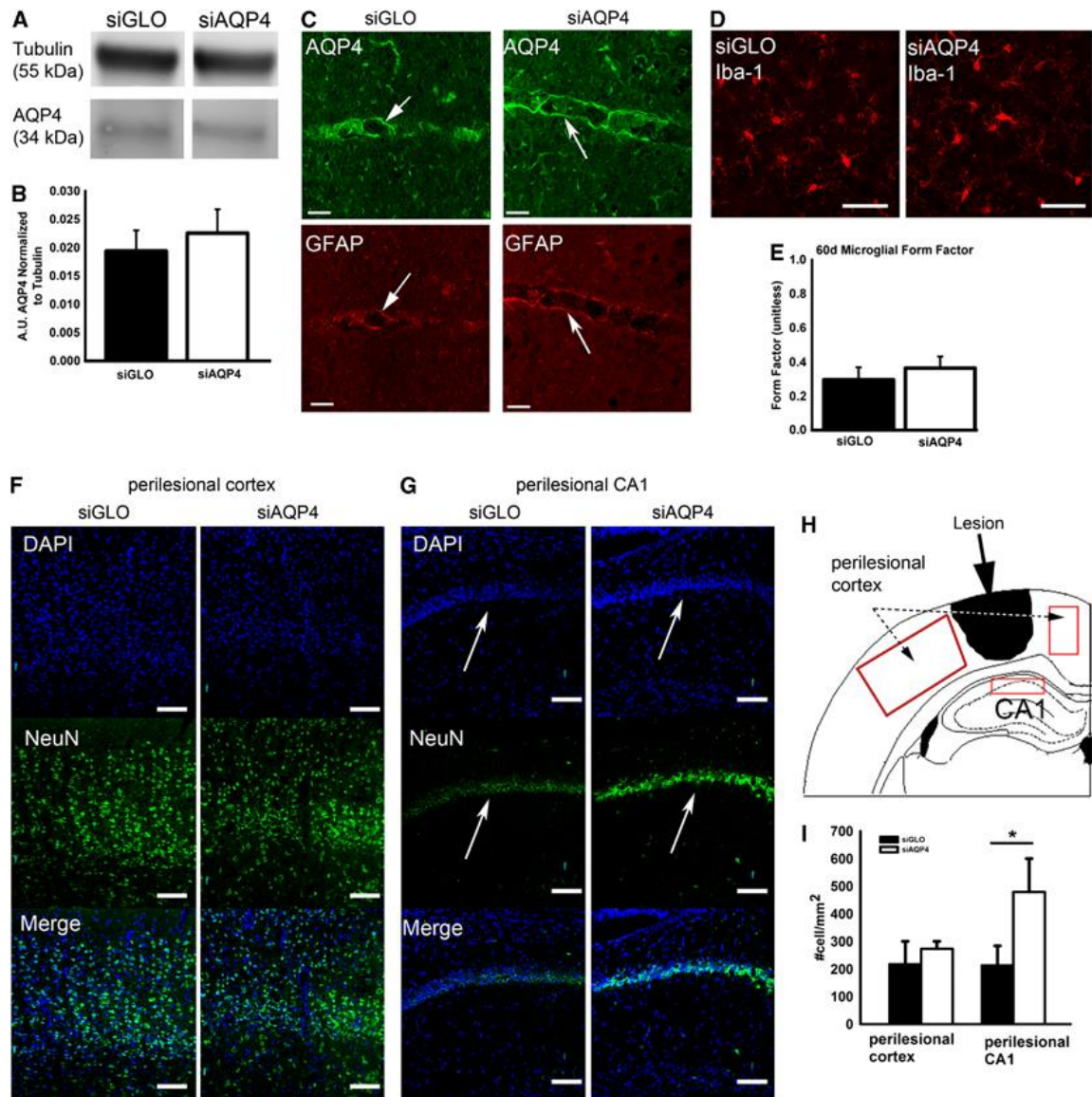
Figure 6. siAQP4 treatment increases the neuronal survival in hippocampus at 60d.
At 60d, AQP4 expression did not differ significantly between siAQP4 and siGLO as quantified via Western Blot (A) (B). AQP4 and GFAP staining did not show overall obvious visible differences in staining intensity or staining pattern between the groups as shown in the exemplary confocal picture (C). The arrows represent penetrating arteries stained in both siGLO and siAQP4 (C). At 60d, there were no visible differences in microglial staining visualized via Iba-1 immunohistochemistry between the siGLO and siAQP4 animals (D). Form factor analysis showed no significant differences between the animals, signifying no differences in microglial activation status (E). In the perilesional cortex of 60d animals, NeuN cell count showed no significant differences (F) (I). However, in the perilesional CA1 (arrow), siAQP4 animals had significantly higher number of NeuN positive cells (G) (*, p<0.05, I). A schematic drawing showing the regions of interests (in red) used to quantify NeuN numbers are shown (H). Scale bar C, D=50μm; F, G=100μm.

Improved Sensorimotor, Proprioception and
Spatial Memory after siAQP4 Treatment

Concomitant with the observed decrease in edema and histological improvements, motor functions were improved in siAQP4 treated rats. siAQP4 pups had fewer foot-faults at 1 and 3d (respectively 34% and 46%, $p < 0.05$, Fig 7A). After 7d, there were no more significant differences in the number of foot faults (Fig. 7A). Similarly, siAQP4 treated rats were able to stay on a rotarod 40% longer than siGLO treated rat pups at 3d (Fig 7B), that returned to baseline at 7d post injury. Long-term improvements were tested up to 60 days post injury, with a battery of tests assessing several cognitive repertoires. The open field test did not show significant difference between the groups in overall locomotor activity (data not shown) and supported the MWM cued test showing no differences in the ability to swim (data not shown). Similarly, the zero maze tests did not show differences between the groups with the same time spent in the "dark" quadrants (data not shown). During the spatial learning on the day1 of the protocol, both groups were able to perform the task similarly (Fig 7C). However on the second day of the MWM protocol, when the platform is moved to a second location, siAQP4 animals spent more time than the non-treated group in trying to find the new location of the platform on the first block (Fig 7D). This suggests that siAQP4 animals have a better memory of the previous platform location and thus spent more time at the previous site (Fig 7E). This data is also supported by the probe test to assess the spatial memory. The siAQP4 treated rats spent significantly longer times than the siGLO group in the quadrant that previously contained the platform (Fig 7F). Improvement in spatial memory at 60d post-injury is associated with higher CA1 neuronal survival in siAQP4 treated group (Fig 6).
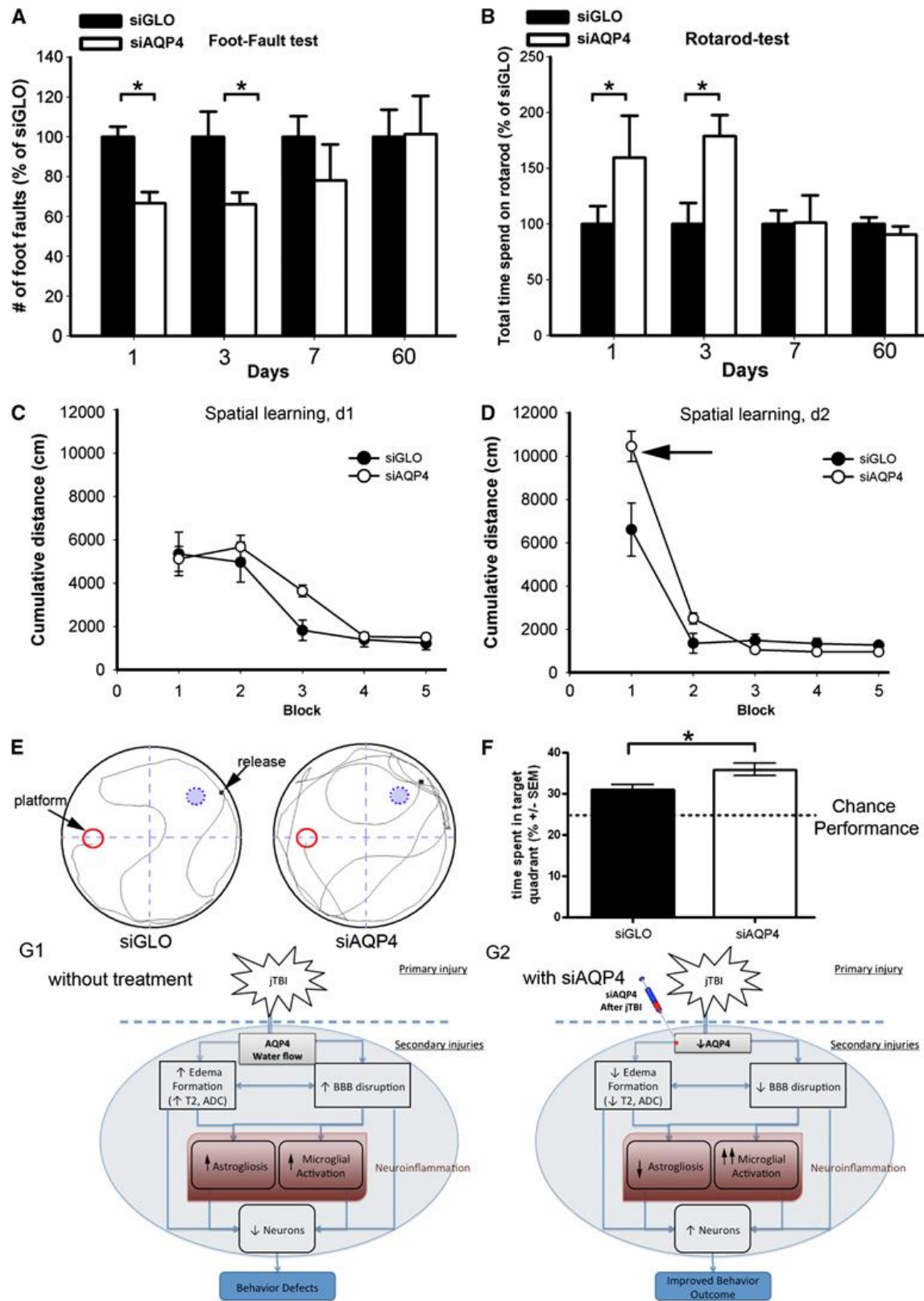
Figure 7. siAQP4 treatment associated with behavioral improvement at short and long-term after jTBI. siAQP4-treated pups had better functional outcomes as revealed by the foot-fault test. siAQP4 group had significantly fewer foot faults than siGLO treated animals at day 1 (34%) and day 3 (46%) after jTBI (*, $p < 0.05$) (A). siAQP4 animals also performed significantly better on the rotarod test at day 3 compared to siGLO by staying on for a significantly longer time before falling (*, $p<0.05$) (B). After jTBI, siAQP4 treatment improves the proprioception and sensorimotor outcomes in association with a better neuronal and a decreased edema formation acutely. In MWM test, the groups did not show overall significant difference in the rate of spatial learning at day 1 (d1, C) and day 2(d2, D). However, the siAQP4 treated animals exhibited higher cumulative distance value on the first block on d2 (arrows) compared to the non-treated group, suggesting a better memory of the platform's previous location. The video track (E, dark line) shows that the siAQP4 animals spent more time in the quadrant of platform's previous location (location noted by blue dotted circle) than the siGLO rats, in accordance with a better memory. The actual location of the platform is noted by the red circle (E) and at the opposite location to the previous one. The probe test confirmed this hypothesis with a significantly higher time spent in the quadrant where the platform was located for the siAQP4 treated rats compared to the siGLO animals (F). All these data showed that siAQP4 treatment improve the short and long-term behavioral outcomes.

In summary (G1 and G2), the primary injury induces a cascade of secondary of injuries involving AQP4 and water flow in brain tissue, which contributes to the edema formation (measured with T2 and ADC) and BBB disruption after jTBI. Downstream to these changes, there is neuroinflammation with astrogliosis and microglia activation, accompanied by neuronal cell death during the first days after the injury. The neuronal cell death is associated with functional impairments (G1). The injection the siAQP4 after jTBI (G2) induces a decrease in the AQP4 expression, which contributes to less entry of water and edema (measured with T2 and ADC) and also fewer constraints on the BBB. Therefore, these changes are associated with less astrogliosis and higher activation of the microglia, which could be beneficial. With these improvements, the neuronal survival is improved and accompanied by a better functional recovery after siAQP4 treatment (G2).

Discussion

We report here for the first time that siAQP4 treatment is an effective mechanism for reducing edema after jTBI and improves functional recovery even up to 60 days after injury. Injection of siAQP4 reduced AQP4 expression by 30% and was associated with significant decrements in edema formation, less BBB disruption, decreased astrogliosis, increased microglia activation, reduced neuronal cell death as well as improved neurological function during the acute phase after injury. We also observed that the siAQP4 treated animals had improved hippocampal neuronal cell count and memory recall at long-term: up to 60 days after injury as well. The uniqueness of our approach in implementing siRNA targeting AQP4 to improve functional outcomes after jTBI at both short and long-term after injury strongly suggests a potential future for clinical development.

MRI (T2, ADC) was used to temporally monitor edema formation as is done clinically after brain injury(8, 18). Our MRI data showed less post-traumatic edema after siAQP4 treatment (Fig 2) as manifested by significantly reduced T2 values in siAQP4 compared to siGLO-treated rat pups at 3d, suggesting less water accumulation within the lesion/perilesion and hippocampal tissues (Fig 2).

Beneficial effects of siAQP4 on water mobility as reflected by reduced ADC values were also observed. ADC values are dramatically increased in the injury site and likely correspond to cell death leading to an altered tissue matrix. This increase in ADC at the lesion is decreased in siAQP4 compared to siGLO-treated rats, suggesting that siAQP4 mitigates cell death at this early time point but not at 3d (Fig 2). However, in adjacent tissues such as the hippocampus, the ADC values were also significantly

decreased, suggesting that siAQP4 may prevent cell death even at 3d in the hippocampus, by limiting edema expansion. This hypothesis is supported by the increased numbers of neurons in the siAQP4 treated animals at 3d (Fig 6). However, decreased ADC could also be associated with a decrease in AQP4 expression on the astrocyte endfeet (Fig 1) at 3d in accordance with our previous studies (14). In fact, decreased AQP4 expression has been correlated with decreased ADC (14, 19) and increased AQP4 expression has been correlated with increased ADC (20) in rats. This suggests that water diffusion is limited by the decrease of AQP4 in the siAQP4-treated pups (Fig. 1). Together, the MRI data demonstrate that siAQP4 treatment prevents edema formation with decreased T2 and ADC values in the lesion and ipsilateral hippocampus. At 3d, T2 values are significantly higher in the lesion/perilesion suggesting an increase in water content in the tissue due to ongoing vasogenic edema formation in the untreated animals; while the decrease in the siAQP4 treated rats suggest that siAQP4 prevents vasogenic edema formation. This hypothesis is supported by the evidence of less BBB disruption (decreased IgG extravasation, increased EBA and claudin-5 staining) in siAQP4 compared to siGLO treated animals. In fact, injection of siAQP4 after jTBI may prevent water entry into astrocytes and block subsequent swelling of these cells at 1d as indicated by the lower values of ADC in siAQP4 animals compared to siGLO. Less osmotic stress on the astrocytes may prevent BBB disruption by maintenance of the physical and mechanical properties of the endothelial cells and also neurovascular unit (Fig 3, 4). Therefore, less BBB disruption appears to be associated with less astrogliosis, which has been correlated with the severity of brain injury (21).

The next question was whether beneficial effects could still be observed at long-term after injury, and whether there were significant down regulation of AQP4. This is an important question when considering the hypothesized biphasic and dual role that AQP4 plays not only in edema formation but also in edema clearance and maintaining regular water homeostasis (22-23). It has been hypothesized and several experimental observations hint that the presence of AQP4 is detrimental acutely after injury because they contribute to the entry of water into the brain parenchyma so acute down regulation of AQP4 may be beneficial, but chronic AQP4 depletion may be detrimental as AQP4 is also needed for water clearance and maintenance of normal water homeostasis (24-27). To this end, we performed a Western blot at 60d and also performed immunohistochemistry to see if there were visible differences in AQP4 expression levels. At 60d, we observed no differences in AQP4 levels or staining, thus injection of siAQP4 right after injury down-regulates AQP4 acutely but does not lead to chronic, long-term depletion of AQP4. This is another beneficial effect of using siRNA as it allows conditional down-regulation limited in the time of the target protein of interest.

The beneficial effects of siAQP4 treatment were also observed in the higher number of neurons (NeuN positive cells) in siAQP4 compared to siGLO treated rats at both acute and long-term after injury. These improvements led to improved neurological outcomes at 1 and 3d in siAQP4 treated rats (Fig 7A, B). This improvement in motor function was not visible at 7d, which may be a natural recovery or loss of some neurons in perilesional cortex as shown at 60 days (Fig. 6). Interestingly, at 60d, there were a significantly higher number of NeuN positive cells in the CA1 region of siAQP4 compared to siGLO; an effect of which can be observed in memory improvement. Our

93

unique data strongly suggest that the early decrease in AQP4 mitigates development of secondary injuries such as edema resulting in chronic neuroprotection for the perilesional structures, such as the hippocampus.

siAQP4 treatment resulted in greater microglial activation around the injection site at 3d but not at 60d. Microglial activation after siAQP4 treatment is in accordance with previous observations in brain injury models using AQP4$^{-/-}$ mice (28-29). However, acute microglial activation is hypothesized to be beneficial after injury (30), whereas a chronic microglial activation is hypothesized to be detrimental (30), so it is likely that at this time point, increased microglial activation due to siAQP4 treatment is contributing to the beneficial effects observed in our model. This observation suggests a potential relation between the level of AQP4 (Fig 1), astrogliosis and microglia activation (Fig 4, 7G1-G2).

We have previously speculated in a previous review (23) two of the possible mechanisms responsible the relationship between AQP4 and microglial activation. The first potential mechanism may be due to cross-talk that occurs between astrogliosis and microglial activation (31). It is possible that the decreased extent of injury-induced reactive astrogliosis is a result of knocking down AQP4 resulting in increased microglial activity. A second possible mechanism behind the changes observed in post-traumatic microglial activation in response to injection of siRNA against AQP4 may be because of the stretch-activated chloride channels expressed in microglia cells (32). Stretch-activated; also known as swelling-activated chloride channels, are activated by osmotic stress (33). Activation of these stretch-activated chloride channels contributes to the maintenance of the non-activated (ramified) phenotype of microglia (32). Because AQP4

is responsible for water transport, down-regulation of AQP4 through siRNA could have decreased the osmotic stress on the microglia, thus limiting the activation of the swelling activated chloride channels, resulting in microglial activation.

Both of these mechanisms are equally possible based on the data that we report, because at 3d, when both AQP4 levels and astrogliosis are decreased in the siAQP4 treated rats, we observe an increase in microglial activation. However, at 60d, when AQP4 levels and extent of astrogliosis are not changed between the groups, no significant differences in microglial activation are observed.

Our results are in accordance with studies using knockout animals showing that AQP4$^{-/-}$ had improved outcomes compared to WT mice in cerebral pathologies such as hyponatremia (34), bacterial meningitis (34), water intoxication (25), focal cerebral ischemia (25), spinal cord injury (35), and encephalomyelitis (36). Thus, the importance of the development of an AQP4 inhibitor cannot be underestimated. However, as noted earlier no specific effective drug directly against AQP4 is now available (8), despite promising studies using agents such as bumetanide (11), acetazolamide (37-38) and methazolamide (38-39). Our study provides a novel therapeutic strategy to successfully target AQP4, leading to better outcomes after injury when edema is a prominent pathological feature. Our findings are unique, demonstrating proof of concept that siAQP4 treatment when given twice after injury reduces AQP4 expression by 30% and this is sufficient to achieve beneficial functional outcomes on edema formation as well as functional improvements, even long term after injury. Despite the relative modest changes of each individual measurement, the combined effect on the neurovascular unit is synergistic, with less neuronal cell death and functional improvements up to 60d post-

jTBI. Furthermore, acute siAQP4 treatment does not lead to chronic or complete

depletion of AQP4, which in itself could be detrimental to the recovery and overall health

The next step would be to investigate the most efficient method to deliver an

AQP4 inhibitor to the brain without craniotomy. One potential administration route

would be intranasal delivery, which bypasses the BBB, is noninvasive, and easily

performed (40). Our novel findings provide compelling evidence for the effectiveness of

siAQP4 as a potential therapeutic agent not only for jTBI, but also for other brain

disorders in which edema is a significant contributing factor.

Disclosure/Conflict of Interest

The authors declare no conflict of interest.

References

1. Faul M XL, Wald MM, Coronado VG. Traumatic brain injury in the United States: emergency department visits, hospitalizations and deaths 2002-2006.: Atlanta (GA): Centers for Disease Control and Prevention, National center for Injury Prevention and Control2010.

2. Pop V, Badaut J. A Neurovascular Perspective for Long-Term Changes After Brain Trauma. Transl Stroke Res. 2011 Dec 1;2(4):533-45.

3. Moran LM, Taylor HG, Rusin J, Bangert B, Dietrich A, Nuss KE, et al. Quality of Life in Pediatric Mild Traumatic Brain Injury and its Relationship to Postconcussive Symptoms. J Pediatr Psychol. 2011 Oct 12.

4. Margulies S, Hicks R. Combination therapies for traumatic brain injury: prospective considerations. J Neurotrauma. 2009 Jun;26(6):925-39.

5. Ajao D, Pop V, Kamper J, Adami A, Rudobeck E, Huang L, et al. Traumatic brain injury in young rats leads to progressive behavioral deficits coincident with altered tissue properties in adulthood. J Neurotrauma. 2012 Jun 14.

6. Fukuda AM, Pop V, Spagnoli D, Ashwal S, Obenaus A, Badaut J. Delayed increase of astrocytic aquaporin 4 after juvenile traumatic brain injury: possible role in edema resolution? Neuroscience. 2012 Oct 11;222:366-78.

7. Pop V, Sorensen DW, Kamper JE, Ajao DO, Murphy MP, Head E, et al. Early brain injury alters the blood-brain barrier phenotype in parallel with beta-amyloid and cognitive changes in adulthood. J Cereb Blood Flow Metab. 2013 Feb;33(2):205-14.

8. Badaut J, Ashwal S, Obenaus A. Aquaporins in cerebrovascular disease: a target for treatment of brain edema? Cerebrovasc Dis. 2011;31(6):521-31.

9. Badaut J, Brunet JF, Regli L. Aquaporins in the brain: from aqueduct to "multi-duct". Metab Brain Dis. 2007 Dec;22(3-4):251-63.

10. Tait MJ, Saadoun S, Bell BA, Papadopoulos MC. Water movements in the brain: role of aquaporins. Trends Neurosci. 2008 Jan;31(1):37-43.

11. Migliati E, Meurice N, DuBois P, Fang JS, Somasekharan S, Beckett E, et al. Inhibition of aquaporin-1 and aquaporin-4 water permeability by a derivative of the loop diuretic bumetanide acting at an internal pore-occluding binding site. Mol Pharmacol. 2009 Jul;76(1):105-12.

12. Igarashi H, Huber VJ, Tsujita M, Nakada T. Pretreatment with a novel aquaporin 4 inhibitor, TGN-020, significantly reduces ischemic cerebral edema. Neurol Sci. 2011 Feb;32(1):113-6.

13. Brower V. RNA interference advances to early-stage clinical trials. J Natl Cancer Inst. 2010 Oct 6;102(19):1459-61.

14. Badaut J, Ashwal S, Adami A, Tone B, Recker R, Spagnoli D, et al. Brain water mobility decreases after astrocytic aquaporin-4 inhibition using RNA interference. J Cereb Blood Flow Metab. 2011 Mar;31(3):819-31.

15. Badaut J, Ashwal S, Tone B, Regli L, Tian HR, Obenaus A. Temporal and regional evolution of aquaporin-4 expression and magnetic resonance imaging in a rat pup model of neonatal stroke. Pediatr Res. 2007 Sep;62(3):248-54.

16. Hirt L, Ternon B, Price M, Mastour N, Brunet JF, Badaut J. Protective role of early aquaporin 4 induction against postischemic edema formation. J Cereb Blood Flow Metab. 2009 Feb;29(2):423-33.

17. Gobbel GT, Bonfield C, Carson-Walter EB, Adelson PD. Diffuse alterations in synaptic protein expression following focal traumatic brain injury in the immature rat. Childs Nerv Syst. 2007 Oct;23(10):1171-9.

18. Chastain CA, Oyoyo UE, Zipperman M, Joo E, Ashwal S, Shutter LA, et al. Predicting outcomes of traumatic brain injury by imaging modality and injury distribution. J Neurotrauma. 2009 Aug;26(8):1183-96.

19. Meng S, Qiao M, Lin L, Del Bigio MR, Tomanek B, Tuor UI. Correspondence of AQP4 expression and hypoxic-ischaemic brain oedema monitored by magnetic resonance imaging in the immature and juvenile rat. Eur J Neurosci. 2004 Apr;19(8):2261-9.

20. Tourdias T, Dragonu I, Fushimi Y, Deloire MS, Boiziau C, Brochet B, et al. Aquaporin 4 correlates with apparent diffusion coefficient and hydrocephalus severity in the rat brain: a combined MRI-histological study. Neuroimage. 2009 Aug 15;47(2):659-66.

21. Myer DJ, Gurkoff GG, Lee SM, Hovda DA, Sofroniew MV. Essential protective roles of reactive astrocytes in traumatic brain injury. Brain. 2006 Oct;129(Pt 10):2761-72.

22. Berezowski V, Fukuda AM, Cecchelli R, Badaut J. Endothelial Cells and Astrocytes: A Concerto en Duo in Ischemic Pathophysiology. Int J Cell Biol. 2012;2012:176287.

23. Fukuda AM, Badaut J. Aquaporin 4: a player in cerebral edema and neuroinflammation. J Neuroinflammation. 2012;9:279.

24. Kimura A, Hsu M, Seldin M, Verkman AS, Scharfman HE, Binder DK. Protective role of aquaporin-4 water channels after contusion spinal cord injury. Ann Neurol. 2010 Jun;67(6):794-801.

25. Manley GT, Fujimura M, Ma T, Noshita N, Filiz F, Bollen AW, et al. Aquaporin-4 deletion in mice reduces brain edema after acute water intoxication and ischemic stroke. Nat Med. 2000 Feb;6(2):159-63.

26. Verkman AS, Binder DK, Bloch O, Auguste K, Papadopoulos MC. Three distinct roles of aquaporin-4 in brain function revealed by knockout mice. Biochim Biophys Acta. 2006 Mar 10.

27. Tait MJ, Saadoun S, Bell BA, Verkman AS, Papadopoulos MC. Increased brain edema in aqp4-null mice in an experimental model of subarachnoid hemorrhage. Neuroscience. 2010 Apr 28;167(1):60-7.

28. Shi WZ, Zhao CZ, Zhao B, Zheng XL, Fang SH, Lu YB, et al. Aquaporin-4 deficiency attenuates acute lesions but aggravates delayed lesions and microgliosis after cryoinjury to mouse brain. Neurosci Bull. 2012 Feb;28(1):61-8.

29. Lu DC, Zador Z, Yao J, Fazlollahi F, Manley GT. Aquaporin-4 Reduces Post-Traumatic Seizure Susceptibility by Promoting Astrocytic Glial Scar Formation in Mice. J Neurotrauma. 2011 Sep 22.

30. Loane DJ, Byrnes KR. Role of microglia in neurotrauma. Neurotherapeutics. 2010 Oct;7(4):366-77.

31. Liu W, Tang Y, Feng J. Cross talk between activation of microglia and astrocytes in pathological conditions in the central nervous system. Life Sci. 2011 Aug 1;89(5-6):141-6.

32. Eder C, Klee R, Heinemann U. Involvement of stretch-activated Cl- channels in ramification of murine microglia. J Neurosci. 1998 Sep 15;18(18):7127-37.

33. Lewis RS, Ross PE, Cahalan MD. Chloride channels activated by osmotic stress in T lymphocytes. J Gen Physiol. 1993 Jun;101(6):801-26.

34. Papadopoulos MC, Verkman AS. Aquaporin-4 gene disruption in mice reduces brain swelling and mortality in pneumococcal meningitis. J Biol Chem. 2005 Apr 8;280(14):13906-12.

35. Saadoun S, Bell BA, Verkman AS, Papadopoulos MC. Greatly improved neurological outcome after spinal cord compression injury in AQP4-deficient mice. Brain. 2008 Apr;131(Pt 4):1087-98.

36. Li L, Zhang H, Verkman AS. Greatly attenuated experimental autoimmune encephalomyelitis in aquaporin-4 knockout mice. BMC Neurosci. 2009;10:94.

37. Huber VJ, Tsujita M, Yamazaki M, Sakimura K, Nakada T. Identification of arylsulfonamides as Aquaporin 4 inhibitors. Bioorg Med Chem Lett. 2007 Mar 1;17(5):1270-3.

38. Tanimura Y, Hiroaki Y, Fujiyoshi Y. Acetazolamide reversibly inhibits water conduction by aquaporin-4. J Struct Biol. 2009 Apr;166(1):16-21.

39. Huber VJ, Tsujita M, Kwee IL, Nakada T. Inhibition of aquaporin 4 by antiepileptic drugs. Bioorg Med Chem. 2009 Jan 1;17(1):418-24.

40. Thorne RG, Hanson LR, Ross TM, Tung D, Frey WH, 2nd. Delivery of interferon-beta to the monkey nervous system following intranasal administration. Neuroscience. 2008 Mar 27;152(3):785-97.

CHAPTER FOUR

SMALL INTERFERENCE RNA AGAINST CONNEXIN-43 AFTER JUVENILE

TRAUMATIC BRAIN INJURY LEADS TO FUNCTIONAL RECOVERY

By

Andrew M Fukuda[a,b], Nina Nishiyama[c], Germaine Paris[c], Jerome Badaut[a,b]

[a]Department of Physiology, Loma Linda University, Loma Linda, CA 92354

[b]Department of Pediatrics, Loma Linda University Medical Center, Loma Linda, CA 92350

[c]Loma Linda University, Loma Linda, CA 92354

Abstract

Juvenile traumatic brain injury (jTBI) is the leading cause of death and disability for children and adolescents in the United States of America, but there is no pharmacological treatment after injury. Perivascular astrocytes and the astrocyte network is known to be affected by many brain pathologies and is hypothesized to be responsible for the secondary injury cascade, where cells and regions further from the actual site of injury are affected detrimentally. One such secondary injury pathway is blood brain barrier disruption and edema, for which several astrocyte proteins are highly likely to be responsible. We have previously published one of these key perivascular astrocyte proteins, aquaporin 4 (AQP4), to be increased after jTBI at multiple timepoints after injury and have shown that decrease of AQP4 expression with small interference RNA against AQP4 mitigates edema formation and the presence of reactive astrocytes after juvenile traumatic brain injury (jTBI). Due to the proximity of the AQP4 water channels and gap junctions and the possibility of water diffusion via gap junctions, the potential role of the astrocytic gap junction forming connexins were studied. In the first part of the experiment, changes in proteins involved in the formation of the astrocyte network gap junctions: Cx30 and Cx43, were evaluated after jTBI. In a second experiment, we evaluated the effect of small interference RNA against Cx43 on edema formation, reactive astrogliosis, and motor recovery.

Cx proteins make up the gap junctions which connect neighboring astrocytes, allowing for the flow of ions, metabolites, neurotransmitters, and water. It has been speculated that these Cxs are responsible for the secondary injury cascade because of this flow from the primary injury site to distant sites, and AQP4 may be functionally coupled

102

to Cx43. We observed that Cx43 was increased at 3d, 7d, and 60d in the perilesional cortex, and Cx30 was increased at 1d and 3d. We also observed Cx43 to be increased at 3d and 7d in the CA1 and Cx30 increased at 1d in the same region. Additionally, astrogliosis was increased after jTBI at 1d, 3d, 7d, and 60d as seen via GFAP analysis. siCx43 did result in improved motor recovery and decreased GFAP immunoreactivity but did not result in differences in edema formation as measured via T2 (water content) or ADC (water mobility) using MRI at 1d or 3d. From this, we can speculate that although decreasing Cx43 has beneficial roles, the protein may not be contributing to the initial edema formation phase after jTBI in our model.

Introduction

In the US, the annual incidence of non-military related traumatic brain injury (TBI) is approximately 1.7 million, of which 327,000 are hospitalized and 52,000 die (Faul et al., 2010). Juvenile traumatic brain injury (jTBI), which is the leading cause of death and disability in children and adolescents (Faul et al., 2010), is of especially severe concern because the population group most affected (emergency department visit, hospitalization, and death) are those younger than five, followed by teenagers 15 – 19 years old (Faul et al., 2010). The effect of jTBI is two-fold: primary injury and secondary injury. Primary injury results mainly from the direct and immediate biomechanical disruption of the brain tissue. Secondary injuries are the result of an indirect and more delayed molecular mechanism occurring at sites directly surrounding the impacted site and evolves toward regions at a distance from the initial impact site (Bauer and Fritz, 2004). Primary injury can only be lessened by taking preemptive caution such as wearing helmets, so the goal of potential therapeutics is to lessen the damage caused by the secondary injury (Morales et al., 2005). Some of the major determiners for secondary injury cascade are blood brain barrier (BBB) disruption and edema and cellular swelling (Bauer and Fritz, 2004). However, no pharmacological treatments exist against this ruthless epidemic.

Although various cell types such as neurons, oligodendrocytes, and endothelial cells swell after injury, astrocytes are the first cell types to swell, and the swelling lasts the longest; in fact, perivascular astrocyte endfeet can swell within minutes after injury (Grange-Messent and Bouchaud, 1994), and this swelling may spread from primary injury site to distant sites: thus being responsible for the secondary injury cascade.

Therefore the need to study the astroglial pathophysiology after jTBI is necessary to successfully target these injury cascades such as edema. We have previously published a study in which the expression level of aquaporin 4 (AQP4) - a key perivascular astrocyte endfeet protein responsible for water homeostasis under normal condition and the edema process after injury - was shown to increase at multiple timepoints after jTBI that coincided with both the peak of edema formation at 3d and edema resolution at 7d (Fukuda et al., 2012a), and early downregulation of this protein via small interference RNA after brain injury showed beneficial effects after jTBI both during the acute and chronic phase due to decreased edema (Fukuda et al., 2013).

However, the aforementioned spread of secondary injury is not only due to the entrance of water from the peripheral blood stream to the brain parenchyma across AQP4, but most likely also due to the astrocyte network, which is mediated by gap junctions. Astrocytic gap junctions form the connection between neighboring astrocytes, allowing the flow of various molecules and water, and the proteins that make up these gap junctions are the connexins (Giaume et al., 2010). Six connexin proteins form a connexon, which is a hemichannel, and when a hemichannel from one cell attaches with another hemichannel of an adjacent cell, that is called a gap junction. Therefore, 12 connexins make up one gap junction (Giaume et al., 2010). The connexin subtypes are named according to their molecular weight, thus Cx43 has a molecular weight of 43 kiloDalton and Cx30 has that of 30 kiloDalton. Of these connexins, Cx43, which is predominantly astrocytic (Giaume et al., 2010; Rash et al., 2001), is one of the most studied connexin in the brain and highly expressed in astrocytes, which far outnumber other cell types in the brain, including neurons (Sofroniew and Vinters, 2010). Connexin

43 form a hemichannel that has an aqueous pore and selectively permits flow of small endogenous molecules such as second messengers, amino acids, nucleotides, small peptides, and also water (Giaume et al., 2010; Goodenough and Paul, 2003; Herve and Derangeon, 2012; Wallraff et al., 2006). The hypothesized spread of detrimental factors and toxic metabolites such as sodium and calcium ions, apoptotic factors, lysophospholipids, cAMP, and IP3 from the primary injury site to more distant sites mediated by gap junctions is referred to as "bystander effect (Andrade-Rozental et al., 2000; Perez Velazquez et al., 2003)," and several studies have shown astrocytic connexin levels to be increased in affected brain regions after cerebrovascular pathologies such as stroke (Chew et al., 2010). However, no study has been done to characterize the levels of the astroglial gap-junction forming connexins after jTBI.

Several studies using general gap junction inhibitors such as carbenoxolone and octanol have shown better outcome in several ischemic stroke models (Andersson et al., 2011; Frantseva et al., 2002; Perez Velazquez et al., 2006; Rawanduzy et al., 1997). Of note, Wu et al. have recently shown that injection of antisense-oligodeoxynucleotide against Cx43 (AS-ODN Cx43) into the lateral ventricle one hour prior to TBI in adult rats led to decreased edema (as measured via the wet-dry brain weight method) and decreased astrogliosis up to 48 hrs after injury compared to control group (Wu et al., 2013). But to date, there is no study done for a jTBI model in which Cx43 was specifically inhibited. We have previously shown small interference RNA against aquaporin 4, another astrocyte protein essential in the edema process after jTBI (Fukuda et al., 2012a), to be beneficial after injury (Fukuda et al., 2013). Therefore, in this study, the therapeutic potential of small interference RNA against Cx43 (siCx43) will be pursued after jTBI.

Methods to inhibit Cx43 specifically by targeting its mRNA have been effective in several *in vitro* models (Chew et al., 2010), and the use of siCx43 *in vivo* in a model of corneal endothelial injury have also shown beneficial results (Grupcheva et al., 2012). Thus, siCx43 would be a specific and effective method to downregulate Cx43 protein to study the functional behavior outcome after jTBI. Furthermore, edema, astrogliosis, and blood brain barrier (BBB) disruption will be studied because they are common pathophysiological targets of jTBI influenced by the astrocyte network (Fukuda et al., 2013).

Materials and Methods

General Experimental Setup

Two groups of studies were planned and performed. The first groups of studies were constructed in order to examine the changes in the astrocyte network connexin proteins (Cx43, Cx30) and GFAP levels after juvenile traumatic brain injury. The second group of studies were constructed in order to examine the effect of small interference RNA against Cx43 (siCx43) injection after juvenile traumatic brain injury on astrocyte network connexin proteins (Cx43, Cx30), GFAP, blood brain barrier permeability (IgG), edema (ADC, T2), and behavior/motor activities.

Animal Care

All animal care and experiments were conducted according to the Guidelines for Care and Use of Experimental Animals approved by Loma Linda University. All protocols and procedures were in compliance with the U.S. Department of Health and

Human Services Guide and were approved by the Institutional Animal Care and Use

Committee of Loma Linda University. Postnatal day 17 (P17) Sprague Dawly rat pups

were housed in a temperature controlled (22-25°C) animal facility on a 12-hour light/dark

cycle with standard lab chow and water *ad libitum*.

siRNA Preparation

An *in vivo* Cx43 silencing protocol was adapted as described in our previous

studies.(Badaut et al., 2011) Briefly, SMART-pool® containing 4 siRNA-duplexes

against Cx43 (400ng, siCx43, Dharmacon Research) and non-targeted siRNA (siGLO

RISC-free-control-siRNA, Dharmacon Research) were mixed with interferin® (Polypus-

transfection, Illkirch, France) diluted in a saline solution (0.9%) containing 5% glucose

for a final volume of 5 µL and incubated on ice for 20 min before injection.

Controlled Cortical Impact and siRNA Injection

Controlled cortical impact (CCI) was carried out on P17 old rat pups as

previously described (Ajao et al., 2012; Fukuda et al., 2012a; Fukuda et al., 2013). Rats

were anesthetized with isoflurane and placed in a stereotaxic apparatus (David Kopf

Instrument, Tujunga, USA). A 5 mm diameter craniotomy over the right hemisphere 3

mm posterior from bregma and 4 mm lateral to midline was performed. Animals were

subjected to CCI using an electromagnetic impactor with a 2.7 mm round tip set to

impact with a velocity of 6 m/s and a depth of 1.5 mm below the cortical surface (Leica,

Richmond, IL). Sham animals received the craniotomy, but without the cortical impact.

The craniotomy did not cause damage to the dura mater and was intact in both the jTBI

and sham groups. After CCI, none of the animals had major bleeding or cortical tissue herniation.

siRNA administration was performed as previously described (Fukuda et al., 2013). Injection of siRNA was performed 10 min after the injury lateral to the site of the impact using a 30-gauge needle on a Hamilton syringe (3 mm posterior to bregma, 6 mm lateral to midline, and 1.0 mm below cortical surface). The syringe was attached to a nanoinjector (Leica, Richmond, IL) and 4 µL of either siCx43 or siGLO was administered at a rate of 0.5 µL/min. After suturing, all pups were placed on a warm heating pad for recovery before being returned to their dams. A second siRNA injection was repeated 2 days after the CCI in all pups that received siRNA using the same injection protocol.

Magnetic Resonance Imaging (MRI)

MRI was performed at 1 and 3d to follow the process of edema formation and to observe water content and water mobility at the peak of edema in this model (Fukuda et al., 2012a; Fukuda et al., 2013). Pups were lightly anesthetized using isoflurane (1.0%) and imaged on a Bruker Avance 11.7 T (Bruker Biospin, Billerica, MA)(Fukuda et al., 2013) Two imaging data sets were acquired: 1) a 10 echo T2- and 2) a diffusion weighted imaging (DWI) sequence in which each sequence collected 20 coronal slices (1 mm thickness and interleaved by 1 mm). The 11.7T T2 sequence had the following parameters: TR/TE = 2357.9 / 10.2 ms, matrix = 128 x 128, field of view (FOV) = 2 cm, and 2 averages. The DWI sequence had the following parameters: TR/TE = 1096.5 / 50

ms, two b-values (116.960, 1044.422 s/mm^2), matrix = 128 x 128, FOV = 2 cm, and 2 averages.

Region of Interest (ROI) and Volumetric Analysis

T2 and apparent diffusion coefficient (ADC) values were quantified using previously published standard protocols (Badaut et al., 2011). Regions of interest (ROIs) were placed on the imaging section with the maximally detected injury using Cheshire (Parexel International Corp. Waltham, MA). Lesion and ipsilateral hippocampus were delineated on T2 images and overlaid onto corresponding T2 and ADC maps. The mean, standard deviation, and area for each ROI were extracted.

Behavioral Testing

Foot-fault and rotarod testing was performed at 1d and3d in both the siCx43 and Control group. The foot-fault test evaluated sensorimotor, coordination, and proprioception while the rotarod test evaluated sensorimotor coordination and balance as previously reported in our earlier studies.(Ajao et al., 2012) All tests at each time-point were carried out on siGLO and siCx43 treated rats within a 3-hours morning time-block (8 − 11 am). siGLO and siCx43 treated rats were interleaved in testing sequence. To further control potential confounds, the same tests were administered in the same order at all of the time points, by the same investigators blinded to the experimental groups.

Foot-fault testing was carried out on an elevated platform (50 cm X 155 cm, ClosetMaid, Ocala, FL) with parallel wire bars 1.5 cm apart and raised 100 cm above the floor. Rats were placed in the middle of the platform to freely roam around. When a

rodent's paw (fore- or hindlimb) slipped completely through the wire mesh, it was considered as an individual fault. The average foot-fault score was calculated from the total number of faults from two 60 sec trials.

Rotarod evaluation was performed on all the animals at 1d and 3d (SD Instruments, San Diego, CA). A rotating 7 cm-wide spindle with a continuous speed (10RPM and 20 RPM) was used to evaluate performance during two trials per speed. Latency to fall was the outcome measure used as a measure of motor coordination and balance. The maximum time spent on the test was 60s, if the rat did not fall, at which point the rotation was halted and the rat was taken off of the spindle. The average time from the 2 trials was calculated and expressed in total time (s) for 2 trials.

Immunohistochemistry and Image Analysis

For the first set of experiments in which the connexin and GFAP expression was studied between animals who received CCI and sham group, at 1d, 3d, 7d, and 60d animals were transcardially perfused with 4% paraformaldehyde and brains were extracted and put in 30% sucrose for 48 hours, then stored in -22°C. Coronal sections were cut at 20 μm thickness at -22°C on a cryostat (Leica, Richmond, IL) and mounted on slides for immunohistochemical analysis (Badaut et al., 2007; Badaut et al., 2011; Hirt et al., 2009). For the second set of experiments in which siRNA was injected after jTBI, animals were transcardially perfused at 3d.

The primary antibodies used for immunohistochemistry were rabbit polyclonal antibodies for Cx43 (1:100, Abcam, Cambridge, MA), rabbit polyclonal antibodies for Cx30 (1:100, Abcam, Cambridge, MA), and chicken polyclonal antibodies for GFAP

(1:1000, Millipore, Billerica, MA). The secondary antibodies used were IRDye 800 conjugated affinity purified donkey-anti-rabbit IgG (1:1000, Rockland, Gilbertsville, PA), IRDye 680 conjugated affinity purified donkey-anti-chicken IgG (1:1000, Rockland, Gilbertsville, PA), Alexa 594 conjugated affinity purified goat anti-rabbit IgG (1:1000, Invitrogen, Carlsbad, CA), Alexa 488 conjugated affinity purified goat anti-rabbit IgG (1:1000, Invitrogen, Carlsbad, CA), Alexa 568 conjugated affinity purified goat anti-chicken IgG (1:1000, Invitrogen, Carlsbad, CA), and Alexa 488 conjugated affinity purified goat anti-chicken IgG (1:1000, Invitrogen, Carlsbad, CA).

For immunohistochemistry, sections were washed with PBS, blocked with 1% BSA in PBS, incubated with the respective primary antibodies in PBS containing 0.1% Triton X-100 and 1% bovine serum albumin overnight, then incubated for 2 hours at room temperature with affinity purified secondaries conjugated to the desired wavelength in PBS containing 0.1% Triton X-100 and 1% bovine serum albumin. After washing, sections were scanned on an infra-red (IR) scanner (Odyssey) to quantify fluorescence for the different ROIs as previously described (Badaut et al., 2011) or imaged under a confocal laser microscope (Zeiss). For sections to be imaged under a confocal microscope, sections on glass slides were cover-slipped with anti-fading medium VectaShield containing 4',6-diamidino-2-phenylindole (DAPI) (Vector, Vector laboratories, Burlingame, CA, USA).

All image acquisition parameters for the same proteins were kept constant for all of the animals for analysis and visualization purposes and all analysis was carried out in a non-biased, blinded manner. For the analysis of Cx43, Cx30, and GFAP, the following method was used as previously described (Fukuda et al., 2013). The slides with the above

112

mentioned primary antibodies with the secondaries conjugated to the infrared wavelength (680 or 800 nm) were scanned on an infrared scanner (Odyssey, Lincoln, NE), and images were saved with a resolution of 21 μm per pixel. Identical circular regions of interests (ROIs) were drawn in the perilesional cortex and in the ipsilateral CA1 at three different bregma levels (-1.40mm, -2.56mm, and -3.80mm): the bregma level where lesion area was largest, one slice anterior and one posterior. The average fluorescence of these regions of interests was calculated to show immunoreactivity of each of the protein and between groups.

Negative control staining where the primary antibody or secondary antibody was omitted showed no detectable labelling.

For immunoglobulin (IgG) extravasation immunohistochemistry, sections were washed with PBS, blocked with 1% BSA in PBS, then incubated for 2 hours at room temperature with IRDye 800 conjugated affinity purified goat-anti-rat IgG (1:500, Rockland, Gilbertsville, PA) in PBS containing 0.1% Triton X-100 and 1% bovine serum albumin. After washing, sections were scanned on an infra-red (IR) scanner (Odyssey) to quantify fluorescence for the different ROIs and also to measure the area of extravasation divided by the total brain area per ROI.

<center>Western Blot</center>

At 3d and 7d, the brains were freshly extracted from another set of sham and jTBI animals, the cortical tissue adjacent to the site of impact was collected and frozen for western blot analysis as previously published (Fukuda et al., 2012a). Tissues were placed in a tube with RIPA buffer with protease inhibitor cocktail (PIC, Roche, Basel,

Switzerland) and sonicated for 30s and stored in -20C. These samples were then assayed for total protein concentration by bicinchoninic acid assay (BCA, Pierce Biotechnology Inc., Rockford, IL). Ten micrograms of protein was then subjected to SDS polyacrylamide gel electrophoresis on a 4–12% gel (Nupage, Invitrogen, Carlsbad, CA, USA). Proteins were then transferred to a polyvinylidene fluoride membrane (PerkinElmer, Germany). The blot was incubated with a rabbit polyclonal antibody against Cx43 (1:1000, Abcam, Cambridge, MA) or Cx30 (1:1000, Abcam, Cambridge, MA) and a monoclonal antibody against tubulin (Sigma, Switzerland, 1:25,000) in Odyssey blocking buffer (LI-COR, Bioscience, Germany) for 2 h at room temperature. After washing in PBS for 3x10min, the blot was incubated with two fluorescence-coupled secondary antibodies (1:10,000, anti-rabbit Alexa-Fluor-680 nm, Molecular Probes, Oregon and anti-mouse infra-red-Dye-800-nm, Roche, Germany) for 2 h at room temperature. After washing in PBS, the degree of fluorescence was measured using an infra-red scanner (Odyssey, LI-COR, Germany) as previously published (Fukuda et al., 2013). The value of Cx43 and Cx30 was normalized to tubulin and compared between jTBI and sham at each timepoint.

Statistics

One way ANOVA was used for immunohistochemistry analysis and western blot to compare the mean between the sham and jTBI group at each timepoint. One way ANOVA was used for immunohistochemistry analysis to compare the mean between siGLO and siCx43 group as well. Two-way repeated measures analysis of variance with a

114

post hoc Bonferroni test was used for the behavior and MRI data. A p value less than 0.05 was considered to be statistically significant.

Results

Chronic Increase of Connexin 43 Expression after jTBI

Cx43 protein changes were first evaluated using infra-red immunohistochemistry at 1d, 3d, 7d and 60d post-jTBI. At 1d, there was no significant difference (Fig. 1A). However, during the edema period from 3d to 7d in this model (Fukuda et al., 2012b), increase in the level of Cx43 immunofluorescence at 3d and 7d compared to age-matched sham operated animals in the perilesional cortex was observed (Fig. 1A, $p<0.05$). Furthermore, the increase of the Cx43 immunoreactivity was still observed up to 60d, suggesting a signature involvement of the reactive astrocytes. Similar increase at 3d was observed ($p<0.05$) in ipsilateral hippocampus located under the site of the impact, when compared to age-matched sham operated animals (Fig. 1B). However, after 3d there were no significant changes in Cx43 in the hippocampus. No differences were observed between groups in the contralateral cortex and hippocampus.

The immunohistochemistry data was confirmed by western blot analysis for the time points 3 (Fig. 1C) and 7days (Fig. 1D). Cx43 western blot showed an expected band at 43 kda in both groups, with a higher intensity for the jTBI group compared to sham animals. The level of intensity of Cx43 was normalized to beta-tubulin, used as a housekeeping protein (Fig. 1C-F). The quantification of the band showed a significant increase for the two time points, with 30% increase at 3d (Fig. 1E) and 200% increase at 7d (Fig. 1F).
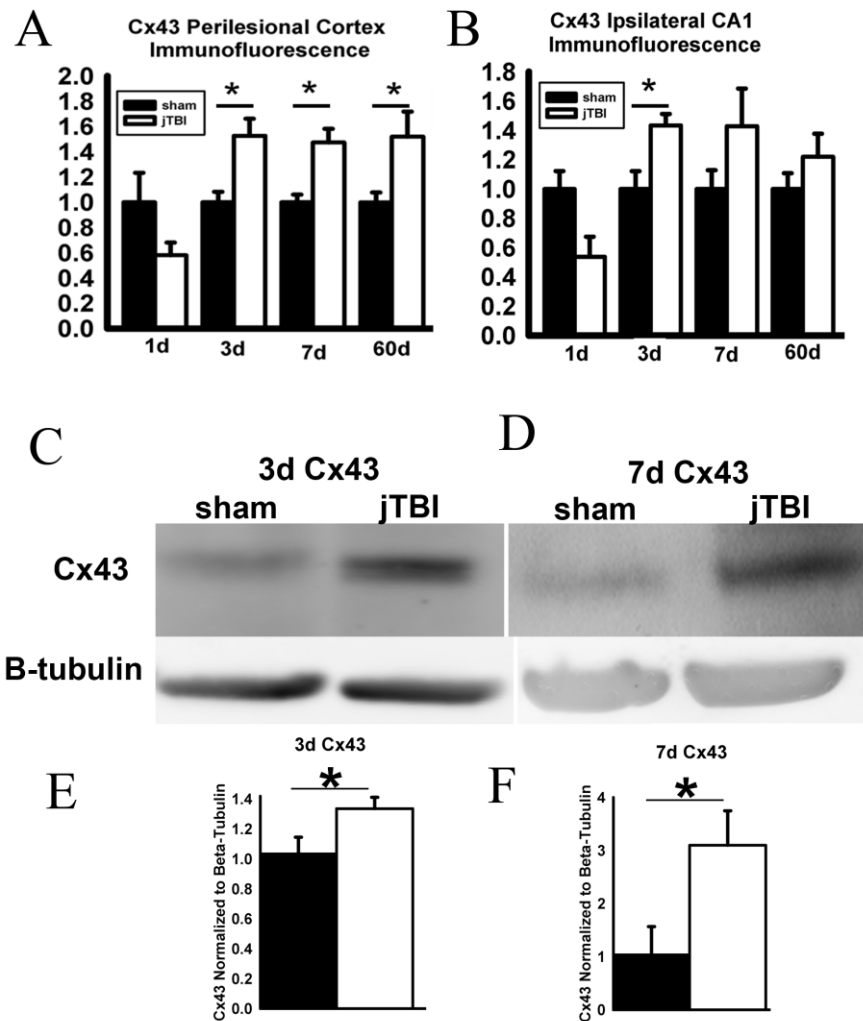
Figure 1. Chronic increase of Connexin 43 expression after jTBI. (A) Cx43 staining quantification in the perilesional cortex showed increased Cx43 immunoreactivity at 3d, 7d, and 60d after jTBI as compared to sham. (B) Cx43 immunoreactivity in the ipsilateral hippocampus showed a significant increase at 3d (*p<0.05). Western blot of Cx43 at 3d (C) and 7d (C) shows a distinct band of Cx43 at around 43kDa. jTBI shows a significantly higher expression of Cx43 at both 3d (E) and 7d (F) compared to sham. (Cx43, connexin 43; kDa, kilo Dalton; jTBI, juvenile traumatic brain injury; *p<0.05).

Connexin 30 is Upregulated Acutely after jTBI

Cx30 protein changes were first evaluated using infra-red immunohistochemistry at 1d, 3d, 7d and 60d post-jTBI. At 1d and 3d, a significant increase was observed in immunoreactivity in the perilesional cortex in the injured animals compared to age-matched sham operated control animals (Fig. 2A, $p<0.05$). However, no significant difference was observed in the perilesional cortex at 7d and 60d. In the ipsilateral hippocampus located under the site of the impact, a significant increase in Cx30 immunoreactivity was observed at 1d ($p<0.05$) when compared to age-matched sham operated animals but not at the other timepoints (Fig. 2B).

The immunohistochemistry data was confirmed by western blot analysis for the time points 3 (Fig. 2C) and 7days (Fig. 2D). Cx30 western blot showed an expected band at 30 kDa in both groups, with a higher intensity for the jTBI group compared to sham animals at 3d. The level of intensity of Cx43 was normalized to beta-tubulin, used as a housekeeping protein (Fig. 2C-F). The quantification of the band showed a 200% increase at 3d (Fig. 2E, $p<0.05$), but no significant difference at 7d (Fig. 2F).
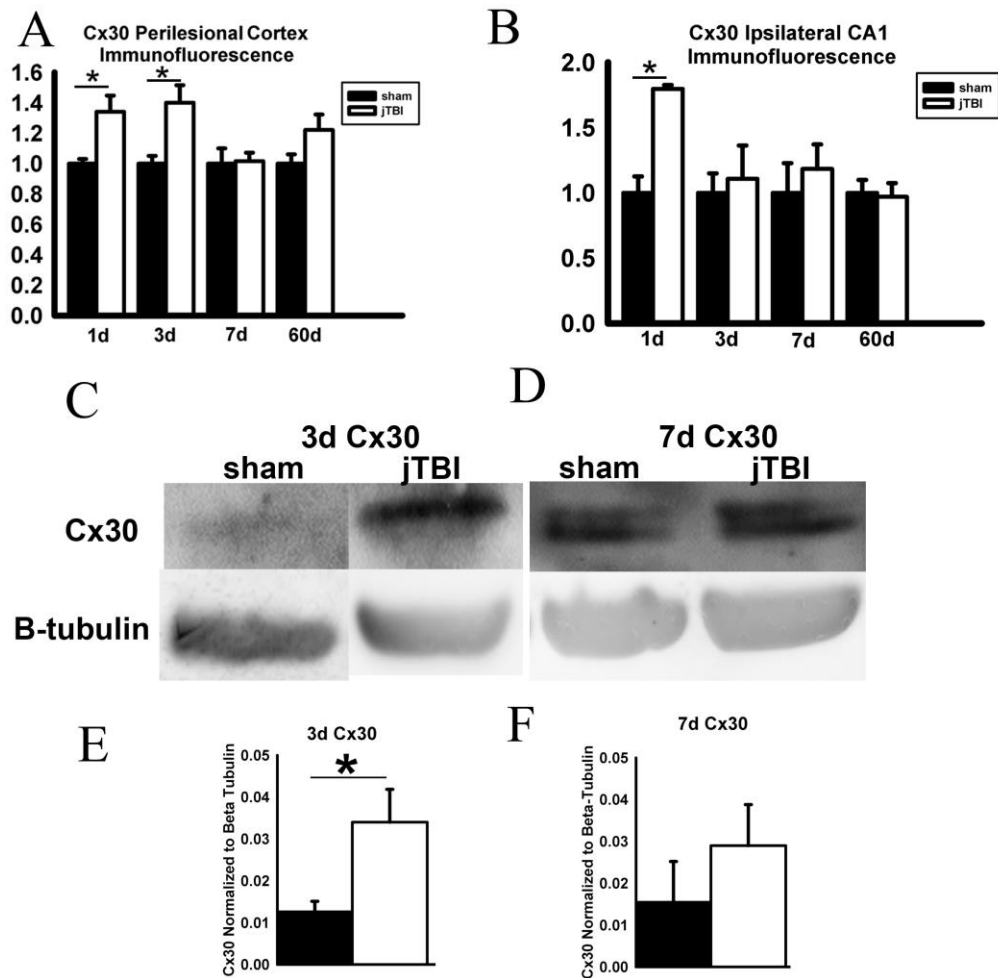
Figure 2. Connexin 30 is upregulated acutely after jTBI. (A) Cx30 staining quantification in the perilesional cortex showed increased Cx30 immunoreactivity at 1d and 3d after jTBI as compared to sham. (B) Cx30 immunoreactivity in the ipsilateral hippocampus showed a significant increase at 1d (*p<0.05). Western blot of Cx30 at 3d (C) and 7d (C) shows a distinct band of Cx30 at around 30kDa. jTBI shows a significantly higher expression of Cx30 at 3d (E) but not at 7d (F) compared to sham. (Cx30, connexin 30; kDa, kilo Dalton; jTBI, juvenile traumatic brain injury; *p<0.05).

Astrogliosis Occurs and is Maintained after jTBI.

The extent of astrogliosis was studied via glial fibrillary astrocytic protein (GFAP)-immunoreactivity (Fig. 3). GFAP is found in the astrocyte cytoskeleton and routinely used for studying astrocytes. GFAP staining intensity was increased in the perilesional cortex in jTBI induced rat pups compared to the age-matched control group at 1d, 3d, 7d, and 60d (Fig. 3A). Unlike the perilesional cortex in which a significant increase in astrogliosis was observed at all timepoints tested, in the ipsilateral hippocampus, a significant increase ($p<0.05$) was only observed at 1d (Fig. 6C).
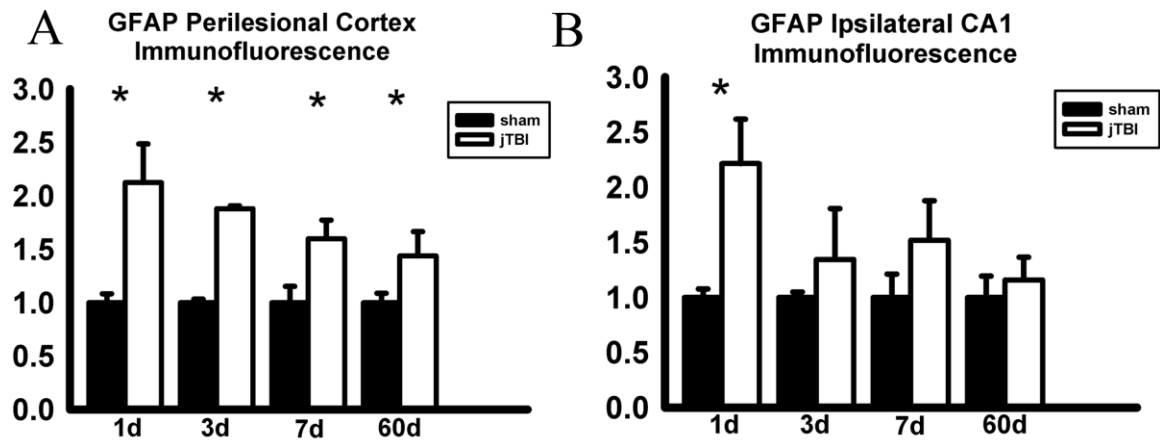
Figure 3. Astrogliosis occurs and is maintained after jTBI. (A) GFAP staining quantification in the perilesional cortex showed increased GFAP immunoreactivity at 1d, 3d, 7d, and 60d after jTBI as compared to sham. (B) GFAP immunoreactivity in the ipsilateral hippocampus showed a significant increase at 1d (*p<0.05). (GFAP, glial fibrillary acidic protein; jTBI, juvenile traumatic brain injury; *p<0.05).

siCx43 Injection Reduces Cx43 Expression
Acutely after Injury

Once the normal pathological change of astrocyte connexin was studied using jTBI and sham control animals, the next step was to test the effect of decreasing this protein. Because Cx43 expression after injury has been studied more extensively and thus far has been proposed to play a more central role in pathophysiological cascades after injury (Chew et al., 2010; Grupcheva et al., 2012; Nakase et al., 2004; Ohsumi et al., 2010; Theodoric et al., 2012; Wu et al., 2013; Yoon et al., 2010), for our study Cx43 was chosen as the potential target. For this purpose, siRNA against Cx43 (siCx43) was injected in the lesion site after injury. To see if siCx43 was effective in decreasing Cx43 expression, Cx43 protein changes were evaluated using infra-red immunohistochemistry at 3d post-jTBI. Injection of siCx43 induced a significantly lower level of Cx43 compared to siGLO control group 3d after the injury (19% decrease) in the perilesional cortex (Fig. 4A), but no significant difference was observed in the ipsilateral hippocampus (Fig. 4B).
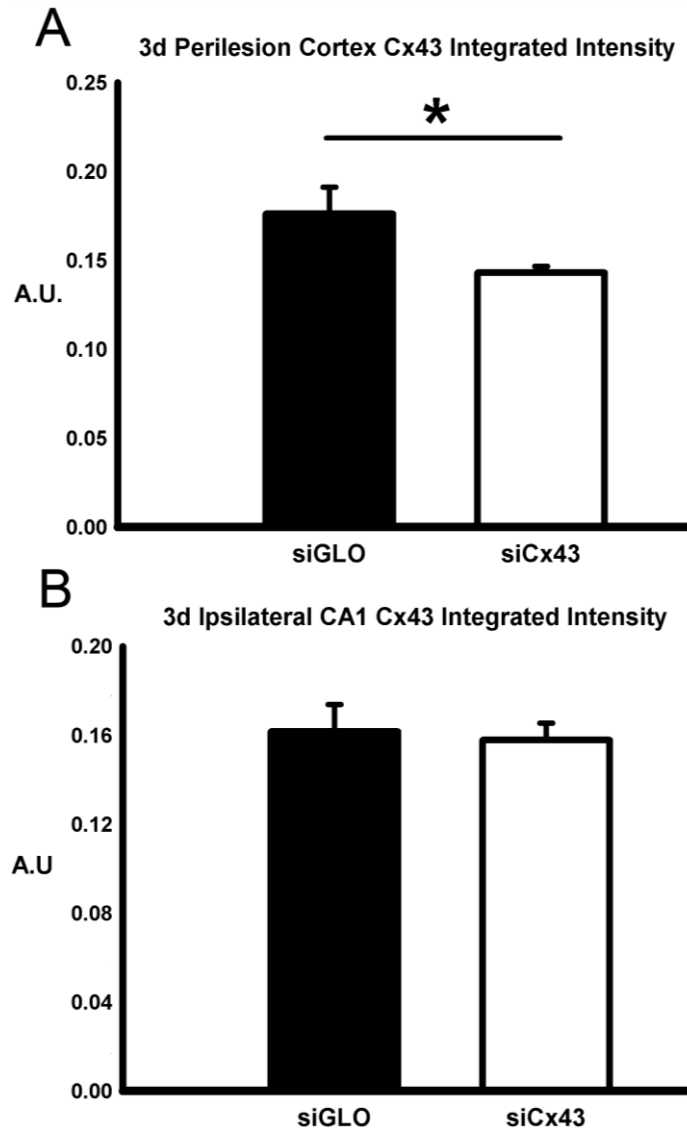
Figure 4. siCx43 Injection Reduces Cx43 Expression Acutely after Injury. Cx43 immunoreactivity was quantified and confirmed a significant decrease in Cx43-immunoreactivity in the siCx43 compared to siGLO treated rats in the (A) perilesional cortex but not in the (B) ipsilateral hippocampus (*, $p < 0.05$). (Cx43; connexin 43).

siCx43 Injections did not Result in Changes in
Cx30 Expression Acutely after Injury

To test whether siCx43 injection had any acute effect on Cx30 expression due to either off targets effects or a compensatory mechanism, Cx30 protein changes were evaluated using infra-red immunohistochemistry at 3d post-jTBI as well. Injection of siCx43 did not result in a significant Cx30 immunoreactivity changes compared to siGLO control group 3d after the injury in neither the perilesional cortex (Fig. 5A) nor the ipsilateral hippocampus (Fig. 5B).
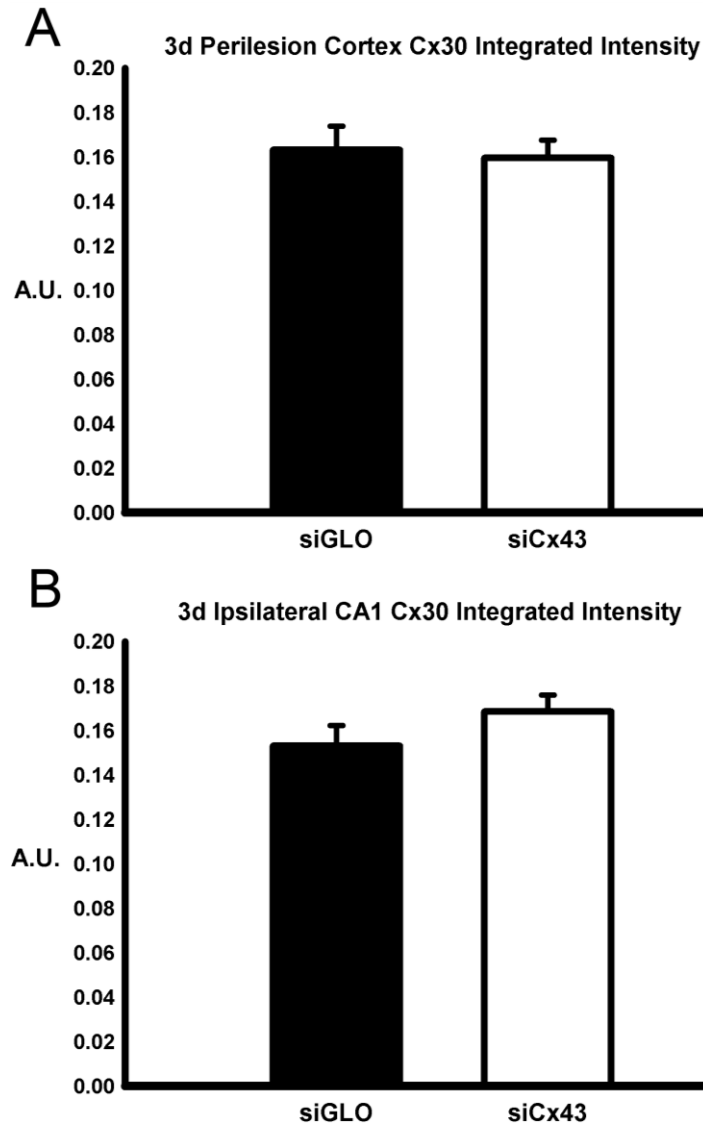
Figure 5. siCx43 Injections did not Result in Changes in Cx30 Expression Acutely after Injury. Cx30 immunoreactivity was quantified and showed no significant decrease in Cx30-immunoreactivity in the siCx43 compared to siGLO treated rats in both the (A) perilesional cortex and (B) ipsilateral hippocampus. (Cx30; connexin 30).

siCx43 Injection Resulted in Improved
Behavior Outcome after jTBI

To test whether Cx43 downregulation resulting from siCx43 injection had a beneficial effect regarding motor function recovery after injury, foot-fault and rotarod testing was performed at 1d and 3d. The foot-fault test evaluated sensorimotor, coordination and proprioception while the rotarod test evaluated sensorimotor coordination and balance. siCx43 pups had fewer foot-faults at 1 and 3d (respectively 24% and 36%, $p < 0.05$, Fig 6A). Although a trend was observed in which siCx43 animals were staying on the rotarod longer than siGLO control animals, the difference was not statistically significant (Fig. 6B).
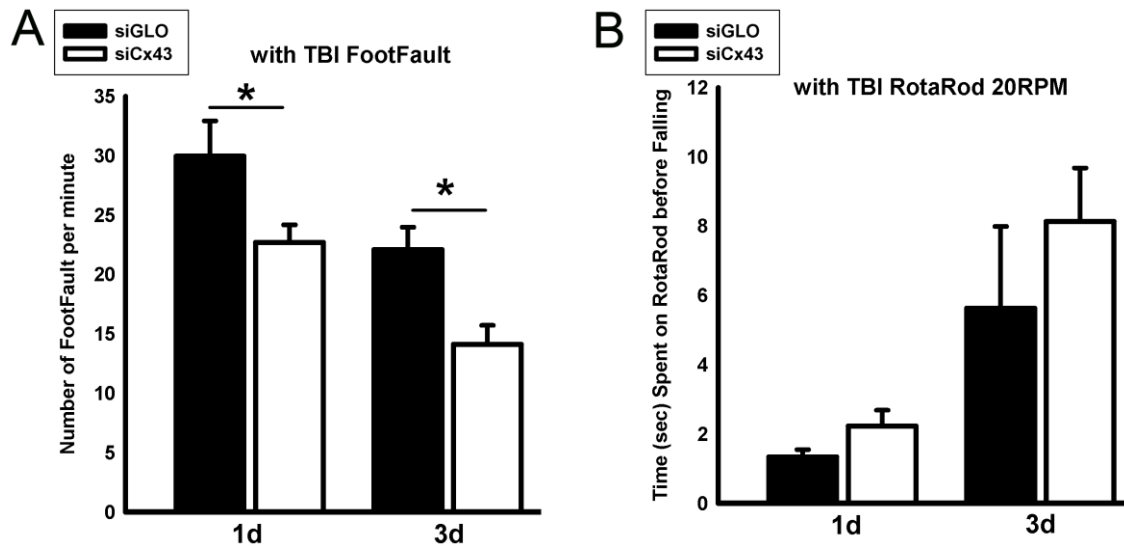
Figure 6. siCx43 Injection Resulted in Improved Behavior Outcome after jTBI. siCx43-treated pups had better functional outcomes as revealed by the foot-fault test. siCx43 group had significantly fewer foot faults than siGLO treated animals at day 1 (24%) and day 3 (36%) after jTBI (*, p < 0.05) (A). However, siCx43 animals' performance on the rotarod did not significantly differ with that of siGLO at neither 1d nor 3d (B).

siCx43 Animals had Reduced Astrogliosis after jTBI

Transgenic mice with Cx43 knocked out was associated with a decreased GFAP expression (Nakase et al., 2003) and Cx43 blockade has been shown to decrease GFAP immunoreactivity after injury (Wu et al., 2013). To study whether this was still valid in our model of jTBI, GFAP-infrared immunohistochemistry was used to assess the effects of siCx43 on neuroinflammation /astrogliosis after jTBI. There was a 17% decrease in GFAP immunofluorescence in the perilesional cortex of the siCx43 rat pups as compared to the siGLO control group (p<0.05, Fig. 7A). However, no significant difference was observed in the ipsilateral hippocampus (Fig. 7B).

Because astroglial connexins have been hypothesized to play a role in BBB permeability (Ezan et al., 2012) and BBB disruption is a major pathophysiology after jTBI, the BBB permeability was assessed via immunoglobulin G (IgG) immunohistochemistry. Under normal circumstance IgG is not observed in the brain, however IgG is observed after injury in which the BBB is disrupted because IgG is extravasated from the peripheral bloodstream into brain tissue. IgG extravasation was calculated as the percentage of the area of IgG staining to total brain slice area. At 3d, there was no significant difference in the extent of IgG extravasation between siCx43 (18.92%) and siGLO control (18.40%) (Fig. 7C), signifying no difference in the extent of BBB permeability between treated and untreated animals.
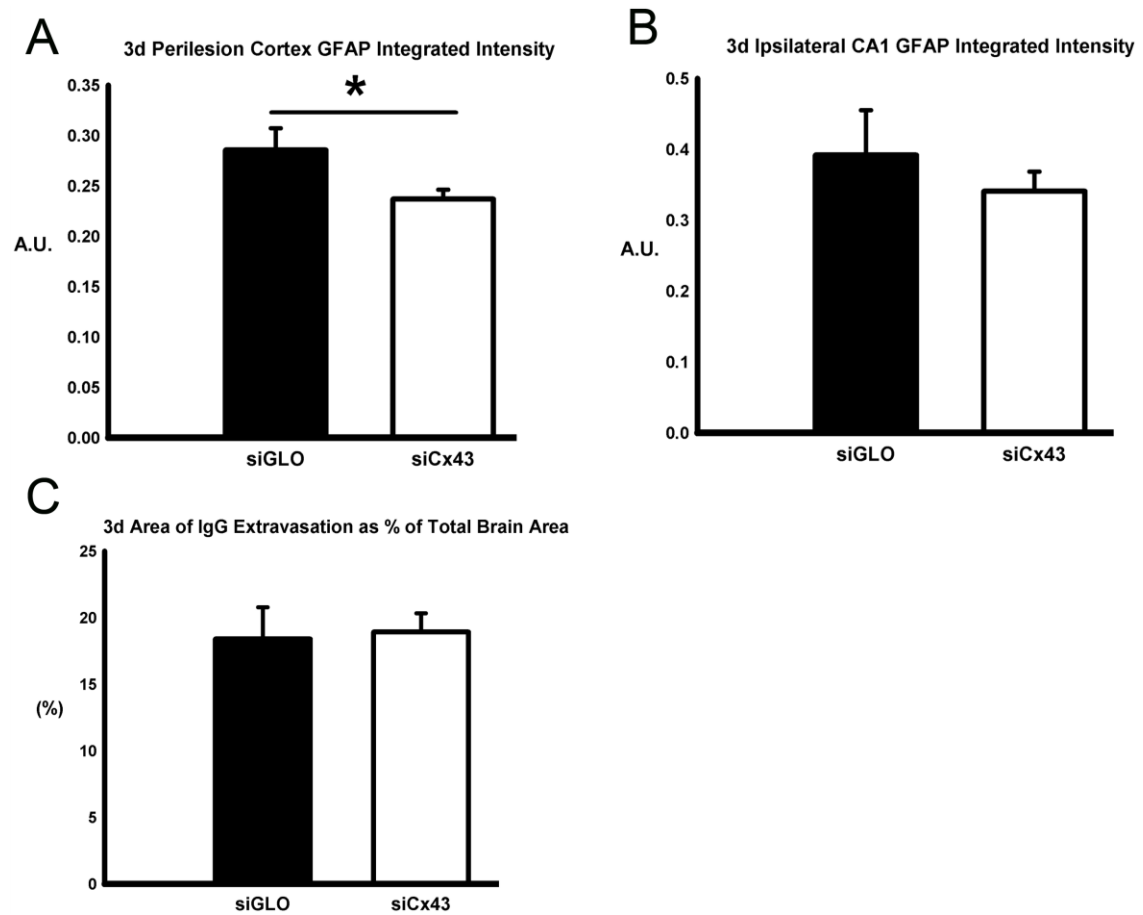
Figure 7. siCx43 animals had reduced astrogliosis after jTBI. GFAP staining quantification in the (A) perilesional cortex showed significant decrease in siCx43 compared to siGLO animals but not in (B) the ipsilateral hippocampus. (C) The extent of IgG extravasation was not significantly different between siGLO and siCx43 animals, signifying most likely the same extent of BBB disruption/permeability (*p<0.05). (GFAP, glial fibrillary acidic protein; jTBI, juvenile traumatic brain injury; IgG, Immunoglobulin G; *p<0.05).

Significant Difference in T2 and ADC was not Observed
Acutely between siCx43 and Control

To address the question of whether decreased Cx43 protein level via siCx43

injection would alter edema formation, MRI was utilized to obtain T2 and ADC values at

1d and 3d. T2 was chosen as a measurement of edema/water content and ADC was used

as a measurement of water mobility. T2 and ADC values were analyzed in the

perilesional cortex and ipsilateral hippocampus at 1d and 3d in all of the animals from the

siCx43 and siGLO groups. In the perilesional cortex, there was no significant difference

in T2 values between siGLO (1d – 116.58 +/- 6.82 ms; 3d – 93.54 +/- 3.47 ms) and

siCx43 (1d – 107.75 +/- 7.85 ms; 3d- 101.27 +/- 7.86 ms) (Fig. 8A). Similarly, in the

ipsilateral hippocampus, no significant difference was observed between siGLO (1d -

121.53 +/- 7.45 ms; 3d - 99.29 +/- 3.01 ms) and siCx43 (1d – 114.66 +/- 8.47 ms; 3d –

109.45 +/- 7.45ms) (Fig. 8B).

For ADC values in the perilesional cortex, no significant difference was observed

between siGLO (1d – 720.25 +/- 69.01 $x10^{-6}mm^2$/sec; 3d – 690.11 +/- 57.56 $x10^{-6}mm^2$/sec) and siCx43 (1d – 763.56 +/- 38.25 $x10^{-6}mm^2$/sec; 3d – 766.65 +/- 61.93 $x10^{-6}mm^2$/sec) (Fig. 8C). No significant difference was observed in the ipsilateral

hippocampus either between siGLO (1d – 708.02 +/- 62.70 $x10^{-6}mm^2$/sec; 3d – 703.98

+/- 70.18 $x10^{-6}mm^2$/sec) and siCx43 (1d – 769.96 +/- 59.07 $x10^{-6}mm^2$/sec; 3d – 815.10

+/- 91.68 $x10^{-6}mm^2$/sec) (Fig. 8D).
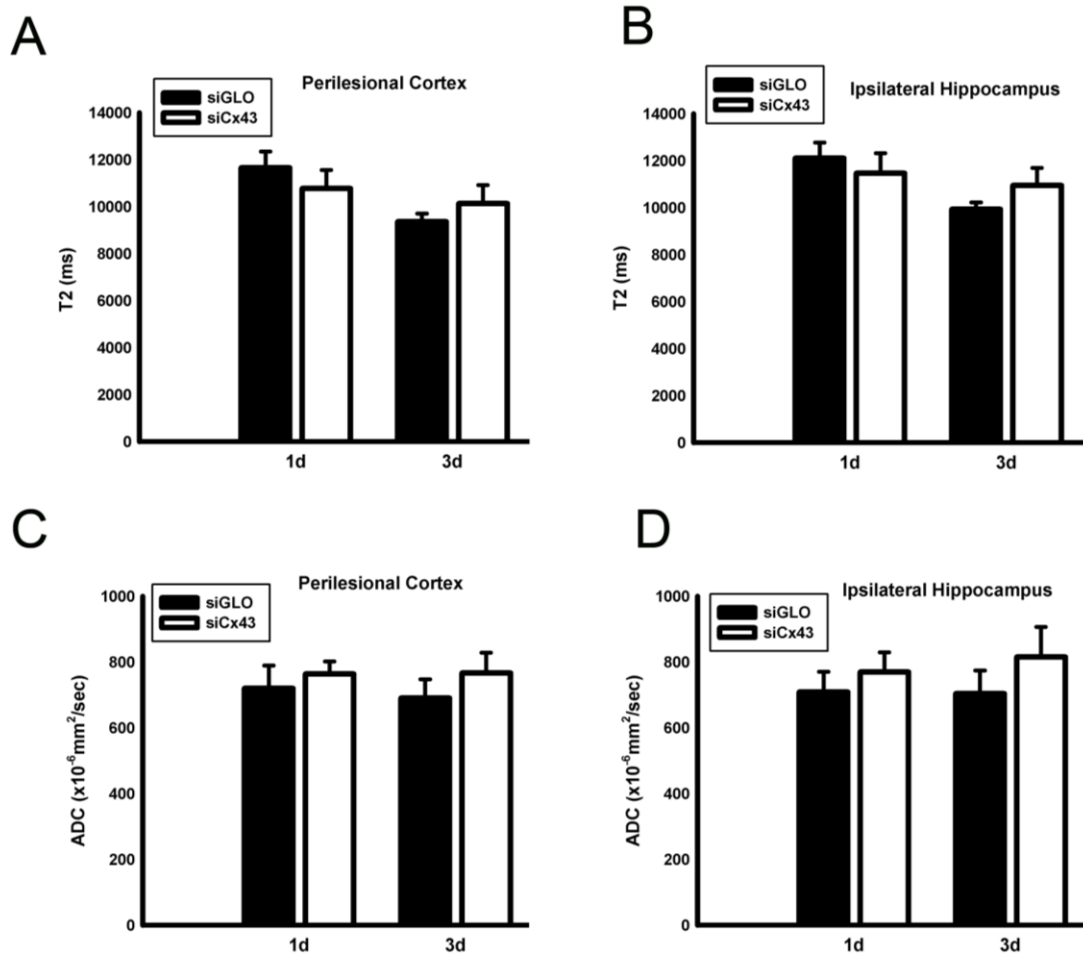
Figure 8. Significant difference in T2 and ADC was not Observed Acutely between siCx43 and Control. The extent of edema formation was assessed via MRI using T2 (water content) and ADC (water mobility). The T2 value did not significantly differ between siCx43 and siGLO pups within the (A) perilesional cortex or (B) ipsilateral hippocampus at neither 1d nor 3d (B). The ADC value did not significantly differ between siCx43 and siGLO pups within the (C) perilesional cortex or (D) ipsilateral hippocampus at neither 1d nor 3d. This most likely signifies that siCx43 did not result in changes in the edema formation after jTBI.

Discussion

Our novel study is the first to characterize the changes in Cx43 and Cx30 proteins after jTBI and also to assess the effect of a post injury administration of siCx43 in a model of jTBI during the acute period.

Cx30 and Cx43 were increased in the perilesional cortex and ipsilateral CA1 after jTBI, although in a different pattern. GFAP was also used to assess the extent of astrogliosis after jTBI, and was observed to be increased after jTBI as well.

siCx43 treatment after jTBI resulted in an improved neurobehavioral outcome and decreased reactive astrogliosis, resulting from a decreased Cx43 level. To the best of our knowledge, this is the first study to use neurobehavioral test as an outcome assessor after specific inhibition of Cx43 in a TBI model.

Changes Seen in Astrocytic Connexins after jTBI

Astrocytes form a network in which individual astrocytes connect with each other, allow neurotransmitter and ionic flow, and influence each other and the network as a whole. Appropriately, the term, astrocyte network (Giaume et al., 2010) is frequently used to describe this characteristic in which astrocytes are interconnected with each other through gap junctions that are made of connexin proteins: predominantly connexin 43, and also connexin 30, that facilitate intercellular communication (Giaume et al., 2010; Seifert et al., 2006). Despite this interest, there is yet much more to be studied for the ultimate goal of finding therapeutics for those suffering from presently untreatable or incurable cerebral dysfunctions. Astrocytes and the network they form are essential for normal brain function, and disruption of this network due to traumatic brain injury leads

to pathological cascades such as excitotoxicity, apoptosis, neuroinflammation, and edema (Fukuda et al., 2012a; Kimelberg, 2005; Woodcock and Morganti-Kossmann, 2013; Zhang et al., 2006). In the brain, the main astrocytic gap junction forming proteins are connexin 43 and connexin 30 (Nagy et al., 2004).

Although Cx43 and Cx30 are both the main astrocytic connexin proteins, especially in the perivascular endfeet, the pattern of change was different between the two proteins, where Cx30 was acutely increased after injury but Cx43 was decreased initially, and upregulated chronically afterwards. In terms of edema, it is interesting to note that Cx30 is increased but Cx43 is not during the edema formation phase (1d), both Cx30 and Cx43 is increased during the peak of edema (3d) and only Cx43 is increased during the edema resorption phase (7d). In a model of stab wound injury, Cx43 showed an increase after injury but Cx30 did not (Theodoric et al., 2012). A model of neonatal cerebral hypoxia ischemia injury also showed different changes in expression pattern of the two proteins, in which Cx30 showed a slight increase acutely then normalized, whereas Cx43 protein levels did not change after injury (Zeinieh et al., 2010).

Thus, acutely, the expression profile of Cx43 follows that of AQP4 as we previously described (Fukuda et al., 2012a), where a slight initial decrease, although not significant, at 1d is observed, followed by an increase at 3d and 7d (Fig 1). However, Cx43 was observed to still be increased even at 60d, whereas AQP4 was not. In contrast there is increased Cx30 levels starting from 1d, and maintained up to 3d (Fig 3), but not until 7d. This might signify that AQP4 and Cx43 may have a functional role together during the acute period. Accordingly, in astrocyte cell cultures, AQP4 downregulation led to decreased expression of Cx43 (Nicchia et al., 2005), and in a transgenic mice lacking

132

Cx43 and Cx30, decreased expression of AQP4 was observed (Ezan et al., 2012). Thus, Cx43 follows the pattern of AQP4, and may be contributing to the edema resorption at 7d after injury as speculated previously (Fukuda et al., 2012b).

Increased connexins after injury has been proposed to be detrimental in several studies (Chew et al., 2010), but some have speculated connexins to be beneficial as well and there is no universal consensus (Andrade-Rozental et al., 2000; Farahani et al., 2005; Perez Velazquez et al., 2003). In adult models of TBI using a lateral fluid percussion injury model in adult rats, a similar pattern of Cx43 immunoreactivity was seen as our model of jTBI in which an initial reduction was followed by an increase in the hippocampus and the cortex (Ohsumi et al., 2006). However, it is interesting to note that this acute reduction was observed at 6h, and the immunoreactivity started to increase at 24 hours (Ohsumi et al., 2006). This apparent shift of the time course of events may be due to a different injury model and/or different age, highlighting the importance of treating jTBI as a different pathology than adult TBI (Giza et al., 2007; Kochanek, 2006). Thus, it is most likely that the determining factors of whether connexin overexpression is beneficial or detrimental are the injury type and the timepoint after injury. Indeed it is possible that the connexins may have different functional roles during the acute and chronic phase after injury. And it is possible that the increased level of Cx43 could be beneficial during certain timepoints but not at others; as hypothesized for AQP4 where inhibition of AQP4 would be beneficial during the edema formation phase, but not during the edema resolution phase (Fukuda et al., 2012a; Fukuda et al., 2013).

We hypothesized that astrocytes most likely play a multi-faceted role in the edema process because of Cx43 and AQP4. First, via a key protein expressed in the

perivascular astrocyte endfeet, aquaporin 4 (AQP4), a member of the water channel

proteins expressed abundantly in the brain that permit water entry into the brain across

the BBB. Second, through the astrocyte network, which facilitates intercellular

communication through gap junction channels formed mainly by connexin 43 (Cx43)

proteins, allowing the spread of water accumulation from the primary injured astrocytes

to surrounding cells, causing them to swell as well. Furthermore, non-gap junction

forming hemichannels may have an additional effect via excitotoxicity through

extracellular signaling of ATP and glutamate (Bennett et al., 2012; Kar et al., 2012).

In order to test the hypothesis of whether decreasing Cx43 after jTBI would result

in decreased edema leading to improved recovery, we injected siCx43 after jTBI to assess

the effect.

The Effect of siCx43 Injection after jTBI

We observed a decrease in GFAP immunoreactivity after siCx43 injection after

jTBI (Fig. 7). This decrease in GFAP is in accordance with the aforementioned adult TBI

study with the AS-ODN pretreatment (Wu et al., 2013) and another study in which gap

junction inhibitors, carbenoxolone and octanol, was administered in adult rats that

underwent a needle stab wound to mimic brain injury (Andersson et al., 2011). Although

the exact function and implication of changes in GFAP immunoreactivity is debated, it is

commonly regarded to be associated with reactive astrogliosis (Kimelberg, 2005;

Sofroniew, 2009; Sofroniew and Vinters, 2010). Some evidences suggest that reactive

astrogliosis may contribute to worsened secondary injury depending on the timepoint and

injury model (Laird et al., 2008). In order to study the edema process, magnetic

resonance imaging (MRI) was used. Because diffusion weighted imaging (DWI) and T2-weighted imaging is routinely used as a measure of edema in clinics (Chastain et al., 2009; Galloway et al., 2008; Hou et al., 2007), and we routinely use it in juvenile animals (Badaut et al., 2007; Badaut et al., 2011; Fukuda et al., 2012a; Fukuda et al., 2013), it was used to map out the time course of the evolution of edema. Apparent diffusion coefficient (ADC) is a DWI parameter which can be thought of as a measure of cerebral water mobility and T2 can be thought of as cerebral water content. In a previous study using siAQP4, both ADC and T2 were decreased in jTBI animals injected with siAQP4, signifying decreased edema, which was associated with improved behavior outcome and decreased reactive astrogliosis (Fukuda et al., 2013). Thus it was hypothesized that the inhibition of edema and suppression of secondary injury spread by limiting water diffusion through the astroglial network as a whole could be achieved by either blocking water channels (astrocyte-BBB) or gap junctions (astrocyte-astrocyte communication). However, contrary to our initial hypothesis, post-injury administration of siCx43 did not result in a significant decrease in edema or BBB disruption.

There are several possible explanations for this observation. First, there is a possibility that both Cx43 and Cx30 (another astrocytic connexin) must be knocked down in order to decrease edema. Indeed, it is very plausible that water is still being propagated across the astrocyte network from the primary injury site to secondary injury sites through Cx30, compensating for the downregulated Cx43 channels; leading to no significant observable difference in water content or mobility. Second, pre-treatment/pre-conditioning seems to yield a greater difference between treatment and control group, as seen in two studies which showed that pre-treating the animals with a gap junction

135

inhibitor resulted in a larger difference between the control than post-treatment (Andersson et al., 2011; Perez Velazquez et al., 2006). Thus, AS-ODN Cx43 may have resulted in decreased edema due to the pre-injury injection of the drug. Third, Cx43 in juvenile animals may not be a key player for the edema process. Water propagation or clearance may be a function that is more central to other astrocytic proteins, namely the AQP4 (Badaut et al., 2011). And it is entirely possible that a combination of the above given explanations may be true. Indeed, a conditional double knockout mice of astrocytic Cx43 and Cx30 was shown to have weaker BBB and astrocyte endfeet swelling (Ezan et al., 2012). Also in a model of global ischemia on sheep, Cx43 inhibition through a specific mimetic peptide was shown to result in increased neuronal and oligodendrocyte cell count if the peptide was given after the ischemia, but not before and during ischemia (Davidson et al., 2013).

Although TBI studies on astrocytic Cx43 is sparse, increased Cx43 has been associated with post-injuries in other brain pathology as well (Chew et al., 2010). Furthermore, studies of other cerebropathologies such as ischemic stroke have reported beneficial results from the specific inhibition of Cx43 *in vitro* (Chew et al., 2010), and general gap junction inhibition *in vivo* (Andersson et al., 2011; Perez Velazquez et al., 2006; Rawanduzy et al., 1997). This may be due to the inhibition of a proposed phenomenon known as the "bystander effect." The bystander effect refers to the hypothesized spread of detrimental factors and toxic metabolites such as sodium and calcium ions, apoptotic factors, lysophospholipids, cAMP, and IP3 from the primary injury site to more distant sites mediated by gap junctions connecting the astrocyte network (Andrade-Rozental et al., 2000; Cronin et al., 2008; Grange-Messent and

Bouchaud, 1994; Perez Velazquez et al., 2003). Thus, siCx43 may be a unique and useful new technical approach to study the *in vivo* Cx43 involvement as well as a potential therapeutic tool in other brain injury models as well. However, it is interesting to note that in models of cerebral hemorrhage, detrimental effects for general gap junction inhibitors such as carbenoxolone and octanol have been reported: intracerebral hemorrhage (Manaenko et al., 2009) and experimental subarachnoid hemorrhage (Ayer et al., 2010). As proposed by the authors, these brain hemorrhages may follow a different pathway than TBI and stroke – namely that the detrimental factors are extracellular, and the intra-astrocellular bridges formed by gap junctions may not be as important (Ayer et al., 2010).

In conclusion, we show here for the first time the temporal changes in Cx43, Cx30, and GFAP after jTBI. We also show that siCx43 injection after injury on juvenile animal results in improved sensorimotor, coordination, and balance recovery, associated with decreased Cx43 and reactive astrogliosis, but is not associated with the edema formation process. Future studies could further examine the affected pathways underlying the beneficial effects such as decreased cell death, neuroinflammation, or decreased excitotoxicity.

References

Ajao, D.O., Pop, V., Kamper, J.E., Adami, A., Rudobeck, E., Huang, L., Vlkolinsky, R., Hartman, R.E., Ashwal, S., Obenaus, A., Badaut, J., 2012. Traumatic brain injury in young rats leads to progressive behavioral deficits coincident with altered tissue properties in adulthood. J Neurotrauma. 29**,** 2060-74.

Andersson, H.C., Anderson, M.F., Porritt, M.J., Nodin, C., Blomstrand, F., Nilsson, M., 2011. Trauma-induced reactive gliosis is reduced after treatment with octanol and carbenoxolone. Neurol Res. 33**,** 614-24.

Andrade-Rozental, A.F., Rozental, R., Hopperstad, M.G., Wu, J.K., Vrionis, F.D., Spray, D.C., 2000. Gap junctions: the "kiss of death" and the "kiss of life". Brain Res Brain Res Rev. 32**,** 308-15.

Ayer, R., Chen, W., Sugawara, T., Suzuki, H., Zhang, J.H., 2010. Role of gap junctions in early brain injury following subarachnoid hemorrhage. Brain Res. 1315**,** 150-8.

Badaut, J., Ashwal, S., Tone, B., Regli, L., Tian, H.R., Obenaus, A., 2007. Temporal and regional evolution of aquaporin-4 expression and magnetic resonance imaging in a rat pup model of neonatal stroke. Pediatr Res. 62**,** 248-54.

Badaut, J., Ashwal, S., Adami, A., Tone, B., Recker, R., Spagnoli, D., Ternon, B., Obenaus, A., 2011. Brain water mobility decreases after astrocytic aquaporin-4 inhibition using RNA interference. J Cereb Blood Flow Metab. 31**,** 819-31.

Bauer, R., Fritz, H., 2004. Pathophysiology of traumatic injury in the developing brain: an introduction and short update. Exp Toxicol Pathol. 56**,** 65-73.

Bennett, M.V., Garre, J.M., Orellana, J.A., Bukauskas, F.F., Nedergaard, M., Saez, J.C., 2012. Connexin and pannexin hemichannels in inflammatory responses of glia and neurons. Brain Res. 1487**,** 3-15.

Chastain, C.A., Oyoyo, U.E., Zipperman, M., Joo, E., Ashwal, S., Shutter, L.A., Tong, K.A., 2009. Predicting outcomes of traumatic brain injury by imaging modality and injury distribution. J Neurotrauma. 26**,** 1183-96.

Chew, S.S., Johnson, C.S., Green, C.R., Danesh-Meyer, H.V., 2010. Role of connexin43 in central nervous system injury. Exp Neurol. 225**,** 250-61.

Cronin, M., Anderson, P.N., Cook, J.E., Green, C.R., Becker, D.L., 2008. Blocking connexin43 expression reduces inflammation and improves functional recovery after spinal cord injury. Mol Cell Neurosci. 39**,** 152-60.

Davidson, J.O., Green, C.R., Nicholson, L.F., Bennet, L., Gunn, A.J., 2013. Connexin hemichannel blockade is neuroprotective after, but not during, global cerebral ischemia in near-term fetal sheep. Exp Neurol. 248**,** 301-8.

Ezan, P., Andre, P., Cisternino, S., Saubamea, B., Boulay, A.C., Doutremer, S., Thomas, M.A., Quenech'du, N., Giaume, C., Cohen-Salmon, M., 2012. Deletion of astroglial connexins weakens the blood-brain barrier. J Cereb Blood Flow Metab.

Farahani, R., Pina-Benabou, M.H., Kyrozis, A., Siddiq, A., Barradas, P.C., Chiu, F.C., Cavalcante, L.A., Lai, J.C., Stanton, P.K., Rozental, R., 2005. Alterations in metabolism and gap junction expression may determine the role of astrocytes as "good samaritans" or executioners. Glia. 50, 351-61.

Faul, M., Xu, L., Wald, M.M., Coronado, V., 2010. Traumatic brain injury in the United States: emergency department visits, hospitalizations, and deaths, 2002–2006. . National Center for Injury Prevention and Control. Atlanta, GA: CDC.

Frantseva, M.V., Kokarovtseva, L., Naus, C.G., Carlen, P.L., MacFabe, D., Perez Velazquez, J.L., 2002. Specific gap junctions enhance the neuronal vulnerability to brain traumatic injury. J Neurosci. 22, 644-53.

Fukuda, A.M., Pop, V., Spagnoli, D., Ashwal, S., Obenaus, A., Badaut, J., 2012a. Delayed increase of astrocytic aquaporin 4 after juvenile traumatic brain injury: possible role in edema resolution? Neuroscience. 222, 366-78.

Fukuda, A.M., Pop, V., Spagnoli, D., Ashwal, S., Obenaus, A., Badaut, J., 2012b. Delayed increase of astrocytic aquaporin 4 after juvenile traumatic brain injury: Possible role in edema resolution? Neuroscience.

Fukuda, A.M., Adami, A., Pop, V., Bellone, J.A., Coats, J.S., Hartman, R.E., Ashwal, S., Obenaus, A., Badaut, J., 2013. Posttraumatic reduction of edema with aquaporin-4 RNA interference improves acute and chronic functional recovery. J Cereb Blood Flow Metab.

Galloway, N.R., Tong, K.A., Ashwal, S., Oyoyo, U., Obenaus, A., 2008. Diffusion-weighted imaging improves outcome prediction in pediatric traumatic brain injury. J Neurotrauma. 25, 1153-62.

Giaume, C., Koulakoff, A., Roux, L., Holcman, D., Rouach, N., 2010. Astroglial networks: a step further in neuroglial and gliovascular interactions. Nat Rev Neurosci. 11, 87-99.

Giza, C.C., Mink, R.B., Madikians, A., 2007. Pediatric traumatic brain injury: not just little adults. Curr Opin Crit Care. 13, 143-52.

Goodenough, D.A., Paul, D.L., 2003. Beyond the gap: functions of unpaired connexon channels. Nat Rev Mol Cell Biol. 4, 285-94.

Grange-Messent, V., Bouchaud, C., 1994. Effects of soman on cerebral astrocyte plasma membranes: a freeze-fracture study. Neurosci Lett. 178, 77-80.

Grupcheva, C.N., Laux, W.T., Rupenthal, I.D., McGhee, J., McGhee, C.N., Green, C.R., 2012. Improved corneal wound healing through modulation of gap junction communication using connexin43-specific antisense oligodeoxynucleotides. Invest Ophthalmol Vis Sci. 53**,** 1130-8.

Herve, J.C., Derangeon, M., 2012. Gap-junction-mediated cell-to-cell communication. Cell Tissue Res.

Hirt, L., Ternon, B., Price, M., Mastour, N., Brunet, J.F., Badaut, J., 2009. Protective role of early aquaporin 4 induction against postischemic edema formation. J Cereb Blood Flow Metab. 29**,** 423-33.

Hou, D.J., Tong, K.A., Ashwal, S., Oyoyo, U., Joo, E., Shutter, L., Obenaus, A., 2007. Diffusion-weighted magnetic resonance imaging improves outcome prediction in adult traumatic brain injury. J Neurotrauma. 24**,** 1558-69.

Kar, R., Batra, N., Riquelme, M.A., Jiang, J.X., 2012. Biological role of connexin intercellular channels and hemichannels. Arch Biochem Biophys. 524**,** 2-15.

Kimelberg, H.K., 2005. Astrocytic swelling in cerebral ischemia as a possible cause of injury and target for therapy. Glia. 50**,** 389-97.

Kochanek, P.M., 2006. Pediatric traumatic brain injury: quo vadis? Dev Neurosci. 28**,** 244-55.

Laird, M.D., Vender, J.R., Dhandapani, K.M., 2008. Opposing roles for reactive astrocytes following traumatic brain injury. Neurosignals. 16**,** 154-64.

Manaenko, A., Lekic, T., Sozen, T., Tsuchiyama, R., Zhang, J.H., Tang, J., 2009. Effect of gap junction inhibition on intracerebral hemorrhage-induced brain injury in mice. Neurol Res. 31**,** 173-8.

Morales, D.M., Marklund, N., Lebold, D., Thompson, H.J., Pitkanen, A., Maxwell, W.L., Longhi, L., Laurer, H., Maegele, M., Neugebauer, E., Graham, D.I., Stocchetti, N., McIntosh, T.K., 2005. Experimental models of traumatic brain injury: do we really need to build a better mousetrap? Neuroscience. 136**,** 971-89.

Nagy, J.I., Dudek, F.E., Rash, J.E., 2004. Update on connexins and gap junctions in neurons and glia in the mammalian nervous system. Brain Res Brain Res Rev. 47**,** 191-215.

Nakase, T., Fushiki, S., Naus, C.C., 2003. Astrocytic gap junctions composed of connexin 43 reduce apoptotic neuronal damage in cerebral ischemia. Stroke. 34**,** 1987-93.

Nakase, T., Sohl, G., Theis, M., Willecke, K., Naus, C.C., 2004. Increased apoptosis and inflammation after focal brain ischemia in mice lacking connexin43 in astrocytes. Am J Pathol. 164**,** 2067-75.

Nicchia, G.P., Srinivas, M., Li, W., Brosnan, C.F., Frigeri, A., Spray, D.C., 2005. New possible roles for aquaporin-4 in astrocytes: cell cytoskeleton and functional relationship with connexin43. FASEB J. 19**,** 1674-6.

Ohsumi, A., Nawashiro, H., Otani, N., Ooigawa, H., Toyooka, T., Yano, A., Nomura, N., Shima, K., 2006. Alteration of gap junction proteins (connexins) following lateral fluid percussion injury in rats. Acta Neurochir Suppl. 96**,** 148-50.

Ohsumi, A., Nawashiro, H., Otani, N., Ooigawa, H., Toyooka, T., Shima, K., 2010. Temporal and spatial profile of phosphorylated connexin43 after traumatic brain injury in rats. J Neurotrauma. 27**,** 1255-63.

Perez Velazquez, J.L., Frantseva, M.V., Naus, C.C., 2003. Gap junctions and neuronal injury: protectants or executioners? Neuroscientist. 9**,** 5-9.

Perez Velazquez, J.L., Kokarovtseva, L., Sarbaziha, R., Jeyapalan, Z., Leshchenko, Y., 2006. Role of gap junctional coupling in astrocytic networks in the determination of global ischaemia-induced oxidative stress and hippocampal damage. Eur J Neurosci. 23**,** 1-10.

Rash, J.E., Yasumura, T., Davidson, K.G., Furman, C.S., Dudek, F.E., Nagy, J.I., 2001. Identification of cells expressing Cx43, Cx30, Cx26, Cx32 and Cx36 in gap junctions of rat brain and spinal cord. Cell Commun Adhes. 8**,** 315-20.

Rawanduzy, A., Hansen, A., Hansen, T.W., Nedergaard, M., 1997. Effective reduction of infarct volume by gap junction blockade in a rodent model of stroke. J Neurosurg. 87**,** 916-20.

Seifert, G., Schilling, K., Steinhauser, C., 2006. Astrocyte dysfunction in neurological disorders: a molecular perspective. Nat Rev Neurosci. 7**,** 194-206.

Sofroniew, M.V., 2009. Molecular dissection of reactive astrogliosis and glial scar formation. Trends Neurosci. 32**,** 638-47.

Sofroniew, M.V., Vinters, H.V., 2010. Astrocytes: biology and pathology. Acta Neuropathol. 119**,** 7-35.

Theodoric, N., Bechberger, J.F., Naus, C.C., Sin, W.C., 2012. Role of gap junction protein connexin43 in astrogliosis induced by brain injury. PLoS One. 7**,** e47311.

Wallraff, A., Kohling, R., Heinemann, U., Theis, M., Willecke, K., Steinhauser, C., 2006. The impact of astrocytic gap junctional coupling on potassium buffering in the hippocampus. J Neurosci. 26**,** 5438-47.

Woodcock, T., Morganti-Kossmann, M.C., 2013. The role of markers of inflammation in traumatic brain injury. Front Neurol. 4**,** 18.

Wu, Z., Xu, H., He, Y., Yang, G., Liao, C., Gao, W., Liang, M., He, X., 2013. Antisense oligodeoxynucleotides targeting connexin43 reduce cerebral astrocytosis and edema in a rat model of traumatic brain injury. Neurol Res. 35**,** 255-62.

Yoon, J.J., Green, C.R., O'Carroll, S.J., Nicholson, L.F., 2010. Dose-dependent protective effect of connexin43 mimetic peptide against neurodegeneration in an ex vivo model of epileptiform lesion. Epilepsy Res. 92**,** 153-62.

Zeinieh, M.P., Talhouk, R.S., El-Sabban, M.E., Mikati, M.A., 2010. Differential expression of hippocampal connexins after acute hypoxia in the developing brain. Brain Dev. 32**,** 810-7.

Zhang, X., Alber, S., Watkins, S.C., Kochanek, P.M., Marion, D.W., Graham, S.H., Clark, R.S., 2006. Proteolysis consistent with activation of caspase-7 after severe traumatic brain injury in humans. J Neurotrauma. 23**,** 1583-90.

CHAPTER FIVE

DISCUSSION

Parts of the following work has been published in the peer reviewed journal, *Biochimica et Biophysica Acta*, 2014 May;1840(5):1554-65.

Aquaporin and Brain Diseases

Edema Process: Role of the Aquaporins

Most brain diseases (e.g. stroke, traumatic brain injury, brain tumors, brain inflammation) present the hallmark of edema, which is water accumulation resulting from brain osmotic homeostasis dysfunctions. The main consequence of edema is the swelling of the brain, which aggravates the secondary injuries such as decrease of brain perfusion. Edema has been known in the clinic and pre-clinical science for many years but the molecular and cellular events in edema formation/resolution are still poorly understood. Moreover, there is no efficient treatment to prevent or limit edema formation or expansion in brain disorders. Thus, the discovery of the brain AQPs was a beacon of hope in the development of new therapy to battle the edema process. The knowledge gathered in the past 15 years on AQPs as a potential drug target for edema is summarized in the following parts after a short introduction on the edema build-up phase.

Edema Build-Up Phase: Anoxic, Ionic
and Vasogenic Edema

For 40 years, cerebral edema has been traditionally divided into 2 major classes: cytotoxic and vasogenic (Badaut et al., 2011b). Classically, cytotoxic edema is defined by intracellular water accumulation without blood-brain barrier (BBB) disruption while vasogenic edema appears after BBB disruption, leading to a diffusion of proteins from the blood to the tissue followed by water accumulation in the extracellular space (Badaut et al., 2011b). However, this classical subdivision has been challenged by the recent knowledge in molecular changes during the edema formation and BBB properties, and the classical subdivision represents a simplified view of a more complex pathological process. In regard to vascular brain injuries such as jTBI, the recent cellular and molecular events behind edema suggest that the edema build-up phase can be divided into 3 major types: anoxic, ionic and vasogenic edema (Simard et al., 2007, Badaut et al., 2011b, Berezowski et al., 2012). Anoxic edema is characterized as swelling of the astrocytes and neuronal dendrites that occur within minutes (figure 1B) after oxygen and glucose deprivation in the context of cerebrovascular disease. The depletion of oxygen and energy nutrients induces major changes in the cellular ionic gradients due to the absence of efficient energy dependent co-transporters. This leads to a massive entry of ions into cells which can be observed in phenomenon such as a slow rise in extracellular K^+ concentration (Milner and Campbell, 2002, Dityatev and Schachner, 2003), followed by water entry into the cells, which induces cellular swelling in astrocytes first, and then in neuronal dendrites (Figure 1B). Then, anoxic edema quickly evolves to become ionic edema. The absence of oxygen and nutrients also alters the ionic gradients of endothelial cells, including transcapillary flux of Na^+ (O'Donnell et al., 2004, Simard et al., 2007)

with tissue swelling (Figure 1B). Suffering of endothelial cells therefore results in early transient leakage of the BBB in stroke (de Castro Ribeiro et al., 2006, Hirt et al., 2009) as well as in TBI (Pop et al., 2013). This results in further entry of water through endothelial cells leading to brain swelling as observed from examples in stroke models within 30 minutes after reperfusion (de Castro Ribeiro et al., 2006, Hirt et al., 2009) associated with further increased BBB permeability (Strbian et al., 2008, Hirt et al., 2009). Vasogenic edema follows this cascade of events (Figure 1B) with increased permeability to plasma proteins such as albumin (Badaut et al.) due to a physical disruption of endothelial tight junctions, an extracellular matrix degradation and potentially an increased transendothelial cell transport by the transcytosis mechanism.
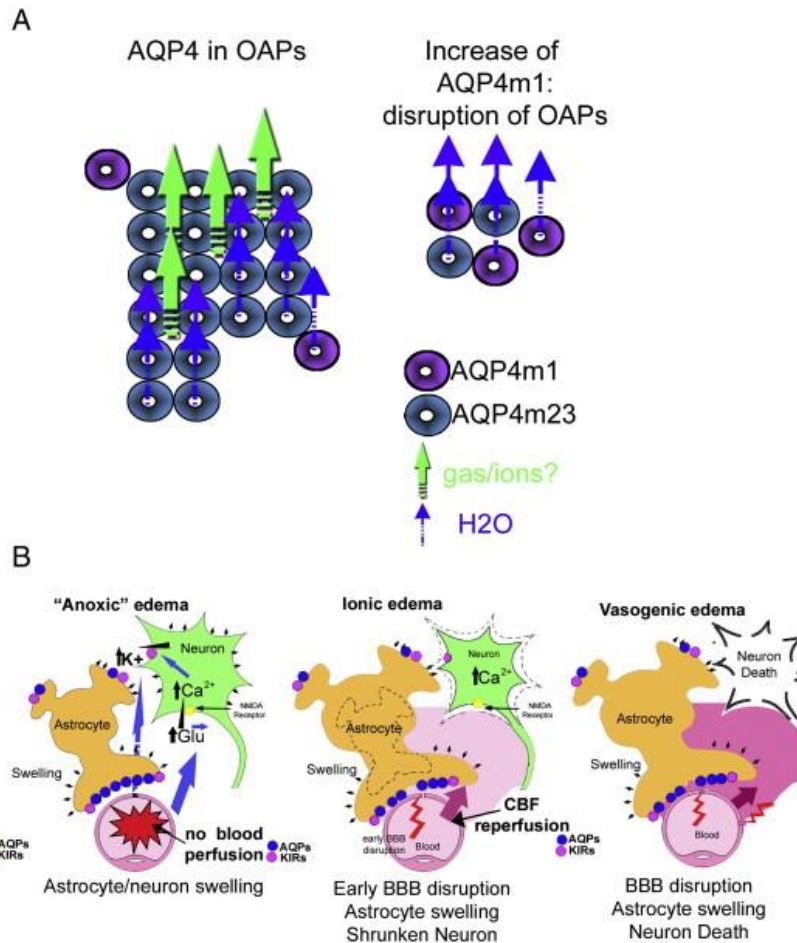
Figure 1. Disorganization of AQP4 in orthogonal particles after brain injuries and edema process. (A) AQP4-m1 (purple circles) and AQP4-m23 (blue circles) isoforms contribute together to form orthogonal array particles (OAPs) in astrocyte endfeet in contact to the blood vessels. It was previously shown that higher expression of AQP4-m23 contributes to the formation of large OAPs. However, increase of AQP4-m1 induced disruption of OAPs with a reduction of the size. This modification is observed in pathological conditions such as stroke. Recent knowledge on AQP leads us to hypothesize that the large OAPs contribute to gas and cation diffusion in the astrocyte membranes through central pores (green arrows) (modified from [33]). (B) Schematic drawing of the events happening during edema formation with 3 different edema phases: anoxic, ionic and vasogenic edema. During the injury with decrease of brain perfusion, the first minutes are characterized by anoxic edema. Anoxic edema is characterized as a swelling of the astrocytes and the neuronal dendrites caused by a disruption of the cellular ionic gradients and the entry of ions followed by water entry and leading to cellular swelling. During the ionic edema, astrocytes become swollen and neuronal death starts to occur resulting in shrinkage of the neurons, shear stress and endothelial dysfunctions on the non-perfused vascular tree, which results in early transient leakage of the BBB. Vasogenic edema is a result of disruption of the tight junctions between the endothelial cells, leading to increased permeability of the cerebral blood-vessels to albumin and other plasma proteins, further contributing to swelling of astrocytes and subsequent neuronal cell death. (adapted from [33]).

146

It is important to mention that this definition was proposed in the context of brain injuries involving acute cerebrovascular dysfunctions and may not be adequately adapted for other brain disorders such as brain tumors (Nico and Ribatti, 2011). In this regard, it is important to underline that clinical treatments solely focusing on osmotic challenges are not efficient or sufficient for treatment of cerebral edema, because of the suggested complexity and diversity in the molecular mechanisms underlying the edema formation process. Although the exact functional contributions of cerebral AQPs are not yet fully understood, because of their localization and their identity as water channel proteins, they most likely play vital roles in the cerebral edema process. We will now review the role of the AQPs within the context of this revised subdivision of edema formation.

AQP4 and Edema Build-Up

Acute brain injuries including trauma (Ke et al., 2001, Fukuda et al., 2012), ischemia (Meng et al., 2004, de Castro Ribeiro et al., 2006), and subarachnoid hemorrhage (Badaut et al., 2003), each have distinct patterns of alteration in the level of AQP4 expression. Early after stroke, AQP4 expression is rapidly up-regulated in the astrocyte endfeet in contact with blood vessels, peaking at 1h after stroke onset in a model of transient occlusion of the middle cerebral artery (de Castro Ribeiro et al., 2006, Hirt et al., 2009). These early changes are associated with the development of ionic brain edema (Figure 1B) and the swelling of the astrocyte processes in stroke models (Risher et al., 2009). However, increased AQP4 expression is not observed in more severe stroke models (Friedman et al., 2009), prompting the hypothesis that under great tissue duress, the brain is not able to synthesize sufficient new AQP4 proteins during the early phase of

reperfusion. Interestingly, in stroke, the ratio of AQP4-m1 and AQP4-m23 is changed in the ischemic hemisphere, with higher induction of AQP4-m1 compared to AQP4-m23 (Hirt et al., 2009), suggesting a disorganization of the OAPs in accordance with previous rat stroke data (Suzuki et al., 1984). However, the functional consequences of AQP4-m1 increase and disorganization in stroke are not yet elucidated (Figure 1A) and in our jTBI model there was no significant difference in the ratio between AQP4-m1 compared to AQP4-m23 between sham and jTBI animals (Fukuda et al., 2012).

The complexity of the role of AQP4 in edema process is outlined by the variety of the changes in AQP4 expression, which seems to depend on both the degree of severity and the pathological model. Indeed, increased AQP4 (Sun et al., 2003, Guo et al., 2006, Ding et al., 2009, Higashida et al., 2011, Tomura et al., 2011) versus decreased AQP4 (Ke et al., 2001, Kiening et al., 2002, Zhao et al., 2005) are likely due to differences in injury type, rodent strains, and age at impact (Fukuda et al., 2012). Moreover, several studies using the AQP4-/- mice showed discrepancies in the outcomes and interpretation of the role of AQP4 in edema process. For example, AQP4-/- mice reveal a protective role for AQP4 in spinal cord injury models with a decrease of edema formation and lesion size at early time point after injury (Saadoun et al., 2010). Using a similar model and transgenic mice, a second set of experiments showed functional improvement for the WT mice compared to the AQP4-/- mice at longterm after contusion spinal cord injury (Kimura et al., 2010), suggesting that AQP4 either plays detrimental roles in the edema process or a protective role by facilitating the clearance of excess water. Several other contradictory results using the non-conditional AQP4-/- mice (Saadoun et al., 2008, Kimura et al., 2010), indicate the limitations of using this genetic tool to solve the

question of the pathophysiological role of AQP4 in edema formation. In our lab, we recently developed *in vivo* application of siRNA targeting AQP4 (siAQP4), showing specific AQP4 decrease with reduced water mobility (Badaut et al., 2011a, Fukuda et al., 2013, *in press*). This new tool is further developed as a molecular approach to address the question of the role of AQP4 in edema formation, which was tested in a model of juvenile traumatic brain injury (jTBI). In this model we showed that AQP4 expression is not changed at 24h during the build-up of edema (Fukuda et al., 2012). Our results suggest that stable AQP4 levels may contribute to water entry leading to cellular swelling (lower apparent diffusion coefficient (ADC)) and increased edema (increased T2) at proximity of the site of impact (Fukuda et al., 2012). Interestingly, application of siAQP4 after jTBI induced a reduction in edema formation associated with cognitive improvement at 2 months post-injury, suggesting that siAQP4 could be used as a specific drug to prevent edema formation by transiently decreasing the level of AQP4 expression (Fukuda et al., 2013, *in press*). This data show that the presence of AQP4 plays a deleterious role during the edema formation by facilitating the entry of water in the astrocytes.

<div align="center">

Edema Resolution in Acute Brain Disease:
Role of AQP in Water Clearance

</div>

As mentioned previously, the data generated using AQP4-/- mice raised the hypothesis of a dual role for AQP4 in the edema process with a deleterious role of AQP4 in edema build-up and its beneficial role in water clearance during the edema resolution (Saadoun and Papadopoulos, Papadopoulos et al., 2004). Despite the lack of a clear answer on the role of AQP4 in edema resolution, several results support this hypothesis.

The first evidence is the infusion of saline solution in brain parenchyma that induced significant increase in the intracranial pressure in AQP4-/- mice compared to the WT (Papadopoulos et al., 2004). In several pathological conditions, increased AQP4 was observed to be associated with edema resolution measured over time using MRI (Meng et al., 2004, Tourdias et al., 2009, Badaut et al., 2011a, Badaut et al., 2011b, Tourdias et al., 2011, Fukuda et al., 2012, Fukuda et al., 2013, *in press*). Frequently, AQP4 expression is increased after 48h in stroke models (de Castro Ribeiro et al., 2006, Hirt et al., 2009), in TBI (Sun et al., 2003, Guo et al., 2006, Ding et al., 2009, Higashida et al., 2011, Tomura et al., 2011, Fukuda et al., 2012) and in neuroinflammatory lesion conditions (Tourdias et al., 2011). Most of the time, the increase of the AQP4 is observed near the lesion site in perivascular astrocyte endfeet, astrocyte processes, and the glia limitans (de Castro Ribeiro et al., 2006, Fukuda et al., 2012). These changes may indicate that excess AQP4 could facilitate edematous fluid elimination through the subarachnoid space (Fernandez-Teruel et al., 2002, Nicchia et al., 2009, Tourdias et al., 2011). As observed in a jTBI model, increased AQP4 in the glia limitans may compensate for water accumulation at 1 and 3 days (higher T2), with a gradual increase of AQP4 at 3 days and normalization of both AQP4 and T2 values by 7 days (Fukuda et al., 2012). In the rat neuroinflammatory lesion model, the ADC monitored time course study indicates a clear distinction between a minor AQP4 expression increase during the edema build-up phase and a shift to strong AQP4 expression during the edema resolution phase (Tourdias et al., 2011). In fact, ADC values are significantly increased when AQP4 expression is at the peak of its expression (Tourdias et al., 2011).

Neuroinflammation in Brain Injury:
Astrocytic AQP4

AQP4 expression is frequently increased during the onset of neuroinflammatory period characterized by microglia activation and astrogliosis. In fact, several interesting recent data suggest a potential relationship between AQP4 and microglial activation, without a clear definition about the link. First, AQP4-/- mice are more vulnerable to seizures compared to WT one month after TBI (Lu et al., 2011). This difference was explained by the neuroinflammatory response showing less astrogliosis and increased microglial activation in AQP4-/- compared to WT mice. Minocycline injection in AQP4-/- reversed the outcome by inhibition of the increase in microglia activation and decreased the severity of post-traumatic seizures (Lu et al., 2011). Similar results were reported in cryo-injury models, where AQP4-/- mice presented increased microglia and reduced astrogliosis compared to WT. In this model, a decrease in the lesion volume and in neuronal loss in AQP4-/- mice compared to WT was reported at 1 day after injury whereas the opposite result was reported at 7 and 14 days (Saubamea et al., 2012). In our lab, we have also observed that the siAQP4 treatment after jTBI showed a decrease in AQP4 associated with less BBB disruption, less edema, more NeuN positive cells, and better behavior outcomes compared to the control group up to 2 months post-injury (Fukuda et al., 2013). As observed in the AQP4-/- mice, we reported an increase in activated microglia and a decrease in astrogliosis around the lesion at 3 days post-injury in siAQP4 treated rats compared to control group. However, this difference is not present anymore at 2 months post-injury (Fukuda et al., 2013). One possible explanation for this observation may be that changes in AQP4 expression are associated with changes in astrogliosis and microglia activation in acute brain injury. Astrogliosis may require the

presence of AQP4 to facilitate the water movement necessary for migration (Saadoun et al., 2005, Auguste et al., 2007) and hypertrophy. However, the mechanism behind the decrease of the AQP4 and activation of microglia is still unknown. One possible mechanism is a modification in the pattern of cytokine release in response to astrocytic AQP4 down regulation or inhibition. The other hypothesis is in relation with the presence of stretch-activated chloride (Cl$^-$) channels expressed in microglia and known to be activated by osmotic stress (Lewis et al., 1993, Eder et al., 1998, Schlichter et al., 2011). The activation of these channels contributes to the maintenance of the non-activated (ramified) phenotype of microglia (Eder et al., 1998). Because AQP4 is responsible for water transport and osmotic pressure, we can hypothesize that inhibition of AQP4 either through genetic deletion or siRNA will modify the osmotic stress within the extracellular space surrounding the microglia. This would change the activation status of the swelling activated chloride channels, resulting in microglia activation. Another possibility lies in the cross talk that occurs between astrogliosis and microglia activation (Liu et al., 2011). The decrease of reactive astrogliosis as a result of the absence of AQP4 may cause an increase in microglial activity. The exact link between microglial activation and decreased astrogliosis in absence of AQP4 needs further investigation. However, it is likely that at 3 days post-jTBI, increased microglia activation due to siAQP4 treatment is contributing to the beneficial effects observed on the cognitive outcome. Indeed, acute microglia activation was hypothesized to be beneficial in contrast to chronic microglia activation (Loane and Byrnes, 2010). These changes of AQP4 in relation with neuroinflammation could also be correlated with imaging signal changes over time after brain injury or in chronic brain disorders.

Future Developments: Drugs Against AQP4?

As mentioned previously, there is no specific inhibitor to block the AQP4 channel and such a compound is critical for evaluating the role of AQP4 and treatment of edema. Using siRNA strategy permitted to show the potential to use a specific inhibitor of AQP4 in jTBI and the contribution of astrocytic AQP4 in neuroimaging (Manley et al., 2000, Fukuda et al., 2013, *in press*). Although non-specific, a range of compounds already commercially available that may block AQP4 have been tested. Bumetanide blocks the AQP4 channel and water permeability in oocytes (Migliati et al., 2009), and bumetanide prevents edema formation after brain ischemia (O'Donnell et al., 2004, Migliati et al.), which correlates with decreased AQP4 expression (Migliati et al.). However bumetanide is also an inhibitor of Na-Cl-K co-transporter expressed in endothelial cells. This multiple site of action of bumetanide is complicating *in vivo* validation and makes teasing out solo effects of AQP4 difficult (O'Donnell et al., 2004). Therefore the benefits of bumetanide on edema could also be due to the inhibition of Na-Cl-K co transporter expressed in endothelial cells. Acetazolamide (AZA), a sulfonamide carbonic anhydrase inhibitor was also proposed for a specific inhibitor of water permeability associated with AQP1 and AQP4 (Huber et al., 2007, Tanimura et al., 2009). However, it was reported that AZA has no effect on water permeability (Sogaard and Zeuthen, 2008, Yang et al., 2008). Similarly, two other inhibitors belonging to sulfonamide carbonic anhydrase inhibitor class, methazolamide and valproic acid have also been tested but without clear effects on the water permeability (Huber et al., 2009, Tanimura et al., 2009). Waiting to have a specific pharmacological drug to block AQP4, the siRNA strategy was used with success in normal brain to silence the AQP4 expression (Badaut et al., 2011a). Decrease of AQP4

is associated with a decrease of ADC values (Badaut et al., 2011a). siAQP4 was used as treatment in jTBI with decrease of the edema formation post-TBI and functional improvement up to 2 months post-injury (Fukuda et al., 2013, *in press*). These results encourage us to use the siRNA strategy as a specific drug to prevent the edema formation. However, heterogeneous alterations in AQP4 expression demonstrate the complexity of modifying edema reduction. This strongly suggests testing the siAQP4 treatment strategy in different brain disorder models to find out which battles will be won with siRNA, and which ones should be avoided.

Connexin 43: Consideration of Potential Post Injury Cascade other than Edema Formation

In our hypothesized model before conducting the studies, AQP4 was thought of as the initial passage into the astrocyte network entering/exiting the network. Cx43, on the other hand, was thought to be the passageway between astrocytes within the network. We thought that siRNA against either protein would decrease edema formation and result in beneficial outcome after jTBI. However, unlike siAQP4 treatment, siCx43 did not result in changes in the edema process after jTBI. But although the edema process did not seem to be altered with siCx43, nevertheless, siCx43 animals did perform better in the foot fault test compared to control.

Thus we speculate that Cx43 most likely plays a role in the injury cascade of jTBI other than edema. In order to shed light onto possible non-edematous roles of Cx43, it is important to consider the functions of non-gap junction forming, or uncoupled, hemichannels; which do not participate in intracellular trafficking of molecules, but rather between the astrocyte and the extracellular environment (Goodenough and Paul,

2003). Eugenin et al. has an excellent review which contains a section on Cx43 astroglial hemichannels (Eugenin et al., 2012). Under normal condition, uncoupled Cx43 hemichannels remain closed but a variety of pathological triggers such as metabolic inhibition, fibroblast growth factor 1, hypoxic condition, ischemic condition, oxidative stress, increased calcium concentration, and acidic environment can open the hemichannel, leading to release of ATP, glutamate, NADH out to the extracellular space (Contreras et al., 2002, Bennett et al., 2012, Eugenin et al., 2012, Kar et al., 2012). This release increases neurotoxicity and neuronal susceptibility to insult, leading to pro-inflammatory cytokine induced neuronal cell death (Froger et al., 2010, Orellana et al., 2011). At this point, it is also important to remember that one of the key hallmarks of injury after brain injury is reactive astrogliosis, which modulates production of pro-inflammatory cytokines (Anderson et al., 2014). Cx43 KO animal has been shown to have decreased astrogliosis and decreased proliferation of astrogliosis after ischemia as well (Nakase et al., 2004). Alas, some pathological functions that have been associated with Cx43 upregulation are apoptosis, excitotoxicity, and neuroinflammation (Bennett et al., 2012), and these functions could be explained by opening of uncoupled hemichannels. In our model, we also observed the siCx43 resulted in a decreased post-injury reactive astrogliosis as interpreted via decreased GFAP immunofluorescence intensity (Ch. 4). Thus, in future studies, the potential effect of siCx43 after jTBI on other mechanisms can be studied such as caspase-3 for apoptosis, NeuN for neuronal survival and IBA for microglial activation as performed in our earlier AQP4 studies (Fukuda et al., 2013).

Additionally, it is also important to consider the potential role and function of the other astrocyte gap junction forming connexin: Cx30. Because Cx30 was discovered in astrocytes later than Cx43 (Nagy et al., 1997, Nagy et al., 1999), Cx43 has been studied in more extensive detail than Cx30 as the main astrocyte connexin. Thus, Cx30's specific functions in the brain are still largely unknown, although Cx30 has been shown to have a functional role in controlling cellular membrane integrity in the inner ear (Schutz et al., 2010, Forge et al., 2013) and glutamate clearance (Pannasch et al., 2014). However, a study which compared a Cx43 KO to Cx30 KO to a Cx43/30 Double KO showed that the double KO mice had white matter intramyelinic edema and astrocyte edema in the CA1 but the single allele deletions did not have any edema, potentially signifying that Cx43 and Cx30 may have redundant roles and may compensate each other in situations where one protein is decreased (Lutz et al., 2009). Additionally Cx43/30 Double KO also showed a weakened state of BBB as well, which could lead to increased vasogenic edema under stress and insult such as jTBI (Ezan et al., 2012). Thus, it is possible that Cx43 and Cx30 both have overlapping roles regarding water homeostasis and the edema process, therefore siCx43 alone did not cause a change in T2 and ADC value due to Cx30 compensation.

And lastly, future studies can better elucidate the potential relationship that AQP4 and Cx43 and Cx30 may have on each other under normal and pathological conditions. Interestingly, a decrease in Cx43 protein expression and a concomitant decrease in gap junction function after administration of siRNA against AQP4 in primary astrocyte culture have been reported (Nicchia et al., 2005). Another brain cell cultures taken from AQP4 -/- mice have also shown lower Cx43 protein level compared to wildtype (Kong et

al., 2008). A transgenic mice lacking Cx43 and Cx30 have also been reported to have decreased AQP4 levels (Ezan et al., 2012).

REFERENCES

Anderson MA, Ao Y, Sofroniew MV (2014) Heterogeneity of reactive astrocytes. Neurosci Lett 565:23-29.

Auguste KI, Jin S, Uchida K, Yan D, Manley GT, Papadopoulos MC, Verkman AS (2007) Greatly impaired migration of implanted aquaporin-4-deficient astroglial cells in mouse brain toward a site of injury. Faseb J 21:108-116.

Badaut J, Ashwal S, Adami A, Tone B, Recker R, Spagnoli D, Ternon B, Obenaus A (2011a) Brain water mobility decreases after astrocytic aquaporin-4 inhibition using RNA interference. J Cereb Blood Flow Metab 31:819-831.

Badaut J, Ashwal S, Obenaus A (2011b) Aquaporins in cerebrovascular disease: a target for treatment of brain edema? Cerebrovasc Dis 31:521-531.

Badaut J, Brunet JF, Grollimund L, Hamou MF, Magistretti PJ, Villemure JG, Regli L (2003) Aquaporin 1 and aquaporin 4 expression in human brain after subarachnoid hemorrhage and in peritumoral tissue. Acta Neurochir Suppl 86:495-498.

Bennett MV, Garre JM, Orellana JA, Bukauskas FF, Nedergaard M, Saez JC (2012) Connexin and pannexin hemichannels in inflammatory responses of glia and neurons. Brain Res 1487:3-15.

Berezowski V, Fukuda AM, Cecchelli R, Badaut J (2012) Endothelial Cells and Astrocytes: A Concerto en Duo in Ischemic Pathophysiology. Int J Cell Biol 2012:176287.

Contreras JE, Sanchez HA, Eugenin EA, Speidel D, Theis M, Willecke K, Bukauskas FF, Bennett MV, Saez JC (2002) Metabolic inhibition induces opening of unapposed connexin 43 gap junction hemichannels and reduces gap junctional communication in cortical astrocytes in culture. Proc Natl Acad Sci U S A 99:495-500.

de Castro Ribeiro M, Hirt L, Bogousslavsky J, Regli L, Badaut J (2006) Time course of aquaporin expression after transient focal cerebral ischemia in mice. J Neurosci Res 83:1231-1240.

Ding JY, Kreipke CW, Speirs SL, Schafer P, Schafer S, Rafols JA (2009) Hypoxia-inducible factor-1alpha signaling in aquaporin upregulation after traumatic brain injury. Neurosci Lett 453:68-72.

Dityatev A, Schachner M (2003) Extracellular matrix molecules and synaptic plasticity. Nat Rev Neurosci 4:456-468.

Eder C, Klee R, Heinemann U (1998) Involvement of stretch-activated Cl- channels in ramification of murine microglia. J Neurosci 18:7127-7137.

Eugenin EA, Basilio D, Saez JC, Orellana JA, Raine CS, Bukauskas F, Bennett MV, Berman JW (2012) The role of gap junction channels during physiologic and pathologic conditions of the human central nervous system. Journal of neuroimmune pharmacology : the official journal of the Society on NeuroImmune Pharmacology 7:499-518.

Ezan P, Andre P, Cisternino S, Saubamea B, Boulay AC, Doutremer S, Thomas MA, Quenech'du N, Giaume C, Cohen-Salmon M (2012) Deletion of astroglial connexins weakens the blood-brain barrier. J Cereb Blood Flow Metab.

Fernandez-Teruel A, Gimenez-Llort L, Escorihuela RM, Gil L, Aguilar R, Steimer T, Tobena A (2002) Early-life handling stimulation and environmental enrichment: are some of their effects mediated by similar neural mechanisms? Pharmacology, biochemistry, and behavior 73:233-245.

Forge A, Jagger DJ, Kelly JJ, Taylor RR (2013) Connexin30-mediated intercellular communication plays an essential role in epithelial repair in the cochlea. J Cell Sci 126:1703-1712.

Friedman B, Schachtrup C, Tsai PS, Shih AY, Akassoglou K, Kleinfeld D, Lyden PD (2009) Acute vascular disruption and aquaporin 4 loss after stroke. Stroke 40:2182-2190.

Froger N, Orellana JA, Calvo CF, Amigou E, Kozoriz MG, Naus CC, Saez JC, Giaume C (2010) Inhibition of cytokine-induced connexin43 hemichannel activity in astrocytes is neuroprotective. Mol Cell Neurosci 45:37-46.

Fukuda AM, Adami A, Pop V, Bellone JA, Coats JS, Hartman RE, Ashwal S, Obenaus A, Badaut J (2013) Posttraumatic reduction of edema with aquaporin-4 RNA interference improves acute and chronic functional recovery. J Cereb Blood Flow Metab.

Fukuda AM, Adami A, Pop V, Bellone JA, Coats JS, Hartman RE, Ashwal S, Obenaus A, Badaut J (2013, *in press*) Post-traumatic reduction of edema with aquaporin-4 RNA interference improves acute and chronic functional recovery. J Cereb Blood Flow Metab.

Fukuda AM, Pop V, Spagnoli D, Ashwal S, Obenaus A, Badaut J (2012) Delayed increase of astrocytic aquaporin 4 after juvenile traumatic brain injury: possible role in edema resolution? Neuroscience 222:366-378.

Goodenough DA, Paul DL (2003) Beyond the gap: functions of unpaired connexon channels. Nat Rev Mol Cell Biol 4:285-294.

Guo Q, Sayeed I, Baronne LM, Hoffman SW, Guennoun R, Stein DG (2006) Progesterone administration modulates AQP4 expression and edema after traumatic brain injury in male rats. Exp Neurol 198:469-478.

Higashida T, Kreipke CW, Rafols JA, Peng C, Schafer S, Schafer P, Ding JY, Dornbos D, 3rd, Li X, Guthikonda M, Rossi NF, Ding Y (2011) The role of hypoxia-inducible factor-1alpha, aquaporin-4, and matrix metalloproteinase-9 in blood-brain barrier disruption and brain edema after traumatic brain injury. J Neurosurg 114:92-101.

Hirt L, Price M, Ternon B, Mastour N, Brunet JF, Badaut J (2009) Early induction of AQP4 contributes the limitation of the edema formation in the brain ischemia. J Cereb Blood Flow Metab 29:423-433.

Huber VJ, Tsujita M, Kwee IL, Nakada T (2009) Inhibition of aquaporin 4 by antiepileptic drugs. Bioorg Med Chem 17:418-424.

Huber VJ, Tsujita M, Yamazaki M, Sakimura K, Nakada T (2007) Identification of arylsulfonamides as Aquaporin 4 inhibitors. Bioorg Med Chem Lett 17:1270-1273.

Kar R, Batra N, Riquelme MA, Jiang JX (2012) Biological role of connexin intercellular channels and hemichannels. Arch Biochem Biophys 524:2-15.

Ke C, Poon WS, Ng HK, Pang JC, Chan Y (2001) Heterogeneous responses of aquaporin-4 in oedema formation in a replicated severe traumatic brain injury model in rats. Neurosci Lett 301:21-24.

Kiening KL, van Landeghem FK, Schreiber S, Thomale UW, von Deimling A, Unterberg AW, Stover JF (2002) Decreased hemispheric Aquaporin-4 is linked to evolving brain edema following controlled cortical impact injury in rats. Neurosci Lett 324:105-108.

Kimura A, Hsu M, Seldin M, Verkman AS, Scharfman HE, Binder DK (2010) Protective role of aquaporin-4 water channels after contusion spinal cord injury. Ann Neurol 67:794-801.

Kong H, Fan Y, Xie J, Ding J, Sha L, Shi X, Sun X, Hu G (2008) AQP4 knockout impairs proliferation, migration and neuronal differentiation of adult neural stem cells. J Cell Sci 121:4029-4036.

Lewis RS, Ross PE, Cahalan MD (1993) Chloride channels activated by osmotic stress in T lymphocytes. J Gen Physiol 101:801-826.

Liu W, Tang Y, Feng J (2011) Cross talk between activation of microglia and astrocytes in pathological conditions in the central nervous system. Life Sci 89:141-146.

Loane DJ, Byrnes KR (2010) Role of microglia in neurotrauma. Neurotherapeutics 7:366-377.

Lu DC, Zador Z, Yao J, Fazlollahi F, Manley GT (2011) Aquaporin-4 Reduces Post-Traumatic Seizure Susceptibility by Promoting Astrocytic Glial Scar Formation in Mice. J Neurotrauma.

Lutz SE, Zhao Y, Gulinello M, Lee SC, Raine CS, Brosnan CF (2009) Deletion of astrocyte connexins 43 and 30 leads to a dysmyelinating phenotype and hippocampal CA1 vacuolation. J Neurosci 29:7743-7752.

Manley GT, Fujimura M, Ma T, Noshita N, Filiz F, Bollen AW, Chan P, Verkman AS (2000) Aquaporin-4 deletion in mice reduces brain edema after acute water intoxication and ischemic stroke. Nat Med 6:159-163.

Meng S, Qiao M, Lin L, Del Bigio MR, Tomanek B, Tuor UI (2004) Correspondence of AQP4 expression and hypoxic-ischaemic brain oedema monitored by magnetic resonance imaging in the immature and juvenile rat. Eur J Neurosci 19:2261-2269.

Migliati E, Meurice N, DuBois P, Fang JS, Somasekharan S, Beckett E, Flynn G, Yool AJ (2009) Inhibition of aquaporin-1 and aquaporin-4 water permeability by a derivative of the loop diuretic bumetanide acting at an internal pore-occluding binding site. Mol Pharmacol 76:105-112.

Migliati ER, Amiry-Moghaddam M, Froehner SC, Adams ME, Ottersen OP, Bhardwaj A (2010) Na(+)-K (+)-2Cl (-) cotransport inhibitor attenuates cerebral edema following experimental stroke via the perivascular pool of aquaporin-4. Neurocrit Care 13:123-131.

Milner R, Campbell IL (2002) Developmental regulation of beta1 integrins during angiogenesis in the central nervous system. Mol Cell Neurosci 20:616-626.

Nagy JI, Ochalski PA, Li J, Hertzberg EL (1997) Evidence for the co-localization of another connexin with connexin-43 at astrocytic gap junctions in rat brain. Neuroscience 78:533-548.

Nagy JI, Patel D, Ochalski PA, Stelmack GL (1999) Connexin30 in rodent, cat and human brain: selective expression in gray matter astrocytes, co-localization with connexin43 at gap junctions and late developmental appearance. Neuroscience 88:447-468.

Nakase T, Sohl G, Theis M, Willecke K, Naus CC (2004) Increased apoptosis and inflammation after focal brain ischemia in mice lacking connexin43 in astrocytes. Am J Pathol 164:2067-2075.

Nicchia GP, Mastrototaro M, Rossi A, Pisani F, Tortorella C, Ruggieri M, Lia A, Trojano M, Frigeri A, Svelto M (2009) Aquaporin-4 orthogonal arrays of particles are the target for neuromyelitis optica autoantibodies. Glia 57:1363-1373.

Nicchia GP, Srinivas M, Li W, Brosnan CF, Frigeri A, Spray DC (2005) New possible roles for aquaporin-4 in astrocytes: cell cytoskeleton and functional relationship with connexin43. FASEB J 19:1674-1676.

Nico B, Ribatti D (2011) Role of aquaporins in cell migration and edema formation in human brain tumors. Exp Cell Res 317:2391-2396.

O'Donnell ME, Tran L, Lam TI, Liu XB, Anderson SE (2004) Bumetanide inhibition of the blood-brain barrier Na-K-Cl cotransporter reduces edema formation in the rat middle cerebral artery occlusion model of stroke. J Cereb Blood Flow Metab 24:1046-1056.

Orellana JA, Froger N, Ezan P, Jiang JX, Bennett MV, Naus CC, Giaume C, Saez JC (2011) ATP and glutamate released via astroglial connexin 43 hemichannels mediate neuronal death through activation of pannexin 1 hemichannels. J Neurochem 118:826-840.

Pannasch U, Freche D, Dallerac G, Ghezali G, Escartin C, Ezan P, Cohen-Salmon M, Benchenane K, Abudara V, Dufour A, Lubke JH, Deglon N, Knott G, Holcman D, Rouach N (2014) Connexin 30 sets synaptic strength by controlling astroglial synapse invasion. Nat Neurosci 17:549-558.

Papadopoulos MC, Manley GT, Krishna S, Verkman AS (2004) Aquaporin-4 facilitates reabsorption of excess fluid in vasogenic brain edema. Faseb J 18:1291-1293.

Pop V, Sorensen DW, Kamper JE, Ajao DO, Murphy MP, Head E, Hartman RE, Badaut J (2013) Early brain injury alters the blood-brain barrier phenotype in parallel with beta-amyloid and cognitive changes in adulthood. J Cereb Blood Flow Metab 33:205-214.

Risher WC, Andrew RD, Kirov SA (2009) Real-time passive volume responses of astrocytes to acute osmotic and ischemic stress in cortical slices and in vivo revealed by two-photon microscopy. Glia 57:207-221.

Saadoun S, Bell BA, Verkman AS, Papadopoulos MC (2008) Greatly improved neurological outcome after spinal cord compression injury in AQP4-deficient mice. Brain 131:1087-1098.

Saadoun S, Papadopoulos MC Aquaporin-4 in brain and spinal cord oedema.
Neuroscience 168:1036-1046.

Saadoun S, Papadopoulos MC, Watanabe H, Yan D, Manley GT, Verkman AS (2005)
Involvement of aquaporin-4 in astroglial cell migration and glial scar formation. J
Cell Sci 118:5691-5698.

Saadoun S, Waters P, Bell BA, Vincent A, Verkman AS, Papadopoulos MC (2010) Intra-
cerebral injection of neuromyelitis optica immunoglobulin G and human
complement produces neuromyelitis optica lesions in mice. Brain 133:349-361.

Saubamea B, Cochois-Guegan V, Cisternino S, Scherrmann JM (2012) Heterogeneity in
the rat brain vasculature revealed by quantitative confocal analysis of endothelial
barrier antigen and P-glycoprotein expression. J Cereb Blood Flow Metab 32:81-
92.

Schlichter LC, Mertens T, Liu B (2011) Swelling activated Cl- channels in microglia:
Biophysics, pharmacology and role in glutamate release. Channels (Austin)
5:128-137.

Schutz M, Scimemi P, Majumder P, De Siati RD, Crispino G, Rodriguez L, Bortolozzi
M, Santarelli R, Seydel A, Sonntag S, Ingham N, Steel KP, Willecke K,
Mammano F (2010) The human deafness-associated connexin 30 T5M mutation
causes mild hearing loss and reduces biochemical coupling among cochlear non-
sensory cells in knock-in mice. Human molecular genetics 19:4759-4773.

Simard JM, Kent TA, Chen M, Tarasov KV, Gerzanich V (2007) Brain oedema in focal
ischaemia: molecular pathophysiology and theoretical implications. Lancet
Neurol 6:258-268.

Sogaard R, Zeuthen T (2008) Test of blockers of AQP1 water permeability by a high-
resolution method: no effects of tetraethylammonium ions or acetazolamide.
Pflugers Arch 456:285-292.

Strbian D, Durukan A, Pitkonen M, Marinkovic I, Tatlisumak E, Pedrono E, Abo-
Ramadan U, Tatlisumak T (2008) The blood-brain barrier is continuously open
for several weeks following transient focal cerebral ischemia. Neuroscience
153:175-181.

Sun MC, Honey CR, Berk C, Wong NL, Tsui JK (2003) Regulation of aquaporin-4 in a
traumatic brain injury model in rats. J Neurosurg 98:565-569.

Suzuki M, Iwasaki Y, Yamamoto T, Konno H, Yoshimoto T, Suzuki J (1984)
Disintegration of orthogonal arrays in perivascular astrocytic processes as an early
event in acute global ischemia. Brain Res 300:141-145.

Tanimura Y, Hiroaki Y, Fujiyoshi Y (2009) Acetazolamide reversibly inhibits water conduction by aquaporin-4. J Struct Biol 166:16-21.

Tomura S, Nawashiro H, Otani N, Uozumi Y, Toyooka T, Ohsumi A, Shima K (2011) Effect of decompressive craniectomy on aquaporin-4 expression after lateral fluid percussion injury in rats. J Neurotrauma 28:237-243.

Tourdias T, Dragonu I, Fushimi Y, Deloire MS, Boiziau C, Brochet B, Moonen C, Petry KG, Dousset V (2009) Aquaporin 4 correlates with apparent diffusion coefficient and hydrocephalus severity in the rat brain: a combined MRI-histological study. Neuroimage 47:659-666.

Tourdias T, Mori N, Dragonu I, Cassagno N, Boiziau C, Aussudre J, Brochet B, Moonen C, Petry KG, Dousset V (2011) Differential aquaporin 4 expression during edema build-up and resolution phases of brain inflammation. J Neuroinflammation 8:143.

Yang B, Zhang H, Verkman AS (2008) Lack of aquaporin-4 water transport inhibition by antiepileptics and arylsulfonamides. Bioorg Med Chem 16:7489-7493.

Zhao J, Moore AN, Clifton GL, Dash PK (2005) Sulforaphane enhances aquaporin-4 expression and decreases cerebral edema following traumatic brain injury. J Neurosci Res 82:499-506.